Universidade de Aveiro Departamento de Química
2017

LÚCIA ISABEL FERREIRA SANTOS

Suportes físicos para imobilização de sistemas de libertação controlada de fármacos bioinspirados pelo processo de polinização

Physical supports for immobilization of drug particles or controlled drug delivery systems by bioinspired pollination

Universidade de Aveiro Departamento de Química
2017

LÚCIA ISABEL FERREIRA SANTOS

Suportes físicos para imobilização de sistemas de libertação controlada de fármacos bioinspirados pelo processo de polinização

Physical supports for immobilization of drug particles or controlled drug delivery systems by bioinspired pollination

Dissertação apresentada à Universidade de Aveiro para cumprimento dos requisitos necessários à obtenção do grau de Mestre em Biotecnologia Industrial e Ambiental, realizada sob a orientação científica da Doutora Ana Sofia Silva, Investigadora Pós-Doutorada do Departamento de Química da Universidade de Aveiro, e do Professor Doutor João Mano, Professor Catedrático do Departamento de Química da Universidade de Aveiro.

o júri

presidente

Professor Doutor Jorge Manuel Alexandre Saraiva
Investigador Auxiliar da Universidade de Aveiro

Doutor Bruno Filipe Carmelino Cardoso Sarmento
Investigador Auxiliar do I3s- Instituto de Investigação e Inovação em Saúde da Universidade do Porto

Professor Doutor João Filipe Colardelle da Luz Mano
Professor Catedrático da Universidade de Aveiro

agradecimentos

Em primeiro lugar, queria agradecer ao professor João Mano pela oportunidade de trabalhar neste tema totalmente inovador, numa área completamente nova para mim. Um enorme obrigado a todo o grupo COMPASS por todo o apoio dado durante este ano. Em especial, queria agradecer à Ana Sofia Silva que me orientou e apoiou, estando presente durante todo o trabalho. E claro, aos fiéis companheiros de mestrado Cláudia, Carla, Diana, Luís, Pedro e Sara ali presentes para o melhor e pior do dia-a-dia no laboratório. Pois na ciência, raramente alguma coisa corre bem à primeira e nada melhor que ter este grupo para animar os dias!
A todos os meus amigos que sentiram a minha ausência durante estes últimos meses (ler restantes páginas se quiserem saber o porquê). Especialmente aos "biotecos" e "amigas da mário", juntos desde o início desta caminhada na ciência e em todos os momentos importantes deste percurso académico. Isto sem vocês não teria a mesma piada nem faria sentido! Sem esquecer, a todos aqueles do grupinho da cozinha, pelos belos momentos passados na residência. Cara vizinha Catarina obrigada pela paciência e boa disposição ao longo destes meses, parece que conseguimos sobreviver!
Um especial obrigado aos meus pais sempre presentes em todos os momentos da minha vida e pelo orgulho demonstrado.

palavras-chave

Abelhas, biomimetismo, libertação transdémica de fármacos, *micropatternig*, pensos, polinização, transportadores de fármaco.

resumo

Nos últimos anos, a administração transdérmica de fármacos foi aponte como uma via de libertação de fármacos de sucesso devido às suas enumeras vantagens. Relativamente aos sistemas convencionais, este é um sistema não doloroso, apresenta menos efeitos secundários e possibilita uma dose menos frequente. Os pensos representam a maior quota do mercado de sistemas de libertação transdérmica de fármaco. No entanto, a sua aplicação tem sido restringida pelos atuais problemas associados à sua administração passiva. Com base no conceito de biomimetismo, um novo e otimizado sistema para administração transdérmica de fármacos é aqui proposto, bioinspirado na capacidade das abelhas aprisionarem e, consequentemente, libertarem o pólen durante o processo de polinização. Assim, foi desenhado um penso hierárico biomimético obtido a partir de polidimetilsiloxano (PDMS) com um micropadrão de pilares (imitando o pêlo presente nas patas das abelhas). A otimização do sistema foi obtida pela conjugação de micropilares espaçados com a mesma distância que o diâmetro das partículas de fármaco. Obteve-se assim uma eficiência de aprisionamento de 24,8 ± 0,4 mg/cm^2, estando acima dos valores obtidos para os pensos atualmente disponíveis no mercado, bem como na maioria dos trabalhos até aqui efetuados. A tetraciclina, um antibiótico modelo, foi aqui utilizado para determinar o perfil de libertação de dois sistemas diferentes: pensos com tetraciclina em pó ou com micropartículas de alginato encapsuladas com esse mesmo fármaco. Enquanto o pó de tetraciclina foi rapidamente libertado, o sistema mais complexo permitiu uma libertação controlada do composto ativo durante 5 dias. Os pensos foram caracterizados por microscopia eletrónica de varrimento, microscopia de fluorescência e resistência à tração. Além disso, a atividade antimicrobiana também foi também verificada. Em suma, os resultados obtidos propõem a aplicação deste penso a nível clínico, proporcionando uma elevada concentração de fármaco que poderá resolver os problemas atuais associados aos sistemas de administração passiva de fármacos.

keywords

Biomimetic, drug carries, honey bees, micropatterning, patches, pollination, transdermal drug delivery.

abstract

In the last years, transdermal drug delivery has been exploited as a successful controlled drug release route due their several advantages (e.g. no painful, less frequent dosage and side effects), being the patches the largest market share of such systems. Nevertheless, current problems associated with passive delivery patches have been limiting their application. Based on the insights behind the biomimetics concept, herein we propose as novel and optimized system for transdermal drug delivery purposes, a bioinspired patch based on the remarkable bee's ability to catch and release the pollen during pollination. For this purpose, a hierarchical biomimetic polydimethylsiloxane (PDMS) micropatterning patch with micropillars (mimicking the hair of bee's legs) was engineered. An optimized system was obtained through the combination of patch with micropillars spaced with the same distance as drug microparticles' diameter. In fact, an entrapment efficiency of 24.8 ± 0.4 mg/cm^2 was achieved, being above the actual commercially available patches and most of the current research works. The release profile was determinate to two different systems: patches with either tetracycline hydrochloride powder or tetracycline loaded alginate microparticles, a model antibiotic. While tetracycline powder was immediately release, the most complex system allowed for a controlled and sustained release of the active pharmaceutical ingredient (API) for 5 days. The engineered patches were characterized by SEM, fluorescent microscopy, tensile strength and antimicrobial activity was also verified. The results herein obtained suggest that the optimized patch could be further developed for clinical applications, providing high drug concentration that could solve the current problems associated with passive drug delivery patches.

Contents

List of figures

List of tables

Abbreviations

AA – Asiatic Acid

Anti-TNF-α-Abs – Anti- tumor-necrosis-factor-alpha-antibodies

API – Ative pharmaceutical ingredient

BMA – Butyl methacrylate

BSA – Bovine serum album

CMC – Carboxymethyl cellulose

CPVP – Crospovidone

CS-PVA – Chitosan-polyvinyl alcohol

DCM – Dichloromethane

DIA – Drug-in adhesive

DDS – Drug Delivery System

EDTA – ethylenediaminetetraacetic acid

FDA – Food and Drug Administration

G – Gauge

GMA – Glycidyl methacrylate

HA – Hyaluronic acid

HEC – Hydroxyl cellulose

HPC – Hydroxyl propyl cellulose

HPMC – Hydoxypropyl methyl cellulose

IgG – Immunoglobulin

LB – Lysogeny broth

MN- Microneedle

PBI – Polyisobutylenes

PBS – Phosphate Buffered Saline

PCL – Polycaprolactone

PDMS – Polydimethylsiloxane

PEG – Poly(ethylene glycol)

PET – Polyethylene terephthalate

PGA – Polyglycolide

PHBHV – Poly(HydroxyButyrate-co-HydroxyValerate)

PHEA – Poly(2-hydroxyethylacrylate)

PMA – Propylene glycol monomethyl ether acetate

PMP – PDMS micropatterning patch

PSA – Pressure adhesive sensitive

PVA – Polyvinyl alcohol

PVP – Polyvinylpyrrolidone

RT – Room temperature

SC – Statum corneum

SEM – Scanning electron microscope

Chapter 1- Motivation

Wound healing is a well-studied process that consists in the repair of a tissue after trauma. One of the most affected tissue is skin, where epidermis and dermis develop a protective barrier that once broken, initiates a cascade of cellular and chemical signals that will promote the damage repair.[1] Wound healing is a complex set of reactions and interactions with cells and "mediators" which is normally divided in three steps: inflammatory, proliferative and remodelling phase **(Figure 1.1)**. Haemostasis is the initial step and allows the foundation of the healing process. On the other hand, the inflammatory phase is characterized by vasodilation and the increase the vascular permeability and is marked by platelet accumulation, coagulation, and leukocyte migration. The proliferative phase is distinguished by re-epithelialization, angiogenesis, fibroplasia, and wound contraction. The final step is the remodelling phase that takes place over a period of months, during which the dermis responds to injury with the production of collagen and matrix proteins and then returns to its preinjury phenotype.[2]

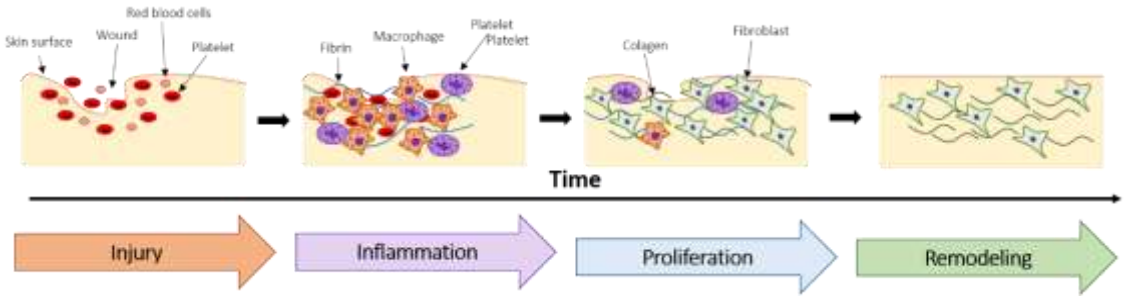

Figure 1.1. Wound healing process- inflammation, proliferation and remodelling.

Many factors can lead to impaired wound leading. This will affect wound characteristics and healing capacity. The main local factors are the wound oxygenation and infection. Oxygen is a critical parameter in the healing process preventing wounds from infections, enhancing collagen synthesis and allowing wounds contraction. The critical point of healing is the infection. When skin is injured an inflammatory response is developed due to presence of microorganisms at skin surface that have access to the underlying tissues. Inflammation is a normal step of wound healing and is responsible for the removal of such microorganisms. When the normal microflora of skin is not restored, inflammation may be prolonged and the wound may enter a chronic state and fail to heal. The impaired wound

healing and the associated inflammatory response are related with age, stress, obesity, sexual hormones, nutrition, medication, diseases like diabetes or alcohol consumption.

After many years of R&D, drug delivery systems (DDS) were appointed as the most effective strategy, improving the pharmacological and therapeutic properties of drug. These systems not only facilitate the handling and administration of drugs and regulate the local or systemic release, but also aid the drug to overcome certain barriers and fit the release process to specific therapeutic demands.[3] Skin allows a large and readily accessible surface area for the application and absorption of a patch-like device to its surface, i.e., a non-invasive procedure that will promote a continuous intervention.[4] In the last years, transdermal drug delivery has been exploited as a successful controlled drug release platform that has received regulatory approval. In fact, there are already a set of products with this concept present in the market.[5] Transdermal DDS must be applied when a drug has a significant first-pass effect in the liver, being prematurely metabolized in the pre-systemic stage. Hence, transdermal drug delivery allows for less frequent dosing or steady delivery profiles and is also a suitable alternative to hypodermic injection, which is painful and makes use of large amounts of dangerous medical devices, increasing the risk of disease transmission (e.g through needles re-use).[6,7]

A large set of distinct transdermal DDS have been developed with different designs, polymeric arrangements and drug particles embedded. Designs with different degrees of development were produced from the humblest system, based on passive drug delivery with little/no permeation enhancement, to the most complex transdermal DDS that enable the delivery of small molecules and macromolecules.[8] The use of these patches with different designs will mostly depend on drug properties (e.g. molecular weight and physicochemical), as well as the required amount to accomplish an effective treatment.[6] Based on the extraordinary potential behind the DDS, drug carriers (either at nano- or micro-scale) can be incorporated in patches in order to improve drug pharmacological properties, prompting a more efficient treatment.[3]

The concept of bio-inspired, bioengineered and biomimetic drug delivery carriers is emerging nowadays, aiming to understand how nature designs, processes and molecular building blocks enable the fabrication of high performance soft materials and polymer composites. These designs allow the engineer of new molecules and materials with novel properties. In fact, a better understanding of biological systems in conjunction with the

advanced biotechnology tools allows the re-engineering of various at micro and nono-scales natural systems enabling their multiple application in the delivery of molecules such as proteins and small interfering RNA, and others therapeutic agents.[9]

Many soft biomimetic synthetic adhesives have also been studied in order to support macroscopic masses, normally inspired by animals and insects. Nevertheless, bioinspired adhesion that is tuned to micro- and nano-scale sizes and forces is poorly exploited. However, such adhesive forces are critical in the adhesion of micro and nanoparticles to surfaces, which are relevant to a wide range of industrial and biological processes such as drug delivery. Honey bees for instance, can carry large amount of pollen in their legs and body, mostly in the space between hair legs. Bees have a typical branched hair with numerous short lateral barbs and pollen grains are caught and held between the barbs of adjacent hair. The hair covering the body allows the temporary retention of pollen, which is then removed by the combing action of the legs' brushes. Together, pollens and bees' hair legs, whose adhesion is critical to plant pollination, are an optimized system that can be used to inspire the develop of a hierarchal system based on the adhesion between particles and micro-patterned soft matter surfaces.[9,10]

Microfabrication allows the production of micro- or nano-structures. In most of the cases the process is based on a variety of patterning-techniques, such as photolithography, that enables the mass production of patterned structures. Nowadays, soft lithography is commonly used in microfabrication and represents a non-photolithographic strategy based on self-assembly and replica moulding for carrying out micro- and nanofabrication. This technique is low in capital cost, easy to learn, straightforward to apply and accessible to a wide range of users and can be apply to a wide variety of materials and surface chemistries. Microfabrication technology has been applied in drug delivery systems fabrication with different materials. This approach can be applied to develop biomimetic systems such as membranes with a micropatterning surface. According to the principles behind the biomimetics, effective drug carries can be developed based on a natural system by construction of a micropatterned structure.

The main goal of this work is the development of a bioinspired system based on adhesion of the grain pollens to the bee’s hair legs. Just as bees are able to capture and release the pollen, a micropatterning patch with micropillars (that mimics bees' hair legs) can be developed to grab a certain amount of drug. These systems are designed for topical

application in skin wounds with a controlled release of antibiotic during the inflammatory phase (five days). For this purpose, a system of thin PDMS micropatterned patch with micropillars (100 to 550 μm) and tetracycline-loaded microparticles, a common antibiotic for skin wounds, is herein developed. Differently sized microparticles were thoroughly tested against patches with different configurations in terms of micropillars geometry arrangement, height and distance between them, in order to support the hypothesis that grains pollen caught by bees' hair legs have similar sizes to the actual leg hair spacing. In fact, Amador and co-workers have recently provided physical insight into the critical process of pollination and suggest that hair spacing on the body is tuned to accumulate more particles and that, to facilitate particles grabbing by the bee's hair legs, particle size to should be comparable to hair leg spacing.[11] Drug release profiles and the antimicrobial activity of the obtained systems will also be investigated. Drugs' microparticles will be incorporated in micro-patterned soft matter surfaces. The most effective system will be elected after testing different particle's size against micropatterned patches with different configurations: distance between micropillars and their height; and different geometry arrangement. Together with a suitable drug release profile, it is envisaged that the hierarchal patch herein developed will be beneficial for an effective treatment of skin wounds.

For the purpose, this master dissertation development is divided into the subsequent chapters:

- Chapter 1: *Motivation*, where some introductory notes are given and the main goal of this thesis is detailed;
- Chapter 2: *Biomaterials for drug delivery patches*, where an insight of current state of the existing/commercial available transdermal drug delivery systems is provided. Future perspectives are also presented;
- Chapter 3: *Materials and Methods*;
- Chapter 4: *Physical supports for immobilization of particles inspired by pollination*, where a novel and robust bioinspired patch is proposed based on the bee's ability to catch and release the pollen during pollination;
- Chapter 5: Final Overview, concluding remarks and future prospects.

References

1. Martin, P. Wound healing--aiming for perfect skin regeneration. *Science*. **276,** 75–81 (1997).
2. Broughton 2nd, G., Janis, J. E. & Attinger, C. E. The basic science of wound healing. *Plast. Reconstr. Surg.* **117,** 12S–34S (2006).
3. Allen, T. M. & Cullis, P. R. Drug Delivery Systems: Entering the Mainstream. *Science.* **303,** (2004).
4. Prausnitz, M. R., Mitragotri, S. & Langer, R. Current status and future potential of transdermal drug delivery. *Nat. Rev. Drug Discov.* **3,** 115–124 (2004).
5. Wiedersberg, S. & Guy, R. H. Transdermal drug delivery: 30+ years of war and still fighting! *J. Control. Release* **190,** 150–156 (2014).
6. Naik, A., Kalia, Y. N. & Guy, R. H. Transdermal drug delivery: overcoming the skin's barrier function. *Pharm. Sci. Technolo. Today* **3,** 318–326 (2000).
7. Guy, R. H. Transdermal Drug Delivery. *Drug Delivey*. **197,** 399–410 (2009).
8. Prausnitz, M. R. & Langer, R. Transdermal drug delivery. *Nat. Biotechnol.* **26,** 1261–1268 (2008).
9. Bhushan, B. Biomimetics: lessons from nature-an overview. *Philos. Trans. R. Soc. A Math. Phys. Eng. Sci.* **367,** 1445–1486 (2009).
10. Bogue, R. Biomimetic adhesives: a review of recent developments. *J. Eur. Ind. Train.* **28,** 282–288 (2008).
11. Amador, G. J. *et al.* Honey bee hairs and pollenkitt are essential for pollen capture and removal. *Bioinspir. Biomim.* **12,** 26015 (2017).

Chapter 2- Biomaterials for drug delivery patches

Lúcia F. Santos [1], A. Sofia Silva[1], João F. Mano[1]

[1] Department of Chemistry, CICECO – Aveiro Institute of Materials, University of Aveiro, Campus Universitário de Santiago, 3810-193 Aveiro, Portugal

Abstract

The limited efficiency of conventional drugs has been instigated the development of new and effective drug delivery systems (DDS). The research and development of transdermal DDS have been promoted due to their various advantages such as no pain and less frequent and greater flexibility of dosing.

The simple design, application and lower cost of patches, makes the transdermal DDS the best seller of the market. Patches are based on passive drug delivery and higher drug concentration must be applied to improve transcutaneous fluxes. These devices have been produced using either biodegradable or non-biodegradable polymers. The biodegradable ones have been receiving high attention due to their safety, biocompatibility, low toxicity and controlled degradation by human enzymes on water. On the other hand, non-biodegradable polymers are related to higher risk of skin irritation. However, patches based on these materials are the most currently available patches in the market and allow greater mechanical resistance and flexibility and non-degradation over the time. Furthermore, patches with higher drug concentration have been achieved with these non-biodegradable polymers. Drug particles have also an important role in patches production. Low size and pre-fabrication of drug carriers not only enhanced drug solubility and permeation but also allowed a more controlled drug release over the time.

This review highlights the latest development of patches for drug delivery, focusing on the different materials that have been proposed and their combination with drug carriers.

***Key words*:** Drug delivery systems, trandermal delivery, patches, polymers, skin, drug carries.

1. Introduction

Drug delivery systems (DDS) has been appointed as an effective way to improve the pharmacological and therapeutic properties of drug. These systems not only facility the handling and administration of drugs and regulate the local or systemic release, but also help the drug to overcome certain barriers and fit the release process to specific therapeutic demands.[1] Skin allows a large and readily accessible surface area for application and absorption of a patch-like device to its surface, constituting a non-invasive procedure that will promote a continuous intervention.[2] In the last years, transdermal drug delivery has been exploited as a successful controlled drug release platform that have received regulatory approval for a series of products. [3] Transdermal DDS must be applied when a drug has a significant first-pass effect in the liver, being prematurely metabolized. Transdermal delivery allows for less frequent dosing or steady delivery profiles and may be easily applied without pain.[4,5]

Distinct designs of transdermal DDS have been proposed from the humblest system, based on passive drug delivery with little/no permeation enhancement, to more complex transdermal DDS that enables the delivery of small molecules and macromolecules.[6] The choice among these patches can mostly depend on the drug properties (e.g. molecular weight and physicochemical characteristics), as well as the required amount and release profile to accomplish an effective treatment.[4] Drug carriers (either at nano- or micro-scale) can be incorporated in patches in order to improve drug pharmacological properties, prompting a more efficient treatment of such device.[1]

This review section will highlight the efforts developed in last years regarding the production of patches with different designs and their potential application in drug delivery. Pros and cons of currently available systems will be discussed and future prospects will be discussed.

1. Drug Delivery Systems

Conventional (“free”) drugs exhibit some limitations that can be improved through their incorporation in DDS. The chemical nature of the drug molecule can be responsible for its poor solubility resulting in drug precipitation when in aqueous media. The use of drug carriers such as lipid micelles or liposomes among others, can surpassed this major limitation

improving drug solubility.[7] Another common problematic is the expeditious breakdown of the drug *in vivo* due to physiological conditions like pH. Such degradation, that leads to a notable loss of drug activity, can be prevented through the use of DDS that will protect the drug from premature degradation.[8] Moreover, drug carriers empower less non-specific distribution, reducing unwanted/toxic side effects in healthy tissues. DDS can be designed to improve selectivity towards the targeted tissues (like for instance, ligand-mediated targeting), allows for an increased drug concentration in the specific site of action, enhancing drug effects in the diseased area.[9,10] Through the association of particular carrier systems with conventional therapeutic molecules, properties such as pharmacokinetics and biodistribution are strongly improved allowing a higher specific response to the target tissue.[11]

2. Transdermal Drug Delivery Systems

Many efforts have been developed to promote topic/transdermal drug delivery. However, systemic route still the main drug administration strategy. A drug administered through the systemic route reaches the systemic circulation (blood) inducing, therefore, a systemic action. On the other hand, drugs given by the topical route are mainly applied on skin or mucous membrane, promoting a localized action. [12,13]

Skin exhibits a large and readily accessible surface area for the absorption and/or application of a patch-like device in a non-invasive procedure, promoting a continuous intervention (system repositioning, removal or replacement). These devices are not capable of rapid drug input but are usually designed to retard and sustain the delivery of the drug.[4] Transdermal drug delivery allows less frequent dosing with a continuous delivery and can be applied to avoid the first-pass effect in the liver, where drugs can be prematurely metabolized.[4] However, these systems also present some drawbacks such the potential toxic effect of the drug.[6]

In the last years, transdermal drug delivery has been exploited as a successful controlled drug release platform that has received regulatory approval for several products, with a large majority already available in the market.[3] The worldwide transdermal patch market approaches £2 billion in USA, yet restricted to ten drugs - scopolamine (hyoscine), nitroglycerine, clonidine, estradiol (with and without norethisterone or levonorgestrel), testosterone, fentanyl, nicotine and lidocaine.[14] There are several parameters that affect the

delivery of the drug from the patch to the skin. Absorption, for instance, depends on the site of application, thickness and integrity of epidermidis, size of drug molecule, permeability of the drug delivery membrane, state of skin hydration, pH of the drug, drug degradation by skin flora, lipid solubility and body conditions, such as body temperature and some additives, that are responsible for blood flow alteration.[15,16] Skin thickness and blood flow are two parameters that vary with age and are responsible for different responses to the same transdermal device, a notable effect on drug's pharmacokinetics.[15]

Transdermal devices can be divided based on their design in reservoir-type and matrix-type patches as briefly represented in **Figure 2.1**.[17] The reservoir-type patches allow the sustaining of the drug in a solution or gel, and its delivery is governed by a rate-controlling membrane that is positioned between the drug reservoir and skin.[18] On the other hand, matrix-type patches, that were introduced in the 80s,[19] are characterized by a simple design based on the incorporation of drug in an adhesive. A mechanical backbone is used as an outer layer to prevent loss of drug from the adhesive. This design does not involve rate-controlling membranes and the rate of drug delivery is achieved through skin permeability.[15] The reservoir-type patches have been showing more advantages in terms of formulation flexibility and tighter control over delivery rate.

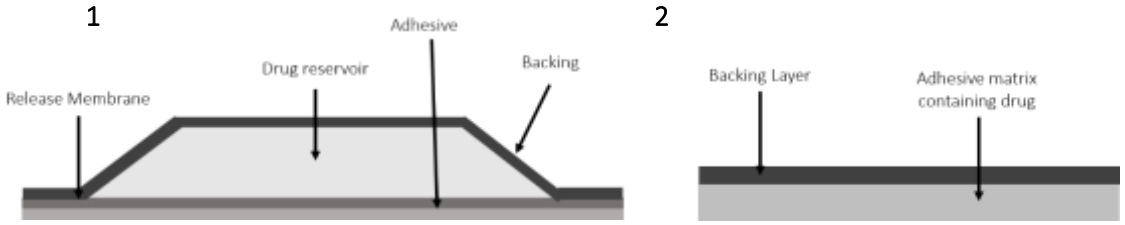

Figure 2.1. Schematic representation of patches design **1.** Reservoir-type **2.** Matrix type.

3. Barriers to transdermal delivers

Skin is a highly efficient barrier that limits molecular transport both from and into the body, preventing molecular permeation. This natural barrier avoids the penetration of foreign molecules such as the flux of toxins, while minimizing the loss of water.[20] Skin is composed by multi-layers, as displayed in **Figure 2.2**. On skin's outer surface there is a non-living layer of keratin-filled cells surrounded by a lipid-rich extracellular matrix named stratum corneum (SC), an extremely thin biomembrane (approximately 100 μm) that is

considered the least permeable of the skin layers. SC has been proposed to play an important role in the barrier function and is the ultimate stage in the epidemical differentiation process, forming a laminate of compressed keratin filled with corneocytes attached in a lipophilic matrix. [21] The matrix lipids allow a continuous phase from the skin surface to SC base. The intercellular lipid lamellae forms a conduit in which the drugs diffuse to access vascular infrastructure and, ultimately, to the systemic system.[4,22] Nevertheless, due to SC high diffusional resistance, the transdermal permeation of a large pool of drugs is highly limited in a mechanism of passive permeation.[20]

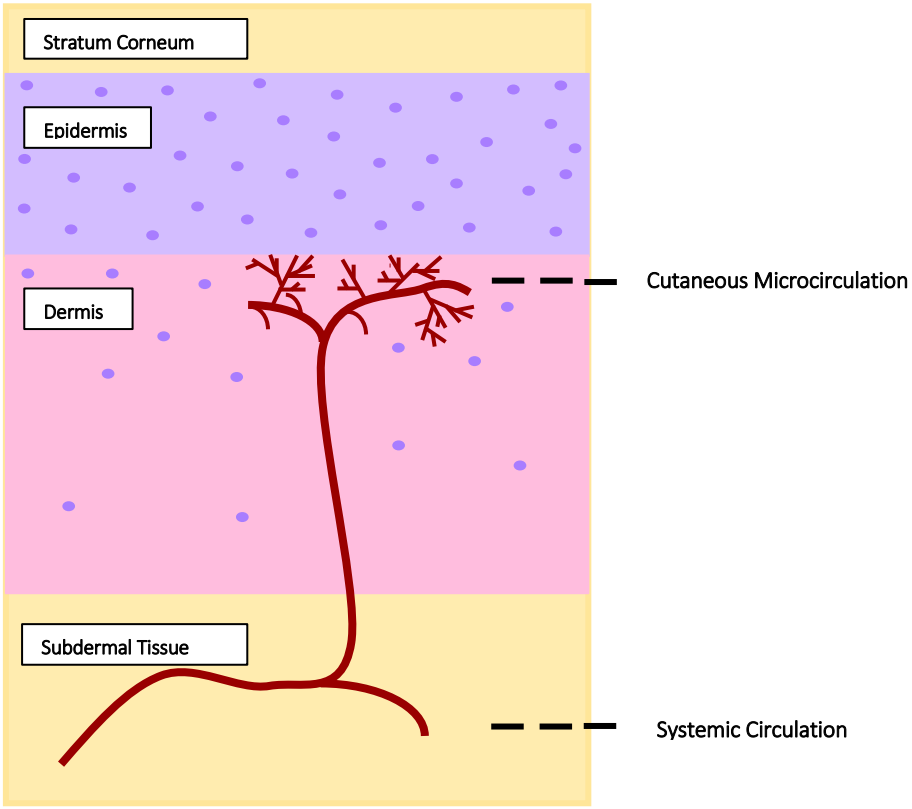

Figure 2.2. Schematic representation of skin layers.

Pharmacologically potent drugs requiring small therapeutic blood concentrations (ng ml^{-1} or less), are usually subjected to passive transdermal delivery. The SC is a very selective barrier and only molecules with the adequate physicochemical properties can be transported across this outer layer.[4,23] The lipophilic nature of SC's barrier promotes a better acceptation of lipophilic molecules. Still, for an accurate passive permeation, the ideal drug should be amphiphilic and sufficiently "mobile" to diffuse across the SC. If the drug is only

hydrophilic, the molecule will be unable to be transfer into the SC. On the other hand, a lipophilic drug will tend to remain on the SC layer.[4,24] Solute diffusivity decreases exponentially as molecular volume (related to molecular weight) increases. A favourable transport across the skin is normally achieved with restriction of drug particles size (less than 500 Da). Also, an increased drug flux is favoured when saturated drugs' solution are used. Conclusively, in order to improve transcutaneous fluxes it is necessary to increase solute concentration and use an amphiphilic drug.[4]

3.1. Enhancing skin permeation

Relatively impermeable molecules can be modified in order to improve their permeation in skin layers. Drugs *per se* can be modified, for example, by a derivatization strategy to alter the lipophilic nature of the drug. Other chemical modifications as well as physical alterations can also be performed in order to improve drugs permeation (**Table 2.1**).[4,25]

However, currently approaches are focused on the enhancement of skin permeation, being devoted to the development of new active and passive methods that improve membrane's permeability. Passive methods include the actual vehicles - creams, gels and "passive" patches. Some modifications have been proposed such as the use of penetration enhancers, supersatured systems or drug carries liposomes. Chemical penetration enhancers have the ability of compromising skin's barrier allowing the entry of poorly penetrating molecules through the membrane.[4] Chemicals like alcohols can solubilize and extract lipid components of the SC or induce lipid fluidization, therefore increasing permeation. Still, this method presents some limitations such as the physiological incompatibility of the high concentrated chemical enhancer used to achieve suitable levels of penetration.[26,27] Supersatured systems are based on the production of a supersatured drug solution, which is a very simple method to increase skin permeation.[28] Commented before, drug carriers improve both drug properties as well as their permeation throughout the skin for a targeted delivery.[29] Nevertheless, due to skin characteristics (low permeability and diffusion), these methods are limited by the amount of drug that can be delivery.[16]

Nowadays, there are an increasing generation of new therapeutically-active molecules with large molecular weight (superior to 500 Da) and mostly hydrophilic. Passive methods of skin delivery are not capable to enhance permeation of these large molecules.

This problem has been solved through the development of active methods of permeation that involve the use of external energy to interfere with the natural barrier of SC to improve transdermal transport.[20] Iontophoresis, electroporation, ultrasound, laser radiation, radiofrequency, microneedles, skin abrasion, puncture and abrasion, magnephoresis and temperature are the main active approaches.[16]

Some physical enhancement techniques have been applied to allow the penetration of emerging "biotechnological" drugs like peptides and oligonucleotides, commonly associated to a difficult penetration.[16] Iontophoresis is one of the most common physical enhancement technologies and makes use of a small electrical current, at a constant pulse, to promote the placement of charged and uncharged species of therapeutic drugs at skin surface.[14,30] Electroporation uses high-voltage short-duration pulses in order to create regions of membrane permeabilization by the production of aqueous pathways in SC with full reversibility within minutes to hours.[25] Ultrasound is also able to compromise the skin's barrier function. This technique applies a frequency greater than 20 kHz and is responsible to increase the pore size, promoting alterations in the SC lipid architecture.[31] Another method based on radiation application has been reported. Laser radiation destroys the target cells that are related to SC ablation without significant damage on epidermis.[32] Radiofrequency is also commonly used for the ablation of malignant tissues due to its ability to induce microchannel formation in skin.[33] Microneedle-based device is another methodology and consists of a drug reservoir and a set of microneedles that penetrates the SC and epidermis to deliver the drug. This type of devices not only presents the ability to overcome barriers properties of SC but also allows a controlled rate for local or systemic effect. The microneedles create channels on the skin that allow the transport of any topically applied drug.[34],[35] Skin abrasion, a common technique used by dermatologists, consists in the direct removal of the most superficial layers of the skin in order to increase the permeation of the drugs. With this procedure, the diffusion of the drug is not restricted by its physicochemical properties.[36] Skin puncture and perforation is another technique that uses needle-like structures to promote the disruption of the skin barrier through the creation of holes and cuts.[20] The majority of these enhancement techniques are invasive. Pressure application has also been appointed as an alternative, providing a non-invasive and simple method to enhance skin permeability through increasing of transappendageal route (including permeation through the sweat glands and across the hair follicles with their

associated sebaceous gland) and drug partition in the SC.[20,37] Another non-invasive methodology is magnetophoresis that consists in the application of a magnetic field to enhance the diffusion of a diamagnetic solute across the skin.[38] Temperature has also an important role in the permeability enhancement. The increase of the temperature improves the drug diffusion and the skin lipid fluidity.[39]

Table 2.1. Advanced techniques to enhance drug delivery via transdermal route.

Techniques	Advantages	Limitations
Passive Methods		
Drug carries (e.g. vesicles) **Supersaturated systems** **Chemical penetration enhancers** [16],[27,28]	Simple methods; Extra equipment not required;	Physiological incompatibility of the high concentrated chemical; Limited by drug amount; Not applied to large and hydrophilic drugs;
Active Methods		
Electroporation[25]	Versatility; Transient changes in tissue;	Non-target transport; Invasive; Require several applicator; Involves skin structural changes;
Iontophoresis [14,30]	Simple design; Without pain sensation;	Possibility of burns; Drug solution must be sufficiently ionized; Invasive;
Ultrasound [31]	No permanent loss of skin barrier; Non-invasive;	Long-time application;
Laser radiation[32]	High precision SC ablation;	Some damages to living tissue; Invasive;
Radiofrequency[33]	Single applicator; Targeted (not affect in proximal muscles);	Involves skin structural changes; Invasive;
Microneedles[34],[35]	Minor skin abrasion; Controlled drug release; Painless;	Local infections at the needle–skin interface; Invasive;
Skin abrasion[36]	Little damage to deeper tissues; Common cosmetic procedure;	Non-target drug delivery; Invasive;
Skin puncture and perforation[20]	Wide drug range; Painless;	Invasive;
Magnetophoresis[38]	No effect on the skin structure; Non-invasive;	Lacks in safety research;
Temperature[39]	No damages to the deeper tissue; Non-invasive;	Skin structure alteration at highest temperatures;

4. Transdermal drug delivery patches

According to Prausnitz and Langer, transdermal delivery systems can be divided in three generations of development. The majority of the actual patches are within the first generation class that carry specific types of drugs (e.g. sufentanil and granisetron) able to cross skin barriers at a therapeutic level but with little or no enhancement. Moreover, this type of patches is limited to drugs with suitable properties such as low-molecular weight, lipophilic and efficacious at low doses. The second generation is characterized by some improvements that allow the delivery of small-molecules by increasing skin permeability. Third generation patches enable the transdermal delivery of small-molecules of drugs or macromolecules such as proteins or DNA, and other vaccines through targeted permeabilization of the skin's SC.[40] **Table 2.2** summarizes the current transdermal patches based on biodegradable and non-biodegradable polymers

5. Patches based on natural and biodegradable polymers

Biocompatible and biodegradable polymers, mostly natural ones have been received careful attention due to their biocompatibility, low toxicity and susceptibility to degradation by human enzymes or by hydrolysis.[41]

5.1.Chitosan

Chitosan is a natural biodegradable polymer derived from chitin, with high potential in patches application. There are several works based on the development of chitosan-based patches. Chitosan possesses a suitable film-forming ability with bioadhesive and absorption enhancement capacity.[42] Sigfridsson and co-workers have developed a polymeric patch based on chitosan layer and an aluminium backing. This patch incorporated 125 mg of Gibenclamide nanocrystals, a hypoglycaemic agent given to diabetic patients. Chitosan decreased the usually nanocrystals precipitation and improved skin permeation of Gibenclamide by nanosizing the drug.[43] The chitosan transdermal patch presents a solution to traditional diabetes treatment that consists in numerous daily injections of insulin, affecting the life quality of diabetic patients. In addition, the insulin injections are also associated to several adverse effects like insulin resistance, glucose intolerance, weight gain and cardiovascular complications.[44–46]

One limitation of patches in prolong treatments is the weak adhesion of the patch to the skin. A novel approach to enhance adhesion and improve mechanical properties of chitosan patches was proposed by Anirudhnan and co-workers and consisted in the grafting of chitosan with glycidyl methacrylate (GMA) and butyl methacrylate (BMA).[47] Amine functionalized hyaluronic acid (HA) (by hydrophobic modification) was used to encapsulate lidocaine, which is a poor water soluble drug used to neuropathic pain and presents a set of secondary effects. The encapsulate drug microparticles were then dispersed in the modified chitosan matrix. This combination offered a matrix with improved mechanical properties, drug retention behaviour and good storage over the time. Chitosan modification with another acrylate confirmed the possibility to improve the mechanical properties of chitosan patches. Modified chitosan with poly(2-hydroxyethylacrylate) (PHEA) offered an efficient transdermal hydrogel patch for levofloxacin (an antibiotic) to wound infection treatment. PHEA enhanced the patch flexibility as well as the hydrogel itself, allowing a higher swelling ability associated with increased drug skin permeation.[48] However, some limitations are observed in crosslinked chitosan patches. Higher crosslinking ratio was associated to a decrease in swelling ratio. Moreover, other limitations were herein also demonstrated such as the restrict drug content (only 5% of the patch) and the hydrogel degradation along the time.

Another modified chitosan matrix was introduced by Hye Kim and co-workers. A silver hybridized porous chitosan-based patch was developed with high mechanical strength and drug delivery efficiency with Rhodamine B (5 mg mL^{-1}) as a model molecule.[49] Silver metal has been appointed as strong bacterial inhibitor with potential applications to prevent wound infections. In this work, silver promoted drug release by enhancement of hybridized films hydrophobicity, which was related to an increase of SC permeability.

Chitosan, has also been receiving particular attention for microneedles patches applications. Due to the safety concerns associated with microneedles break in the skin, biodegradable and biocompatible polymers have been used in order to overcome such limitations, promoting total dissolution of the microneedles and decreasing the contamination risk without waste generation.[50] According to Chen and co-workers, chitosan microneedles patch showed to be a promising device for sustained delivery of hydrophilic macromolecules. **Figure 2.3** presents a chitosan microneedles patch and the resulting microneedle puncture marks on the skin. By using bovine serum album (BSA) as

a model protein, this patch allowed the encapsulation of fragile macromolecules without major changes over the time and enabled a prolonged release (8 days), normally required in therapies with these molecules (e.g. vaccines and DNA therapies). BSA was used in order to determine the applicability of this system to macromolecules. However, in this specific study case, some microneedles fragments remained upon patch removal.[51] Drugs loaded in chitosan carriers could be released through swelling and degradation of the chitosan matrix, leading to a clear sustained-release effect.[52]

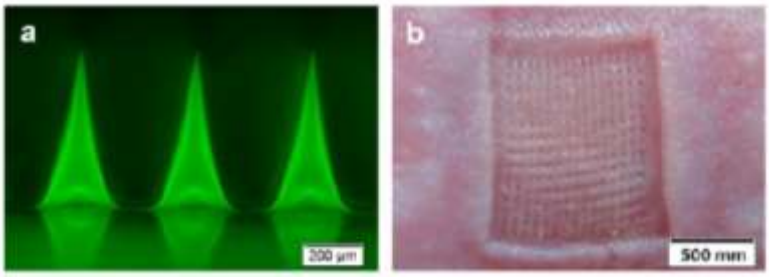

Figure 2.3. Chitosan microneedle patch **a.** Bright-field micrograph of microneedle puncture marks on the skin **b.** Scanning electron micrograph of an inverse replica of skin surface after insertion and removal of microneedles.[51]

More efforts will be needed to improve the properties of chitosan-based patches to enhance the drug encapsulation capability and release kinetics, and important properties such as adhesion and mechanical properties. Combination with inorganic fillers[53],[54] and the nanostructured membranes could be possible.[55,56]

5.2.Cellulose

Cellulose is one of the most common polymers in nature and the largest constituent of the plants. The last decades revealed that cellulose can be also produced by bacteria. The bacterial cellulose has unique physical and mechanical properties, high purity and biocompatibility that promote their application in the biomedical field.[57]

Literature reports show that bacterial cellulose membranes (**Figure 2.4**) have a simple design composed by a single layer with straightforwardness and effeteness to absorb executes and adhere to irregular surfaces, a critical parameter to several clinical situations such as burns and wounds.[58,59] Comparing to the conventional routes, some limitations were appointed to these patches. Particularly, Trovatti and colleagues obtained low drug flux of

diclofenac (hydrophilic drug), an anti-inflammatory normally administrated as a gel.[59] The lower flux was explained through the resistance promoted by the complex tridimensional network of these membranes to the diffusion of drug molecules. The chemical properties of the drug were also pointed out as a limitation. In fact, lower permeation rates were obtain by Silva and colleagues, who incorporated lidocaine hydrochloride in bacterial cellulose membranes and compared those results with the ones obtained through the conventional administration systems. However, when a lipophilic drug was incorporated a three-time higher permeation rate was achieved.[58] These membranes can be applied to pathologies that require lipophilic drugs and long-term release.

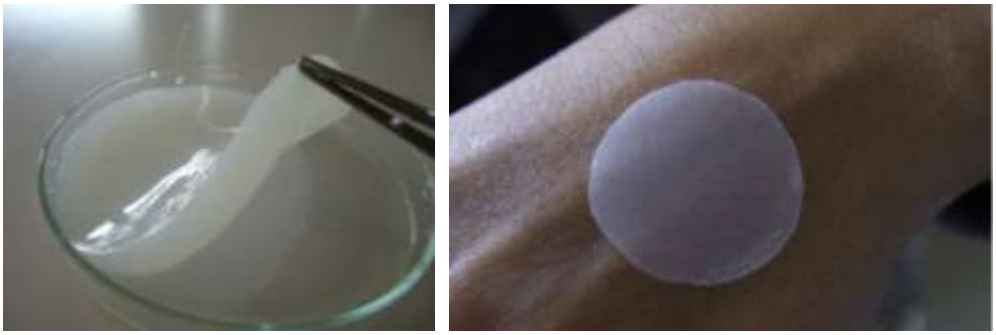

Figure 2.4. Visual images of bacterial cellulose processed and applied as patches.[58]

Cellulose can be also applied to transdermal hydrogel patches. Ahmed and El-Say have reported two cellulose derivatives, hydroxy propyl methyl cellulose (HPMC) and hydroxyl propyl cellulose (HPC) that were incorporated with raberprazole- alginate/chitosan nanoparticles. HPMC showed higher drug flux than HPC. Microspheres of alginate-chitosan have been applied in a wide range of biomedical applications. However, leaching of the drug during the formulation process remains the major drawback. The novel approach of drug encapsulation developed by the authors enhanced the drug entrapment and permeation comparing to the assay with "free" drug (control). However, the diffusion rate was slower than the control one.[60]

These two cellulose derivatives were also used to develop microneedle patches. In the work performed by Kim and co-workers, HPMC combined with drug was used for the tips and carboxymethyl cellulose (CMC) for needles base. This system allowed a rapid release of 179.9μg donepezil hydrochloride to Alzheimer's treatment with a more effective delivery than the conventional oral route. However, the distribution was not uniform and an

applicator is required to solve this limitation. Furthermore, the patch did not allow the loading of high drug amounts but higher patch area can solve this problem.[61]

Hydroxyl cellulose (HEC) is another cellulose derivative reported in the engineering of hydrogel patches, where hydroxyl group allowed an increase of the natural cellulose's solubility. Kong and colleagues described the cross-linking of HEC with HA enhancing skin permeation of isoliquiritigenin, which has beneficial effects on cancer treatment. In cross-linked hydrogels, the drug permeation is limited by the cross-linking degree. HA helped in permeation due to the high water retention capacity, which promoted the looseness of the skin barrier though skin hydration.[62] HA was also associated to higher permeation in the work developed by Korkmaz and co-workers. A dissolving microneedle device was fabricated through the combination of carboxymethyl cellulose (CMC) with HA to delivery of 0.5 mg anti-tumor-necrosis-factor-alpha (anti-TNF-α), a high weight hydrophilic substance that has an important role in autoinflammatory skin diseases. The combination of CMC and HA effectively inhibited antibody diffusion from the delivery site, allowing a targeted drug delivery. Moreover, both side-effects and loss of drug content are herein decreased.[63]

Due the physical and mechanical resistance of cellulose and their functionalized forms, could be developed patches with different design and applicability.

5.3.Starch

Pure starch is a rigid and brittle polymer with poor film-forming properties. These features can be improved by physical blending with other biomaterials improving the mechanical functionality of starch.[70,71] An efficient hydrogel patch of starch nanocrystals was recently developed by Bakrudeen and co-workers that allowed the incorporation of a high amount of acyclovir (200 mg) to antiviral treatment. This hydrogel patch disclosed both good adhesion and stability due to nanocrystals properties, such as crystallinity and morphology. However, the amorphous structure of starch limited its effect as a plasticizer.[72] Moreover, the mixing of starch with other polymers decreased the drug amount embedded. In fact, Ling and Chen proposed a dissolving starch-based microneedles device conjugated with gelatin to delivery insulin, achieving only 2 mg of drug incorporation within the patch. Nevertheless, when compared to conventional treatments, a faster release and similar insulin plasma concentration were achieved, despite of the delayed drug effect.[73]

5.4.Pectin

Pectin and their derivatives are commonly used in hydrogel patches. Hadebe and colleagues have developed an amidated pectin hydrogel patch that allowed an efficient delivery of insulin (16.8 µg insulin/kg patch), used in diabetes treatment.[44] The hydrogel showed good stability and promoted prolong controlled insulin release. However, the non-availability of insulin-containing dermal patches into unit dosage was pointed as possible limitation in patient acceptance. The incorporation of higher amounts of drug was proposed by Mavondo and Tagumirwa that engineered a pectin-based hydrogel that allowed the inclusion of 5 mg asiatic acid (AA)/kg patch. Drug bioavailability was enhanced with higher drug flux *i.e.* great permeability. However, higher levels of drug can turn out to be toxic and exacerbate the disease.[69]

5.5.Hyaluronic acid

HA is a biopolymer commonly used in fabrication of hydrogel patches. It can also be combined with other polymers and be also applied for solid or dissolving microneedle device.[64,65] When compared with dissolving microneedles, solid ones demonstrated less capacity for drug incorporation within the patch. According to Witting and colleagues, only 23 µg of asparaginase (a model enzyme) were incorporated in a solid commercial microneedle device (1 cm^2) through the conjugation of HA with the enzyme. Although the enzymatic activity was maintained by months, microneedle insertion caused a slight skin irritation.[65] On the other hand, Mönkäre and co-workers reported that when HA with Immunoglobulin (IgG) was used in dissolving microneedles, a higher amount of drug was incorporated (10 mg). Skin reactions were also overcome with dissolving microneedles patches. Even though IgG showed no conformal changes or protein aggregates, the patch showed limited use in treatments that need continuous long-term release because of the faster microneedle dissolution. **Figure 2.5** elucidates the process of microneedles dissolution from the outermost layer to the inner one.[64]

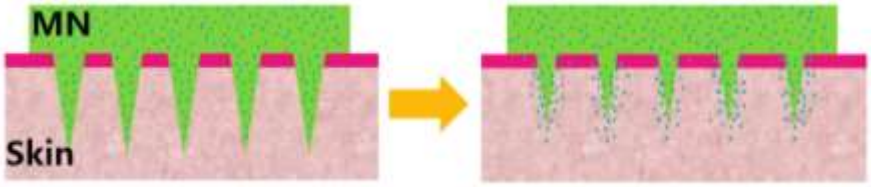

Figure 2.5. Schematic dissolution of microneedles, which sequentially dissolution from the outermost layer to the inner one.[75]

In order to improve both resistance and mechanical properties of dissolving microneedles patches, Liu and colleagues developed a HA microneedle patch reinforced with polyethylene terephthalate (PET) adhesive. This patch improved the permeability of high molecular weight drugs such as fluorescein isothiocyanate-labeled dextran, a common model molecule. However, low drug amount was incorporated (250 µg) and long-time dissolution of base plate (made of PET) was achieved, which results in waste generation. Skin irritation was another limitation promoted by this type of microneedle patch.[66]

HA has been approved by FDA to be use as dermal filler, becoming a polymer with high potential application to the fabrication of microneedle or another devices to skin insertion.

5.6.Natural Rubber

Natural rubber is known by its interesting features such as low cost, biocompatibility, high mechanical resistance, ease manipulation and film formation. However, some works reported allergic reactions induced by natural rubber. Suksaeree and colleagues have reported a methodology to solve such problematic that involves the use of deproteinised natural rubber (DNR).[67] Several studies focus on the development of efficient polymeric patches based on DNR to nicotine delivery, commonly used to smoking cessation. This material is used in the fabrication of matrix and reservoir-type patches.[67,68] Nicotine treatment requires the incorporation of high drug amount to support a continuous release. In the case of matrix patches, lower drug incorporation was achieved (2.5 $mg.cm^{-2}$). Patches with or without backing layer were tested and the addition of backing layer significantly increased the release of the drug.[67] Pichayakorn and co-workers developed a reservoir-type patch with the same material and drug, and a higher drug amount was incorporated (4.25 $mg.cm^{-2}$).[68] However, the impossibility of storage at high temperatures represents a major drawback for the use of this type of patch.

DNR could be blended with another polymers to improve their properties and allow the development of distinctive patches design.

5.7.Polycaprolactone

An efficient dissolving microneedle patch for the delivery of hydrophilic molecules was developed by Ko and colleagues through the combination of polycaprolactone (PCL) and poly(ethylene glycol) (PEG).[79] A model molecule like rhodamine was used and short-term transdermal delivery was achieved. The patch had the ability to incorporate 0.6 mg of drug, higher than most of previously referred patches. However, when hydrophilic molecules with high molecular weight were used, a slower release rate was achieved. Besides that, the patch allowed the permeability enhancement of hydrophilic molecules, commonly impermeable in SC. Other biodegradable aliphatic polyesters should be more explored in the future, as many biomedical products based on such polymers are already approved in the clinics.

6. Patches based on non-biodegradable polymers

Non-biodegradable materials are normally associated with a higher risk of skin irritation and their use is more limited when compared to natural polymers. In the case of solid microneedles patches, some materials can remain inside the skin promoting a set of adverse reactions. These non-dissolving microneedles generate waste that implies treatment to prevent the risk of disease dissemination. Besides their disadvantages, patches based on synthetic materials are commercially available and allow greater mechanical properties, such as mechanical resistance and non-degradation over time.[81] These materials are widely used in drug-in adhesive (DIA) and microneedles patches. DIA patches consist in the incorporation of a drug and possible additives in pressure sensitive adhesives (PSA) that is

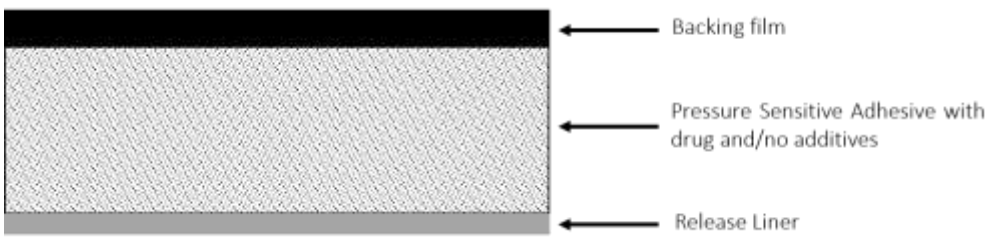

Figure 2.6. Schematic representation of DIA patches.

limited by a backing film and release liner (**Figure 2.6**). Three types of PSA have been used in transdermal patches such as polyisobutylenes (PBI), silicon and acrylics.[82]

6.1.Polyvinyl alcohol

PVA has been showing high potential in biomedical applications due to its rubbery elastic nature, non-toxicity, non-carcinogenicity and rapidly acceptance by the body.[74] The application of PVA in microneedles devices is limited as a result of the insufficient mechanical strength to puncture the SC and their low solubility, which reduces the drug release rate. One solution for this problem was proposed by Lau and colleagues, through the combination of silk fibroin with a PVA pedestal in a multi-layered microneedle patch. The flexible pedestal provided suitable skin adhesion and stress dispersion, while silk fibroin improved drug loading by increasing contact surface. A fast release of insulin (1.0 mg) was achieved with better regulation of the dissolution rate. Nevertheless, storing the patch at dry conditions may represent a limitation since it represents a costly expense.[75] Similarly, Chen and colleagues obtained a support structure through the association of PVA, polyvinylpyrrolidone (PVP) and a polyglycolide (PGA) hydrogel with insulin for the treatment of diabetes. This collective patch allowed an incorporation of 2.0 mg of insulin and enabled a full drug release with complete microneedles insertion. Besides hydrogel's degradation at low concentration, PGA also showed an important role in accelerating the wound healing process, induced by microneedles insertion.[76] Higher drug amount was incorporated in the patch with the combinations of chitosan-polyvinyl alcohol (CS-PVA) hydrogel cross-linked with Maleic anhydride. The drug permeability was enhanced with PVA content by increasing hydrogel swelling and pore formation. Although the incorporation of 10 mg of alprazolam offered a solution to the conventional treatments, by preventing their unwanted side effects, the drug flux was significantly low and not proportional to the entrapped drug amount.[77]

PVA can be also applied to polymeric patches. According to Kataria and colleagues, the combination of PVA with alginate allowed the fabrication of an efficient patch based on nanofibers with total entrapment of the drug within the nanofibers. The delivery of ciprofloxacin promoted a complete and fast wound healing, preventing from infection. The nanofibers were able to absorb exudates, adjusting to wound moisture through their extensive surface and microporous structure.[78]

Due their characteristics, PVA has been applied to the fabrication of distinct patches from the supporting structures of microneedles to hydrogels. In addition, PVA could be blended with another polymers to construct patches with ideal features.

6.2.Polyvinylpryrrolidone

Most treatments, such as the ones for cardiovascular diseases, have the need for simultaneous administration of multiple drugs. Quinn and colleagues reported a dissolving microneedle patch based on the combination of two biocompatible polymers, polyvinylpryrrolidone (PVP) and poly (methylvinylether/maleic acid).[80] This patch allowed the simultaneous delivery of aspirin, lisinopril dihydrate and atorvastatin calcium trihydrate, with rapid microneedles dissolution. Nevertheless, the patch showed some limitations such as poor delivery of hydrophobic drugs, skin irritation after patch's regular use and increased drug concentration after only 48 h, mainly due to water evaporation during the drying period of the patch.

6.3.Acrylic-based polymers

Acrylic and their derivatives are commonly used in commercial patches. One of most sold transdermal patches are contraceptive devices. A DIA patch with acrylic PSA was developed for the efficient delivery of ethynyl estradiol and levonorgestrel.[83] These hormones were applied to female contraceptive devices. Long-time release and great storage in a high range of temperatures, essential conditions to contraceptives patches, were successfully achieved. A set of commercial acrylic patches were used and the results showed that the higher drug release was achieve with an acrylic patch functionalized with hydroxyl group when compared to acrylic patches functionalized with carboxyl groups. Other recent studies support this conclusion. Jung and colleagues, for instance, reported a DIA patch based on acrylic PSA for fluoxetine delivery, commonly used for depression treatment and other psychological diseases.[84] Conventional treatments present several side effects mainly caused by variable plasma drug levels. In this work, a constant high amount of drug was applied to promote prolong release with constant plasma drug level. Drug flux was increased as the drug content also increased from 1% to 20 % (w/w). These acrylic patches functionalized with hydroxyl groups also presented a good storage capability while preventing drug crystallization. However, above 20% content, crystallization of the drug had

been observed. The transdermal patch developed by Xi and colleagues allowed an effective delivery of anastrozole (2 mg), a drug commonly used in breast cancer treatment.[85] However, this drug frequently lacks in specific targeting, being responsible by several damages to healthy tissues. The conjugation of anastrozole with DIA patches allowed the delivery of a high amount of drug in the site of action. Interestingly, non-functionalized acrylic patches showed a higher drug release, when compared to any functionalized ones, mainly due to the lack of interactions between the drug and the patch. Adverse skin reactions attributed to the residual adhesive, are the critical limitations of this type of patches. Additionally, some authors confirmed that acrylic patches with functional groups showed lower drug entrapment.[86,87] D-threo-methylphenidate (1.1 mg) was incorporated in a DIA patch for the treatment of deficit/hyperactivity disorder and although an efficient drug absorption into systemic circulation was achieved, drug plasma concentration was lower than the conventional oral route [87]. The high patient compliance and the non-invasive nature of these patches have been increasing the number of cases of dose dumping. Fentanyl, a drug commonly administrated to pain symptoms and with big interest in obtaining fast-on-set euphoria, was incorporated in a geopolymer, priory to its inclusion in acrylic patches, increasing its resistance to tamper, preventing its abuse without compromising the efficiency of drug delivery. This device allowed the effective delivery of a high amount of drug (149 mg) without compromising the security of these patches. The patches, however, did not show resistance to acidic nor ethanol solutions.[86]

Acrylic patches can also be applied in microneedles devices. The work developed by Guo and co-workers combined the properties of a hydrogel with the solid support of silicon microneedles.[88] This combination allowed the reduction of normal dose of hepatitis B antigen in hepatitis B treatment from 100 μg to 25 μg. The patch promoted higher antibody concentration by increasing skin permeability though the combination of hydrogel and solid microneedles. Nonetheless, the loss of antibody activity with increments of temperature limits the use of this device with sensitive macromolecules. A novel approach to stabilize such type of macromolecules was reported by Qiu and colleagues and consisted in the freeze drying of poly(acrylamide-co-acrylic acid), that enabled the maintenance of proteins stability as well as an easier handling and storage.[89] Such freeze dried patches, however, can only be used with high drug amount. When lower amount was applied, loss of drug activity was achieved. Nevertheless, this combination of an hydrogel patch and a microneedle device

resulting in a powerful device able to incorporate high amounts of insulin (150 mg), representing an effective treatment to diabetes.

Acrylic PSAs functionalized with different groups could have distinct effect on drug release through the variation of the three-dimensional network of the polymer chains.

6.4.Polyisobutylenes

Contraceptive devices based on the delivery of ethynyl estradiol and levonorgestrel were also reported by Schulz and colleagues, where acrylic PSA was changed to polyisobutylenes (PIB). Both devices allowed a long-time release and improved storage in a wide range of temperatures, which is a requisite for this type of applications. However, ethynyl estradiol and levonorgestrel are not soluble on PIB. To solve this problem, drug adsorbates were incorporated onto crospovidone into the PIB blends and an increase of drug release was achieved. Moreover, the drug flux was lower than the one in acrylic patches. The main explanation is the continuous binding of the drug to crospovidone particles (CPVP) due to the low solubility of the drug in the adhesive.[83]

PIB matrices with different molecular weight could vary the drug release, enabling the construction of different patches with sustained and controlled release.

6.5.Silicon

A silicon microneedles patch can incorporate higher drug amount than the silicon patch combined with an acrylic hydrogel proposed by Guo and co-workers,[88] previously mentioned. According to Pamornpathomkul and colleagues, a silicon microneedle patch is able to incorporate, 2.5 mg of fluorescein-isothiocyanate, a model molecule. The combination of solid microneedles with low-frequency sonophoresis allowed the enhancement of skin permeability. However, the extra equipment required also implies high costs for the final product.[90]

The mechanical resistance and great storage capability of silicon allow their application to the construction of robust patches devices.

Table 2.2. Current transdermal patches based on biodegradable and non-biodegradable polymers.

Patches	Active compound	Patch Size	Dose	Design	Advantages	Limitations	Application	Reference
Biodegradable Materials								
Cellulose								
Bacterial Cellulose	diclofenac	0.95cm^2	0.5-1%	Polymeric one layer	Homogenous flexible Adhere to irregular skin surfaces	Lower permeation Long time-release	Anti-inflammation	[58]
	lidocaine hydrochloride	0.95cm^2	2%	Polymeric one layer				[59]
	ibuprofen	0.95cm^2	1%					
Alginate chitosan nanoparticles (HPMC or HPC patches)	rabeprazole	1.76 cm^2	-	Hydrogel and cellulosic membrane	Enhancement of the drug entrapment and permeation.	Slow diffusion	Controls the gastric acid secretion	[60]
HA-hydroxyethyl cellulose	isoliquiritigenin	-	0.5 mM	Hydrogel and cellulosic membrane	Improvement of skin permeation	Lower drug penetration	Cancer treatment	[62]
HA and CMC	Anti-tumor-necrosis-factor-alpha	-	0.5 mg	Polymeric Dissolving microneedles	No inhibition of the binding affinity of anti-TNF-α-Abs Increased antibody residence time	Lower drug incorporation	Auto inflammatory skin diseases	[63]
HPMC and CMC	Donepezil hydrochloride	0.56 cm^2	179.9 µg	Polymeric Dissolving microneedle	More efficacy with same dose of drug Rapidly release	Necessity of applicator Low drug amount	Alzheimer's disease	[61]
Chitosan								
Silver hybridized porous chitosan-based	Rhodamine B	0.4 cm^2	500 µg/ml	Polymeric	Silver promoted increase of drug release and the hydrophilicity	Understand the silver interaction with chitosan to improve their bond strength	Model molecule	[49]
Chitosan and HA	lidocaine	8 cm^2	1 mg	Polymeric	Good storage over the time Improved the mechanical properties and drug retention	Mechanical variations of the patch over the time	Neuropathic pain	[47]

Chitosan	Bovine serum albumin (BSA)	-	0.15%	Microneedle	Encapsulation of fragile biomolecules without considerable exchange Long-time release	Reaming of microneedles fragments	Standard biomolecule	[91]
Chitosan	Glibenclamide (nanocrystals)	1 cm^2	125 mg	Polymeric	Chitosan decreases nanoparticles precipitation Improvement permeation via nanosizing Better patient compliance	Lower patch concentration	Diabetes	[92]
Chitosan with PHEA	levofloxacin	1 cm^2	5%	Hydrogel	PHEA enhances the flexibility Short time-release	Hydrogel degradation Limitation of drug concentration	Wound healing Antibacterial activity	[93]
Starch								
Starch nanocrystals	acyclovir	-	200 mg	Hydrogel	Good adhesion Better stability	Amorphous starch limited its plasticizer effect	Antiviral	[72]
Starch and gelatin	Insulin (biomolucule)	-	2 mg	Polymeric Dissolving microneedle	Quickly release Similar results to conventional routes Good insulin storage	Minimum plasma glucose level was achieved later than by insulin injection	Diabetes	[73]
Pectin								
Pectin	asiatic acid	4 mm^2	5mg/kg pectin	Hydrogel	Enhancement of Asiatic acid bioavailable	Higher levels of AA be toxic and exacerbate disease	Malaria prevention and treatment	[69]
Amidated pectin	insulin	-	9.57-16.80 µg/kg	Hydrogel	Prolong controlled insulin release Good hydrogel stability	Not available patches into unit dosage forms.	Diabetes	[44]
HA								
HA	asparaginase	1 cm^2	10-23 µg	Coated in solid microneedle	The protein activity was maintained for months	MN insertion caused a slight skin irritation	Vaccination	[65]
HA	IgG	-	2-10 mg	Polymeric Dissolving microneedle	Without antibody conformal changes No protein aggregates	Not allowed continuous delivery	Vaccination	[64]

HA and PET	fluorescein isothiocyanate-labeled dextran	250 µg 278 µgcm^{-2}	4 cm^2	Polymeric Dissolving microneedle	Improved permeability of high molecular weight drugs	Long-time release Skin irritation	Model molecule	[66]
Rubber								
Deproteinised natural rubber	nicotine	-	4.25 mgcm^{-2}	Polymeric Reservoir type	Rubber showed excellent properties	Variation on rubber properties Not be storage at high temperature	Cessation of smoking	[68]
		70.88 cm^2	2.5 mgcm^{-2}	Polymeric Matrix type	Slower release and skin permeation without backing layer	Lower drug concentration		[67]
PCL								
PCL/PEG	Rhodamine 6G	0.6 mg	0.91 mm^2	Polymer Microneedle	Short-term delivery of hydrophilic biomolecules	Slower release of high weigh molecules	Model molecule	[79]
Non Biodegradable Materials								
PVA								
Poly vinyl alcohol (PVA) and alginate nanofiber	ciprofloxacin	4 cm^2	35 mg/L	Polymeric	Entrapment to nanofibers of 100% of loaded drug	Gelation of alginate at low polymer concentrations Nanofibers degradation Long-time release	Wound healing	[78]
Maleic Anhydride Cross-Linked Chitosan-PVA	alprazolam	2.54 cm^2	10 mg	Hydrogel	Alprazolam permeability increased with PVA content Better compliance	Low drug flux	Anxiety and depression	[77]
Silk fibroin tips supported on PVA pedestal	Insulin	-	1 mg	Polymeric Multilayered dissolving microneedle	Storage ability at room temperature Better regulation of dissolution rate Rapidly release	Storage at dry condition	Diabetes	[75]
PGA and PVA/PVP	Insulin	-	2.0 mg	PGA Hydrogel in PVA/PVP support	Support structure allowed complete microneedles insertion PGA accelerate wound healing	Degradation at low hydrogel concentration	Diabetes	[76]

				Dissolving microneedle	No cold chain storage Quickly administration			
PVP								
PVP and PMVE/MA	aspirin lisinopril dihydrate atorvastatin calcium trihydrate	0.49 cm^2	5%	Polymeric Dissolving microneedle	Simultaneous administration of multiple drugs Rapid dissolution	Poor delivery of hydrophobic drugs drug concentration by water evaporation Regular use promoted skin reactions	Cardiovascular diseases	[80]
Maleic Anhydride Cross-Linked Chitosan-PVA	alprazolam	2.54 cm^2	10 mg	Hydrogel Polymeric Multilayered dissolving microneedle	Alprazolam permeability increased with PVA content Better compliance Storage ability at room temperature Better regulation of dissolution rate Rapidly release	Low drug flux Storage at dry condition	Anxiety and depression Diabetes	[77] [75]
Silk fibroin tips supported on PVA pedestal	Insulin	-	1 mg					
PGA and PVA/PVP	Insulin	-	2.0 mg	PGA Hydrogel in PVA/PVP support Dissolving microneedle	Support structure allowed complete microneedles insertion PGA accelerate wound healing No cold chain storage Quickly administration	Degradation at low hydrogel concentration	Diabetes	[76]
Acrylic and PIB								
Acrylic patches	anastrozole	1 cm^2	2 mg	Polymeric DIA Circular	Sustained and controlled permeation of the drug Local deposition (Reducing of systemic side effects)	Residual adhesive Functional groups in acrylic PSAs have effect on drug release	Breast cancer	[85]
Acrylic patches	fluoxetine	2.5 cm^2 and 100 cm^2	15 mg/kg (5%)	Polymeric DIA	Plasma concentration equal to oral delivery Long-time release Not variable plasma concentration	High drug concentration promotes crystallization	Serotonin reuptake inhibitor	[84]

Acrylic patch with geopolymer particles	Fentanyl	4.52 cm^2	149 mg	Polymeric	Resistance to tampering Plasma drug concentration was similar to commercial patches	Low resistance to acid pH and ethanol solution	Pain	[86]
Acrylic hydrogel and silicon	hepatitis B antigen	1 cm^2	25 µg	Hydrogel Microneedle	Increasing of permeation Better temperature tolerance Reduction of minimum dose	Loss of antibody activity in hydrogel patch at 37°C (45°C much higher lost)	Hepatitis B (Vaccination)	[88]
Lyophilized poly(acrylamide-co-acrylic acid)	Insulin	1 cm^2	150 mg	Hydrogel matrix Microneedle (pyramidal)	Lyophilized allow more stable proteins and easier handling and storage Possibility of high drug amount	Storage at low temperature Lower drug amount showed loss of insulin activity after lyophilisation	Diabetes	[89]
PCL/PEG	Rhodamine 6G	0.91 mm^2	0.6 mg	Polymeric Microneedle	Short-term delivery of hydrophilic biomolecules	Slower release of high weigh molecules	Model molecule	[79]
Silicon								
Silicon	fluorescein isothiocyanate	225 mm^2	2.5 mg	Polymeric Microneedle with sonophoresis	Enhancement of skin permeability Increase of drug flux	Requirement of equipment. Not easy applicability	Model molecule	[90]

7. Drug particles

Physical and chemical drug properties greatly impact their release. “Free” drug can be directly used in patch production or can be previous encapsulated into carrier systems at the nanoscale such as vesicles (e.g. liposomes), nanoparticles or nanofibers. Vesicles, for instance, allow the delivery of the entrapped molecules into or across the skin. The first papers to report on the effectiveness of vesicles for skin delivery were published in the early 1980. After this, a large set of carries have been developed to delivery different drugs. These carries serve as a rate-limiting membrane barrier for the modulation of systemic absorption, providing a controlled and sustained drug release.[94] Nanoparticles have become frequent drug delivery vehicles due to their high bioavailability, better encapsulation, control release and less toxic properties.[95] Particle size decreasing to the nanoscale is a well-established approach to enhance both drug absorption and solubility especially when dissolution rate is the limiting factor.[43] However, some polymeric carriers are associated to slow degradation and, therefore, prone to accumulate in the body.[96]

Ali and Hanafy report the use of nanocrystals to increase both drug permeation and flux across the skin by a factor of 1.7, when compared to the ‘free’ drug form. Features like bioavailibity, surface area and saturation solubility of the poor soluble drug was enhanced by size diminution.[92] Microparticles of alginate-raberprazole reinforced with chitosan also enhanced the drug entrapment and drug permeation in skin when compared with the assay using the non-encapsulated drug.[60] Another example was lidocaine, a poor water soluble drug, that was encapsulated in amine functionalized HA microparticles and applied to an efficient chitosan patch.[47] The enhancement of drug solubility through encapsulation in nano/microparticles was also reported in the PIB patch developed by Schulz and co-workers. Ethynyl estradiol and levonorgestrel were not soluble in PIB and their incorporation onto crospovidone particles circumvented this problem. These drug carries not only allowed the drug solubilisation in PIB but also increased drug release.[83]

At last, the use of drug carriers to increase both drug’s solubility and permeation, has been showing promising results in the enhancement of drug release.[94]

8. Hydrogels vs non-hydrogel polymeric patches

Hydrogel is a water-swollen, and cross-linked polymeric network produced by the simple reaction of one or more monomers.[97] Hydrogels have received high attention in the past 50 years, due to their exceptional promise in wide range of applications. [98] The first application of hydrogels in biomedical devices were performed in the 60s by Wichterle and Lím. [99] Hydrogels' highly valuable characteristics have been stimulating a growing research for a wide range of applications in the biomedical field: degradable nature, the ability to be injectable or pre-fabricated, the shape and surface, the openness of the pores, water content, chemical modifications with enhancement of drug attachment, the sterilizability and the possibility to add bioactive compounds.[100,101] Hydrogels based on natural, synthetic or combined polymers have been applied for cells encapsulation[102] and tissue engineering,[103,104]with an important role in repairing and regenerating tissues and drug delivery.[105] Hydrogels can be applied through different physical forms such as previous solid forms, microparticles, coatings, membranes and sheets. The last ones are known for their important role in transdermal drug delivery as reservoir in patches.

Hydrogels' application in drug delivery systems is related to its characteristics.[106] The high water content in a hydrogel limits nutrients' permeation into and out of the gel. It also allows the drugs' permeation enhancement reaching an equilibrium swelling level. The amount of water in the hydrogel determines both absorption and diffusion of the solutes through it. Also, drug release depends on the pore volume fraction, pores size and their interconnections, molecule size, and the type and strength of the interactions between the drug and the polymeric chains.[100] However, hydrogels also exhibit some limitations to their application. In most cases hydrogels can be hard to handle, since they are usually mechanical weak, difficult to sterilize and in some cases the loading of the drugs can be problematic in prefabricated matrix. The quantity and homogeneity of drug delivery may be limited, especially with hydrophobic drugs. Furthermore, common hydrogels with high water content and large pore size result in rapid drug release, which limits the applicability to sustained drug delivery.[107]

Polymeric patches were the first to reach the market by the introduction of the scopolamine patch.[19] These patches are mainly present in matrix systems, where polymers have important role and act as PSA which are capable of sticking to the skin by applying a light pressure and can be removed without leaving any visually noticeable residue. However,

ones can also be applied to engineer reservoir type patches.[108] Natural (e.g. cellulose, starch, chitosan) and synthetic polymers (e.g., PVA, PCL, PVP) have been widely used in different design patches. However, the ultimate product should remain stable in storage conditions over a long period.[97] Non-hydrogel polymeric patches often meet these needs. They show higher mechanical resistance, an easier handle and long storage time. In case of long-term treatments, stable patches are required, preserving patch properties along the treatment. This problem is also solved through non-hydrogel polymeric patches. The limitation of these patches is usually by the restriction of the drugs applied. Hydrogels show higher drug permeation, especially in case of molecules with high molecular weight or hydrophilic properties. Nonetheless, higher drug incorporation can result in drug crystallization.[109]

According to their properties, both hydrogels and polymeric patches can be used to engineer efficient transdermal patches. The choice of arrangement strongly depends on drug properties, the amount of drug needed and the required time of treatment.

9. Commercial patches

The desired new product must present a reasonable cost and meeting the unmet medical needs. The first transdermal patch was approved more than 30 years ago for the treatment of motion sickness. Approximately two dozen molecules have been approved for transdermal administration by the regulatory authorities to reach the market. Most of these drugs are for prescription use only, with many being available as generic patches following patent expirations.[110] **Table 2.3** summarizes these available drugs approved by Food and Drug Administration (FDA) and the main characteristics of these transdermal patches: indication, design, dose and patch size and duration of the application.

Although the vast number of patches in the market, scopolamine (hyoscine), nitroglycerine, clonidine, estradiol (with and without norethisterone or levonorgestrel), testosterone, fentanyl, nicotine and lidocaine are the most important patch drugs.[14]

Scopolamine patch was the first transdermal patch to reach the market and allowed the treatment of motion sickness. Until here, scopolamine had a short elimination half-time, expecting a short action duration. The finding of great scopolamine flux through human skin lead the development of a transdermal patch. In 1979, a patch with 2.5 cm^2 was incorporated with 1.5 mg of scopolamine, being until now the smallest patch on the market (Transderm

Scop®; Novartis Consumer Health). This patch not only provided significant effect against motion sickness but also showed few side effects.[110,111]

Until the marketing of the transdermal scopolamine patch, a nitroglycerin ointment was the only transdermal product in the market. Nitroglycerin is common used for angina pectoris and the ointment required frequent dosage. In 1981, nitroglycerin transdermal patches with different structures and dosages were introduced in the market, exhibiting treatment durability up to 12 h. Some years later, the addition of ethanol as a permeation enhancer increased the drug flux, turning this device into the most commercially consumed nitroglycerin patch throughout the market .[110,112]

Another example is clonidine, an efficient drug to hypertension. Transdermal clonidine was developed to reduce drug side effects of the previous treatments and improve patient compliance. In 1980, the first transdermal patch to hypertension therapy was developed and clonidine was the elected drug. The system contained a polyisobutene–clonidine reservoir and contact adhesive layer with a microporous membrane in-between that controlled the drug release rate. However, adverse reactions were observed leading to treatment discontinuation.[110,113]

One of the drugs that led higher number of patches was oestradiol. This drug is frequently used for post-menopausal replacement therapy and was first applied as a gel. This dosage form was messy and had difficult dosage control, which promoted the development of a transdermal patch in 1983. Oestradiol was administrated within a vehicle rich in ethanol, used as percutaneous absorption enhancer. In 1984 the patch reached the market with sufficient drug plasma level to meet the early follicular phase hormone levels. The new device allowed a reduction in the required daily dose, contributing to less side effects.[110,114]

The Alza fentanyl patch, marketed by Johnson & Johnson (J&J) as Duragesic®, has dominated the transdermal market with peak sales greater than $2 billion in 2004. As fentanyl is applied to pain treatment, long-term release is a major demand. In fact, fentanyl patch showed a drug release for at least 12 h and for up to 7 days. The patch ran into difficulties in 2006 with patent expiration and further studies revealed the likelihood of fentanyl leakage out the patch reservoir. As result of J&J's assertive marketing and patent protection, J&J patch sales surpassed $1.2 billion in 2006 and $900 million in 2009.[110,115]

Nicotine is another example of drug patches with commercial success with total sales approaching US $1 billion during their year of introduction. Over a million smokers gave up

smoking with the help of nicotine patches. One of this first systems consisted in an occlusive transdermal pad designed to be attached to the skin with a reservoir liquid nicotine base. The drug delivery was controlled with a microporous membrane with a duration of 30–45 min, thus requiring the application of several patches along the day. A subsequent patent disclosed a monolithic patch with a polyurethane matrix layer. This system solved the problem with nicotine delivery through skin over at least 24 h.[110,116]

Testosterone is another widely-used drug in commercial available transdermal patches to treat hypogonadism. Originally, testosterone was applied as a cream but skin-to-skin transfer of testosterone gel from parents to their young children or from males to their female sexual partners were testified, resulting in precocious puberty or pronounced virilisation. To avoid this, testosterone patches were designed to be applied to the highly permeable scrotal tissue. However, high serum testosterone levels after scrotal application were observed, which can be associated to detrimental effects on the prostate. A non-scrotal skin application overcame these difficulties.[110,117]

Table 2.3. Commercially available transdermal patches approved by the US FDA. Adapted from Pastore and colleagues-[110]

Drug	Trade name (year)	Indication	Patch design	Dose and patch size	Duration
Buprenorphine	Butrans®(2010)	Chronic pain	DIA	5 mg in 6.25 cm^2	7 days
Clonidine	Catapres-TTS®(1984)	Hypertension	Reservoir	2.5 mg in 3.5 cm^2	7 days
Oestradiol	Estraderm®(1986)	Female hormone replacement therapy (HRT)	Reservoir	24 mg in 10 cm^2	3-4 days
	Climara®(1994)		DIA	2 mg in 6.5 cm^2	7 days
	Vivelle®(1994)			4.33 mg in 14.5 cm^2	3-4 days
	Alora®(1996)			0.77 mg in 9 cm^2	3-4 days
	Vivelle-Dot®(1999)			0.39 mg in 2.5 cm^2	3-4 days
	Menostar®(2004)			1 mg in 3.25 cm^2	7 days

	Minivelle®(2012)			0.62 mg in 2.48 cm^2	3-4 days
	Evamist®(2007)		Cutaneous solution	1.53 mg per spray (90 µl)	One spray/ day
Oestradiol/Norethindrone	Combiptach®(1998)	Female HRT	DIA	0.62 mg/2.7mg in 9 cm^2	3-4 days
Ethinyl oestradiol/ Norethindrone	Ortho Evra®(2001)	Female contraception	DIA	0.75 mg/6mg in 20 cm^2	7 days
Oestradiol/Levonorgestrel	Climara Pro®(2003)	Female HRT	DIA	4.40mg/1.39mg in 22 cm^2	7 days
Fentanyl	Duragesic®(1990)	Chronic Pain	DIA	2.1 mg in 5.25 cm^2	72 h
Granisetron	Sancusi®(2008)	Chemotherapy	DIA	34.3 mg in 52 cm^2	Up to 7 days
Methylphenidate	Daytrana®(2006)	ADHD[1]	DIA	27.5 mg in 12.5 cm^2	Up to 9 h
Nitroglycerin	Nitro-Dur®(1995)	Angina pectoris	DIA	20 mg in 5cm^2	12-14 h
	Minitran®(1996)			9 mg in 3.3 cm^2	
Oxybutynin	Oxytrol®(2003)	Overactive bladder	DIA	36 mg in 39 cm^2	3-4 days
Rivastigmine	Exelon®(2007)	Alzheimer's Parkinson's	Matrix	9mg in 5 cm^2	24 h
Rotigtine	Neupro®(2007)	Parkinson's Restless legs syndrome	DIA	2.25 mg in 5 cm^2	24 h
Scopolamine	Transderm®(1981)	Motion sickness	DIA	1.5 mg in 2.5 cm^2	72 h
Selegiline	Emsm®(2006)	Depressive disorder	Reservoir	20 mg in 20 cm^2	24 h
Testosterone	Androderm® (1995)	Hypogonadism	Reservoir	9.7 mg in 32 cm^2	24 h
	Axiron®(2010)		Cutaneous solution	30 mg per pump actuation	2 pump actions per day
Nicotine	Habitrol®(1990)	Smoking cessation	Matrix	17.5 mg in 10 cm^2	24 h
	Nicoderm®(1991)		Reservoir	36 mg in 7 cm^2	24 h

	Nicorette®		Matrix	8.3 mg in 10 cm^2	16 h
	Nicorette®		Matrix	15.75 mg in 9 cm^2	16 h
Sumatripan	Zecuity®(2013)	Migraine	Iontophoretic system	36 mg in 7 cm^2	4 h
Capsaicin	Qutenza®(2009)	Neuropathic pain	DIA	179 mg in 280 cm^2	60 min of up to 4 patches
Diclofenac epolamine	Flector®(2007)	Acute pain	DIA	180 mg in 140 cm^2	12 h
Lidocaine	Lidoderm®(1999)	Post-herpetic neuralgia pain	DIA	700 mg in 140 cm^2	Only once for up to 12h
Lidocaine/Tetracaine	Synera®(2005)	Local analgesia	Eutetic mixture-CHADD®	70 mg/70mg in 50 cm^2	20-30 min
Menthol/Methysalicylate	Salonpas®(2008)	Muscles and joints pain	DIA	3%/10% in 70 cm^2	Up to 8-12 h

[1] Attention deficit hyperactivity disorder (ADHD)

10.Clinical Trials

Currently there are 2060 ongoing clinical trials regarding the use of patches for skin disorders. Still, only 7 represent systems of higher complexity composed of patches with drug particles embedded. Such arrangements are expected to exhibit enhanced performance concerning the storage and consequent release of drug.[94,118] **Table 2.4** displays the main information with regards to these ongoing clinical trials. Bio-medical Carbon Technology (BCT), an antimicrobial dressing invented by Bio-medical Carbon Technology Co., Ltd., particularly consists of activated carbon fibers impregnated with silver particles. One of the clinical trials is based on the investigation of wound healing effects of BCT antimicrobial dressing on deep dermal burn.[119] BCT silver bandage is also evaluated in another clinical trial to achieve its efficacy and safety in obstetrical and gynecological surgical wound healing, being compared to Aquacel® Ag, a commercial dressing.[120] TulleGras M.S (vaseline gauze) and Urgotul (low-adherent dressing) have been experienced on surgical acute wounds, demonstrated both suitable healing rates as well as painless dressing removal.[121] HIV infection is a condition that promoted the development of 3 of the 7 ongoing clinical trials. DermaVir is a synthetic nanomedicine whose active ingredient is a

single plasmid DNA expressing 15 HIV proteins that assemble to HIV-like particles. DermaVir is topically administered to target the nanomedicine to Langerhans cells. These cells migrate to the lymph nodes to induce cytotoxic T- cells that can kill HIV-infected cells. This patch is applied in all ongoing clinical trials related to HIV infection. Safety, tolerability, immunogenicity, and preliminary antiretroviral activity are the main parameters under investigation in these studies.[122–124]

Table 2.4. Clinical trials using patches with drug particles for a wide variety of disorders/diseases.

Clinical Trial	Condition	Drug/ Device	Sponsor	Phase	Status
To Study the Healing Effect of Silver Impregnated Activated Carbon Fiber Wound Dressing on Deep Dermal Burn (clinicaltrials.gov2014)	Burns	Activated carbon fiber impregnated with silver particles	Bio-medical Carbon Technology Co., Ltd.	**N.A.**	Completed
Comparison of Efficacy on Healing, and Safety of Two Dressings Urgotul and TulleGras MS on Surgical Acute Wounds (clinicaltrials.gov2016)	Surgical Acute Wounds	Urgotul: Low-adherent dressing and TulleGras M.S.: Vaseline gauze	Mylan Inc.	Phase 4	Completed
A Comparative Efficacy and Safety Study Between Two Silver Containing Dressings In Post-Op Wound Healing (clinicaltrials.gov2014)	Surgical Wound	BCT Silver Bandage and Aquacel® Ag. Dressing	Bio-medical Carbon Technology Co., Ltd**.**	**N.A**	Terminated
Antiretroviral-Sparing Concept With HIV-specific T Cell Precursors With High Proliferative Capacity (PHPC) (PHPC-02) (clinicaltrials.gov2013)	HIV Infection	DermaVir	Genetic Immunity	Phase 2	Completed
Single DermaVir Immunization in HIV-1 Infected Patients on HAART (GIHU004) (clinicaltrials.gov2013)	HIV Infection	DermaVir	Genetic Immunity	Phase 1	Completed
Repeated DermaVir Immunizations in HIV-1 Infected Treatment-naïve Patients (GIEU006) (clinicaltrials.gov2013)	HIV Infection	DermaVir	Genetic Immunity	Phase 2	Active, not recruiting
Midlife Cholesterol Study (clinicaltrials.gov2014)	Menopause Postmenopause Premenopause Cardiovascular Disease	Tansdermal estradiol patch	Northwester University	Phase 4	Completed

N.A. – not available

An estrogen patch in another example involved in a trial. The postmenopausal state is associated with increased risk of heart diseases due to the loss of estrogen and this subsequent effect in lipids loss. This condition is often treated by estrogen replacement

therapy, having a beneficial effect on lipid levels. The purpose of this research study is to understand how menopause affects lipids and how hormone replacement therapy effects the lipid metabolism of postmenopausal women. A transdermal estradiol patch is here applied to estrogen replacement.[125]

11.Final Remarks

The development of new and effective DDS has been greatly improving treatments efficacy, solving problems commonly associated with the use of conventional “free” drugs. Their administration through transdermal route has been attracting considerable attention due to its numerous advantages, such as less frequent, painless and flexible dosing, as it also generates less amount of dangerous waste. These factors have been stimulating the research and development of transdermal DDS to effective deliver therapeutic molecules to skin targets.

Patches are the most common used transdermal DDS, mostly due to their simple design, application and low production cost. In order to solve the limitations associated with these passive transdermal DDS, higher drug concentration must be applied to improve transcutaneous fluxes. Biodegradable or non-biodegradable polymers have been exploited to engineer robust devices able to deliver accurate amounts of drugs during a prolonged period of time with minimal side effects by different types of patches. The combination of drug particles with patches also enables the development of more efficient systems. Both drug permeation and drug flux across the skin membranes are increased through particle size diminution to micro and nano scales, increasing their bioavailability, surface area and solubility.

Even though different types of patches have been engineered for the last five decades, there is still a need for the development of systems able to retain and release high amounts of drug in a sustained or controlled form. These devices are of major importance in order to deliver specific amounts of drugs in prolonged treatments of particular diseases. We hypothesise that more efforts should be made in the development of patches incorporating micro and/or nanoparticles and/or fabrication of drug carries. From all the aforementioned patches, non-biodegradable ones are able to incorporate larger amount of drugs, being a potential solution to treat cutaneous wounds needing prolonged treatments. Polymeric patches showed to solve hydrogels limitations, being easy to handle with higher mechanical

resistance and great storage over the time. However, when compared to hydrogels, lower drug permeation was achieved, especially with hydrophilic drug molecules or with higher molecular weight (> 500Da).

Although major achievements have been attained in the development of more sophiscated patches, some limitations still need to be overcome. Particularly, physicochemical properties of drug continue to play an important role in its transport through the skin layers and low transcutaneous flux, drug incorporation and retention in the patch still limited their application.

Further research should be developed in order to attain a patches with ideal features from the simplest to most complex hierarchical patches with stimuli- and multiple-release of a large pool of drugs.

12.References

1. Allen, T. M., Cullis, P. R. Drug Delivery Systems: Entering the Mainstream. *Science.* **303,** 1818-1821 (2004).
2. Prausnitz, M. R., Mitragotri, S., Langer, R. Current status and future potential of transdermal drug delivery. *Nat. Rev. Drug Discov.* **3,** 115–124 (2004).
3. Wiedersberg, S., Guy, R. H. Transdermal drug delivery: 30 years of war and still fighting! *J. Control. Release* **190,** 150–156 (2014).
4. Naik, A., Kalia, Y. N., Guy, R. H. Transdermal drug delivery: overcoming the skin's barrier function. *Pharm. Sci. Technolo. Today* **3,** 318–326 (2000).
5. Guy, R. H. Transdermal Drug Delivery. *Drug Delivery.* **197,** 399–410 (2010).
6. Prausnitz, M. R., Langer, R. Transdermal drug delivery. *Nat. Biotechnol.* **26,** 1261–1268 (2008).
7. Lukyanov, A. N., Torchilin, V. P. Micelles from lipid derivatives of water-soluble polymers as delivery systems for poorly soluble drugs. *Adv. Drug Deliv. Rev.* **56,** 1273–1289 (2004).
8. Qiu, Y., Park, K. Environment-sensitive hydrogels for drug delivery. *Adv. Drug Deliv. Rev.* **53,** 321–339 (2001).
9. Jain, S. K., Chourasia, M. K. Pharmaceutical approaches to colon targeted drug delivery systems. *J Pharm Pharm. Sci.* **6,** 33–6633 (2003).
10. Han, H.-K., Amidon, G. L. Targeted prodrug design to optimize drug delivery. *The AAPS Journal.* **2,** 48–58 (2000).
11. Takakura, Y., Hashida, M. Macromolecular Carrier Systems for Targeted Drug Delivery: Pharmacokinetic Considerations on Biodistribution. *Pharm. Res.* **13,** 820–831 (1996).
12. Berlin C.M., J. *et al.* Alternative routes of drug administration--advantages and disadvantages (subject review). American Academy of Pediatrics. Committee on Drugs. *Pediatrics.* **100,** 143–52 (1997).
13. Tanner, T., Marks, R. Delivering drugs by the transdermal route: review and comment. *Ski. Res. Technol.* **14,** 249–260 (2008).

14. Barry, B. Novel mechanisms and devices to enable successful transdermal drug delivery. *Eur. J. Pharm. Sci.* **14,** 101–114 (2001).
15. Wokovich, A. *et al.* Transdermal drug delivery system (TDDS) adhesion as a critical safety, efficacy and quality attribute. *Eur. J. Pharm. Biopharm.* **64,** 1–8 (2006).
16. Biradar, D. D. & Sanghavi, N. Technologies in Transdermal Drug Delivery System: A Review. *Small.* **6,** (2014).
17. Tanner, T. & Marks, R. Delivering drugs by the transdermal route: review and comment. *Ski. Res. Technol.* **14,** 249–260 (2008).
18. Suedee, R. *et al.* Development of a reservoir-type transdermal enantioselective-controlled delivery system for racemic propranolol using a molecularly imprinted polymer composite membrane. *J. Control. Release* **129,** 170–178 (2008).
19. Yutaka Konno *et al* Patch. (1985). US 4879119 A.
20. Brown, M. B. *et al.* Dermal and Transdermal Drug Delivery Systems: Current and Future Prospects. *Drug Deliv.* **13,** 175–187 (2006).
21. Christophers, E. Cellular Architecture of the Stratum Corneum. *J. Invest. Dermatol.* **56,** 165–169 (1971).
22. Elias, P. M. Lipids and the epidermal permeability barrier. *Arch. Dermatol. Res.* **270,** 95–117 (1981).
23. Golden, G. M., McKie, J. E., Potts, R. O. Role of Stratum Corneum Lipid Fluidity in Transdermal Drug Flux. *J. Pharm. Sci.* **76,** 25–28 (1987).
24. Lipinski, C. A. Drug-like properties and the causes of poor solubility and poor permeability. *J. Pharmacol. Toxicol. Methods* **44,** 235–249 (2000).
25. Prausnitz, M. R. *et al*. Electroporation of mammalian skin: A mechanism to enhance transdermal drug delivery. *Med. Sci.* **90,** 10504–10508 (1993).
26. Lashmar, U. T., Hadgraft, J., Thomas, N. Topical Application of Penetration Enhancers to the Skin of Nude Mice: a Histopathological Study. *J. Pharm. Pharmacol.* **41,** 118–121 (1989).
27. Pathan, I. B., Setty, M. Chemical Penetration Enhancers for Transdermal Drug Delivery Systems. *Trop. J. Pharm. Res. Ina. Setty Trop J Pharm Res* **8,** 173–173 (2009).
28. Moser, K. *et al.* Passive skin penetration enhancement and its quantification in vitro. *Eur. J. Pharm. Biopharm.* **52,** 103–112 (2001).
29. Elsayed, M. M. A., Abdallah, O. Y., Naggar, V. F. & Khalafallah, N. M. Lipid vesicles for skin delivery of drugs: Reviewing three decades of research. *Int. J. Pharm.* **332,** 1–16 (2007).
30. Tyle, P. lontophoretic Devices for Drug Delivery. *Pharm. Res.* **3,** 318–326 (1986).
31. Mitragotri, S., Blankshtein, D., Langer, R. Ultrasound-mediated transdermal protein delivery. *Science* **269,** 850 (1995).
32. Jacques, S. L. *et al*. Controlled Removal of Human Stratum Corneum by Pulsed Laser. *J. Invest. Dermatol.* **88,** 88–93 (1987).
33. Sintov, A. C. *et al.* Radiofrequency-driven skin microchanneling as a new way for electrically assisted transdermal delivery of hydrophilic drugs. *J. Control. Release.* **89,** 311–320 (2003).
34. Henry, S. *et al.* Microfabricated Microneedles: A Novel Approach to Transdermal Drug Delivery. *J. Pharm. Sci.* **87,** 922–925 (1998).
35. Prausnitz, M. R. Microneedles for transdermal drug delivery. *Adv. Drug Deliv. Rev.* **56,** 581–587 (2004).
36. Gill, H. S. *et al.* Selective removal of stratum corneum by microdermabrasion to

increase skin permeability. *Eur. J. Pharm. Sci.* **38,** 95–103 (2009).
37. Treffel, P. *et al.* Effect of pressure on in vitro percutaneous absorption of caffeine. *Acta Derm. Venereol.* **73,** 200–2 (1993).
38. Murthy, S. N., Sammeta, S. M., Bowers, C. Magnetophoresis for enhancing transdermal drug delivery: Mechanistic studies and patch design. *J. Control. Release* **148,** 197–203 (2010).
39. Park, J.-H. *et al.* The effect of heat on skin permeability. *Int. J. Pharm.* **359,** 94–103 (2008).
40. Prausnitz, M. R., Langer, R. Transdermal drug delivery. *Nat. Biotechnol.* **26,** 1261–1268 (2008).
41. Nair, L. S., Laurencin, C. T. Biodegradable polymers as biomaterials. *Prog. Polym. Sci.* **32,** 762–798 (2007).
42. Ammar, H. *et al.*. Design and Evaluation of Chitosan Films for Transdermal Delivery of Glimepiride. *Curr. Drug Deliv.* **5,** 290–298 (2008).
43. Sigfridsson, K. *et al.* J. A formulation comparison, using a solution and different nanosuspensions of a poorly soluble compound. *Eur. J. Pharm. Biopharm.* **67,** 540–547 (2007).
44. Hadebe, S. I., Ngubane, P. S., Serumula, M. R. & Musabayane, C. T. Transdermal Delivery of Insulin by Amidated Pectin Hydrogel Matrix Patch in Streptozotocin-Induced Diabetic Rats: Effects on Some Selected Metabolic Parameters. *Plos One* **9,** (2014).
45. Lamounier-Zepter, V., Ehrhart-Bornstein, M. Insulin resistance in hypertension and cardiovascular disease. *Best Pract. Res. Clin. Endocrinol. Metab.* **20,** 355-367 (2006).
46. Mason, T., Chan, B., El-Bahrani, B., Goh, T. & Gupta, N. The effect of chronic insulin delivery via the intraperitoneal versus the subcutaneous route on hepatic triglyceride secretion rate in streptozotocin diabetic rats. *Atherosclerosis.* **161,** 345-352 (2002).
47. Anirudhan, T. S., Nair, S. S., Nair, A. S. Fabrication of a bioadhesive transdermal device from chitosan and hyaluronic acid for the controlled release of lidocaine. *Carbohydr. Polym.* **152,** 687–698 (2016).
48. Siafaka, P. I. *et al*. Porous dressings of modified chitosan with poly(2-hydroxyethyl acrylate) for topical wound delivery of levofloxacin. *Carbohydr. Polym.* **143,** 90–99 (2016).
49. Hye Kim, J. *et al*. Simple fabrication of silver hybridized porous chitosan-based patch for transdermal drug-delivery system. *Materials Letters* **95,** 48-51 (2013).
50. Lee, J. W., Park, J.-H., Prausnitz, M. R. Dissolving microneedles for transdermal drug delivery. *Biomaterials* **29,** 2113–2124 (2008).
51. Chen, M.-C. *et al.*. Chitosan Microneedle Patches for Sustained Transdermal Delivery of Macromolecules. *Biomacromolecules* **13,** 4022–4031 (2012).
52. Jie Wang, J. *et al.* Recent-advances-of-chitosan-nanoparticles-as-drug-carriers. *Int. J. Nanomedicine* **6,** 765–774 (2011).
53. Moura, D. *et al.* High performance free-standing films by layer-by-layer assembly of graphene flakes and ribbons with natural polymers. *J. Mater. Chem. B* **4,** 7718–7730 (2016).
54. Luz, G. M., Mano, J. F. Preparation and characterization of bioactive glass nanoparticles prepared by sol–gel for biomedical applications. *Nanotechnology* **22,** 1-11 (2011).
55. Martins, N. I. *et al.* Multilayered membranes with tuned well arrays to be used as regenerative patches. *Acta Biomater.* **57,** 313–323 (2017).

56. Sousa, M. P., Cleymand, F. & Mano, J. F. Elastic chitosan/chondroitin sulfate multilayer membranes. *Biomed. Mater.* **11,** 35008 (2016).
57. Wojciech K. Czaja *et al*. The Future Prospects of Microbial Cellulose in Biomedical Applications. *Biomaterials.* ***8,*** 1-12 (2006).
58. Silva, N. H. C. S. *et al.* Bacterial cellulose membranes as transdermal delivery systems for diclofenac: In vitro dissolution and permeation studies. *Carbohydr. Polym.* **106,** 264–269 (2014).
59. Trovatti, E. *et al.* Bacterial cellulose membranes applied in topical and transdermal delivery of lidocaine hydrochloride and ibuprofen: In vitro diffusion studies. *Int. J. Pharm.* **435,** 83–87 (2012).
60. Ahmed, T. A., El-Say, K. M. Development of alginate-reinforced chitosan nanoparticles utilizing W/O nanoemulsification/internal crosslinking technique for transdermal delivery of rabeprazole. *Life Sci.* **110,** 35–43 (2014).
61. Kim, J.-Y. *et al.* Tip-loaded dissolving microneedles for transdermal delivery of donepezil hydrochloride for treatment of Alzheimer's disease. *Eur. J. Pharm. Biopharm.* **105,** 148–155 (2016).
62. Kong, B. J., Kim, A., Park, S. N. Properties and in vitro drug release of hyaluronic acid-hydroxyethyl cellulose hydrogels for transdermal delivery of isoliquiritigenin. *Carbohydr. Polym.* **147,** 473–481 (2016).
63. Korkmaz, E. *et al.* Tip-Loaded Dissolvable Microneedle Arrays Effectively Deliver Polymer-Conjugated Antibody Inhibitors of Tumor-Necrosis-Factor-Alpha Into Human Skin. *Journal of Pharmaceutical Sciences* **105,** 3453-3457. (2016).
64. Mönkäre, J. *et al.* IgG-loaded hyaluronan-based dissolving microneedles for intradermal protein delivery. *J. Control. Release.* **218,** 53–62 (2015).
65. Witting, M. *et al*. Feasibility study for intraepidermal delivery of proteins using a solid microneedle array. *Int. J. Pharm.* **486,** 52–58 (2015).
66. Liu, S. *et al.* Transdermal delivery of relatively high molecular weight drugs using novel self-dissolving microneedle arrays fabricated from hyaluronic acid and their characteristics and safety after application to the skin. *Eur. J. Pharm. Biopharm.* **86,** 267–276 (2014).
67. Suksaeree, J. *et al.* Characterization, in vitro release and permeation studies of nicotine transdermal patches prepared from deproteinized natural rubber latex blends. *Chem. Eng. Res. Des.* **90,** 906–914 (2012).
68. Pichayakorn, W. *et al.* Deproteinised natural rubber used as a controlling layer membrane in reservoir-type nicotine transdermal patches. *Chem. Eng. Res. Des.* **91,** 520–529 (2013).
69. Alfrd Mavondo, G. A., Tagumirwa, M. C. Asiatic acid-pectin hydrogel matrix patch transdermal delivery system influences parasitaemia suppression and inflammation reduction in *P. berghei* murine malaria infected Sprague-Dawley rats. *Asian Pac. J. Trop. Med.* ***9,*** 1172-1180 (2016).
70. Eui-Jun Choi *et al*. Synthesis and Characterization of Starch-g-Polycaprolactone Copolymer. *Macromolecules.* **32,** 7402-7408 (1999).
71. Demirgöz, D. *et al.* Chemical modification of starch based biodegradable polymeric blends: effects on water uptake, degradation behaviour and mechanical properties. *Polym. Degrad. Stab.* **70,** 161–170 (2000).
72. Bakrudeen, H. B., Sudarvizhi, C., Reddy, B. S. R. Starch nanocrystals based hydrogel: Construction, characterizations and transdermal application. *Mater. Sci. Eng. C* **68,** 880–889 (2016).

73. Ling, M.-H., Chen, M.-C. Dissolving polymer microneedle patches for rapid and efficient transdermal delivery of insulin to diabetic rats. *Acta Biomater.* **9,** 8952–8961 (2013).
74. Hassan, C. M., Peppas, N. A. Biopolymers · PVA Hydrogels, Anionic Polymerisation Nanocomposites. 37–65 (Springer Berlin Heidelberg, 2000).
75. Lau, S. *et al.*. Multilayered pyramidal dissolving microneedle patches with flexible pedestals for improving effective drug delivery. *J. Control. Release* (2016).
76. Chen, M.-C., Ling, M.-H., Kusuma, S. J. Poly-γ-glutamic acid microneedles with a supporting structure design as a potential tool for transdermal delivery of insulin. *Acta Biomater.* **24,** 106–116 (2015).
77. Maji, P. *et al.* Preparation and Characterization of Maleic Anhydride Cross-Linked Chitosan-Polyvinyl Alcohol Hydrogel Matrix Transdermal Patch. *J. PharmaSciTech* **2,** 62–67 (2013).
78. Kataria, K. *et al. In vivo* wound healing performance of drug loaded electrospun composite nanofibers transdermal patch. *Int. J. Pharm.* **469,** 102–110 (2014).
79. Ko, P.-T. *et al.* Polymer microneedles fabricated from PCL and PCL/PEG blends for transdermal delivery of hydrophilic compounds. *J. Taiwan Inst. Chem. Eng.* **51,** 1–8 (2015).
80. Quinn, H. L. *et al*. Design of a Dissolving Microneedle Platform for Transdermal Delivery of a Fixed-Dose Combination of Cardiovascular Drugs. *J. Pharm. Sci.* **104,** 3490–3500 (2015).
81. Donnelly, R. F. *et al.* Microneedle-Mediated Transdermal and Intradermal Drug Delivery 113–151 (John Wiley & Sons, 2012).
82. Tan, H. S., Pfister, W. R. Pressure-sensitive adhesives for transdermal drug delivery systems. *Pharm. Sci. Technolo. Today* **2,** 60–69 (1999).
83. Schulz, M., Fussnegger, B., Bodmeier, R. Drug release and adhesive properties of crospovidone-containing matrix patches based on polyisobutene and acrylic adhesives. *Eur. J. Pharm. Sci.* **41,** 675–684 (2010).
84. Jung, E. *et al.* Development of drug-in-adhesive patch formulations for transdermal delivery of fluoxetine: *In vitro* and *in vivo* evaluations. *Int. J. Pharm.* **487,** 49–55 (2015).
85. Xi, H. *et al.* Transdermal patches for site-specific delivery of anastrozole: *In vitro* and local tissue disposition evaluation. *Int. J. Pharm.* **391,** 73–78 (2010).
86. Cai, B., Engqvist, H., Bredenberg, S. Development and evaluation of a tampering resistant transdermal fentanyl patch. *Int. J. Pharm.* **488,** 102–107 (2015).
87. Zhang, C. *et al.* Transdermal patches for D-threo-methylphenidate (free base): Formulation aspects and in vivo pharmacokinetics. *J. Drug Deliv. Sci. Technol.* **35,** 50–57 (2016).
88. Guo, L. *et al.* Effective transcutaneous immunization against hepatitis B virus by a combined approach of hydrogel patch formulation and microneedle arrays. *Biomed. Microdevices* **15,** 1077–1085 (2013).
89. Qiu, Y. *et al.* Novel lyophilized hydrogel patches for convenient and effective administration of microneedle-mediated insulin delivery. *Int. J. Pharm.* **437,** 51–56 (2012).
90. Pamornpathomkul, B. *et al.* Transdermal delivery of fluorescein isothiocyanate-dextrans using the combination of microneedles and low-frequency sonophoresis. *Asian J. Pharm. Sci.* **10,** 415–424 (2015).
91. Chen, M.-C. *et al.* Chitosan Microneedle Patches for Sustained Transdermal Delivery

of Macromolecules. *Biomacromolecules* **13,** 4022–4031 (2012).
92. Ali, H. S. M. & Hanafy, A. F. Glibenclamide Nanocrystals in a Biodegradable Chitosan Patch for Transdermal Delivery: Engineering, Formulation, and Evaluation. *J. Pharm. Sci.* 1–9 (2016). doi:10.1016/j.xphs.2016.10.010
93. Siafaka, P. I., Zisi, A. P., Exindari, M. K., Karantas, I. D. & Bikiaris, D. N. Porous dressings of modified chitosan with poly(2-hydroxyethyl acrylate) for topical wound delivery of levofloxacin. *Carbohydr. Polym.* **143,** 90–99 (2016).
94. Honeywell-Nguyen, P. L., Bouwstra, J. A. Vesicles as a tool for transdermal and dermal delivery. *Drug Discov. Today Technol.* **2,** 67–74 (2005).
95. Kumari, A., Yadav, S. K., Yadav, S. C. Biodegradable polymeric nanoparticles based drug delivery systems. *Colloids Surfaces B Biointerfaces* **75,** 1–18 (2010).
96. Luten, J. *et al.* Biodegradable polymers as non-viral carriers for plasmid DNA delivery. *J. Control. Release* **126,** 97–110 (2008).
97. Islam, J. *et al.* Exploration of ethyl anthranilate-loaded monolithic matrix-type prophylactic polymeric patch. *J. Food Drug Anal.* **25,** 968-975 (2016).
98. Ahmed, E. M. Hydrogel: Preparation, characterization, and applications: A review. *J. Adv. Res.* **6,** 105–121 (2015).
99. Wichterle, O., Lím, D. Hydrophilic Gels for Biological Use. *Nature* **185,** 117–118 (1960).
100. Hoffman, A. S. Hydrogels for biomedical applications. *Adv. Drug Deliv. Rev.* **64,** 18–23 (2012).
101. Costa, A. M., Mano, J. F. Extremely strong and tough hydrogels as prospective candidates for tissue repair – A review. *Eur. Polym. J.* **72,** 344–364 (2015).
102. Li, R. H., Altreuter, D. H., Gentile, F. T. Transport characterization of hydrogel matrices for cell encapsulation. *Biotechnol. Bioeng.* **50,** 365–373 (1996).
103. Lee, K. Y., Mooney, D. J. Hydrogels for Tissue Engineering. *Chem. Rev.* **101,** (2001).
104. Lima, A. C., Sher, P., Mano, J. F. Production methodologies of polymeric and hydrogel particles for drug delivery applications. *Expert Opin. Drug Deliv.* **9,** 231–248 (2012).
105. Peppas, N. A. Hydrogels and drug delivery. *Curr. Opin. Colloid Interface Sci.* **2,** 531–537 (1997).
106. Ulbrich, K. *et al.* Synthesis of novel hydrolytically degradable hydrogels for controlled drug release. *J. Control. Release* **34,** 155–165 (1995).
107. Hoare, T. R. & Kohane, D. S. Hydrogels in drug delivery: Progress and challenges. *Polymer.* **49,** 1993–2007 (2008).
108. Pichayakorn, W. *et al.* Nicotine transdermal patches using polymeric natural rubber as the matrix controlling system: Effect of polymer and plasticizer blends. *J. Memb. Sci.* **411,** 81–90 (2012).
109. Kandavilli, S., Nair, V., Panchagnula, R. Polymers in Transdermal Drug Delivery Systems. *Pharm. Technol.* **26,** 62–81 (2002).
110. Pastore, M., Kalia, Y., Horstmann, M. Transdermal patches: history, development and pharmacology. *Br. J.* (2015).
111. Price, N. M. *et al.* Transdermal scopolamine in the prevention of motion sickness at sea. *Clin. Pharmacol. Ther.* **29,** 414–419 (1981).
112. Steven Sablotsky, John M. Questel, J. A. T. Adhesive transdermal dosage layer. (1991). US 5186938 A.
113. David J. Enscore, R. M. G. Matrix composition for transdermal therapeutic system. (1983). US 4559222 A.

114. Good, W. R. *et al*. A new transdermal delivery system for estradiol. *J. Control. Release* **2,** 89–97 (1985).
115. Gale RM, Goetz V, Lee ES, Taskovich LT, Y. S. Transdermal administration of fentanyl and device therefor. (1984). US 4588580 A.
116. Richard W. Baker, Frank Kochinke, C. H. Novel transdermal nicotine patch. (1987). US 4839174 A.
117. Charles D. Ebert, Dinesh Patel, W. H. Method and device for transdermally administering testosterone across nonscrotal skin at therapeutically effective levels. (1991). US 5152997 A.
118. LaVan, D. A., McGuire, T., Langer, R. Small-scale systems for in vivo drug delivery. *Nat. Biotechnol.* **21,** 1184–1191 (2003).
119. ClinicalTrials.gov. To Study the Healing Effect of Silver Impregnated Activated Carbon Fiber Wound Dressing on Deep Dermal Burn. (2014). Available at: https://clinicaltrials.gov/ct2/show/record/NCT01598493?term=dressing+%2B+drug+particle+%2B+skin&rank=1. (Accessed: 23rd January 2017)
120. ClinicalTrials.gov. A Comparative Efficacy and Safety Study Between Two Silver Containing Dressings In Post-Op Wound Healing. (2014). Available at: https://clinicaltrials.gov/ct2/show/NCT01605968?term=dressing+%2B+drug+particles&rank=4. (Accessed: 23rd January 2017)
121. ClinicalTrials.gov. Comparison of Efficacy on Healing, and Safety of Two Dressings Urgotul and TulleGras MS on Surgical Acute Wounds. (2016). Available at: https://clinicaltrials.gov/ct2/show/record/NCT02322710?term=dressing+%2B+drug+particles&rank=5. (Accessed: 23rd January 2017)
122. ClinicalTrials.gov. Repeated DermaVir Immunizations in HIV-1 Infected Treatment-naïve Patients (GIEU006). (2013). Available at: https://clinicaltrials.gov/ct2/show/NCT00711230?term=patch+%2B+drug+particles&rank=11. (Accessed: 23rd January 2017)
123. ClinicalTrials.gov. Single DermaVir Immunization in HIV-1 Infected Patients on HAART (GIHU004). (2013). Available at: https://clinicaltrials.gov/ct2/show/NCT00712530?term=patch+%2B+drug+particle+%2B+skin&rank=2. (Accessed: 23rd January 2017)
124. ClinicalTrials.gov. Antiretroviral-Sparing Concept With HIV-specific T Cell Precursors With High Proliferative Capacity (PHPC) (PHPC-02). (2013).
125. ClinicalTrials.gov. Midlife Cholesterol Study - Full Text View - ClinicalTrials.gov. (2014). Available at: https://clinicaltrials.gov/ct2/show/study/NCT00361075?term=patch+%2B+drug+particles&rank=13. (Accessed: 23rd January 2017)

Chapter 3 - Materials and Methods

1. Materials

All chemicals were purchased from Sigma-Aldrich unless otherwise specified and were used as received. Polydimethylsiloxane (PDMS) - SYLGARD® 184 SILICONE ELASTOMER KIT was purchased by Dow corning and silicon micromolds were designed and fabricated at CENIMAT at NOVA, New University of Lisbon.

2. Methods

2.1.Micropatterned patch fabrication

PDMS micropatterned patch (PMP) were obtained by solving casting process technique, as described previously.[1] Briefly, different silicon wafers were used as masters to obtain PMP (1.44 cm^2) with different distances between the micropillars (40, 80, and 160 µm) and heights (100, 300, and 550 µm). In order to reduce PMP-silicon molds adhesion, silicon molds were treated with a silanization protocol. Silicon molds were cleaned with isopropanol and dried in N_2. After being treated with vacuum air plasma for 3-4 min, the master was placed into a vacuum desiccator along with a small beaker containing a few drops (≈ 20µL/mold) of trichloro(1H,1H,2H,2H-perfluorooctyl)silane for 2 h.[2] Additionally, PMP with variable flexibilities were prepared by using variable base:curing agent ratios, namely 5:1, 10:1, and 15:1. The mixture was then degassed in a vacuum desiccator in order to remove all air bubbles and then poured onto the silicon mold. The molds were cured at 70°C for 2 h.[3] PMP were also produced by double casting process using PDMS master. For easier manipulation purposes and to preserve silicon master molds integrity, the previously fabricated negative PMP were used as masters to positive PMP fabrication, enabling the production of the massive number of negative replicas needed to conduct this study. Same procedure with some modifications was used. PMP were treated with vacuum air plasma for 10 minutes, the master was placed into a vacuum desiccator along with a small beaker containing a few drops (≈ 20µL/mold) of trichloro(1H,1H,2H,2H-perfluorooctyl)silane for 40 min.

PDMS residues were removed from silicon molds as described in literature [4]. A dilute solution of TBAF (1% w/v) in hydrophobic non-hydroxylic aprotic solvent (PMA)

was used to remove the PDMS residues. The solution containing TBAF caused rapid disruption/disintegration of PDMS polymer matrix and removed it by dislodging it from the surface and, to a large extent, by dissolution of the PDMS residues. A key feature of the chemistry used herein is the compatibility of etchant with the flexible PI substrate. The sample was immersed in the solution which was stirred continuously. The solution was maintained at a temperature of 50 °C throughout the cleaning process as this temperature results in faster etching. The cleaning action was performed for a period depending on the amount of polymer residues. An etching rate of 1–1.5 mL/min was showed. After the first etching step, the sample was transported to the first solvent rinse bath comprising of preheated (50 °C) PMA solvent.

2.2. Production of PCL microparticles

In order to prove the previously presented concept a set of PCL microparticles were produced by microfluidics device with different diameters (40, 80 and 160 µm) to test the different responses by the PMP. The different diameters were obtained based on the variation of flow rate and the concentration of the PLC solution. The surfactant that was used in this process was a diluted solution of PVA 2% (w/v). PLC solution was prepared in DCM and PVA in distilled water. The conditions are described in the following table.

Table 3.1. Parameters to PLC microparticles production.

Particle Size (µm)	PVA concentration (%)	Flow rate PVA (mbar)	PLC concentration (%)	Flow rate PCL (mbar)
40	2.0	300	5.0	270

Microfluidic techniques are widely applied in microparticles preparation. Through this method, various shapes and morphologies polymer particles can be obtained.[5] Microfluidcs device was the first trial and was used a chip in “T form” (Figure 4A), where PCL microparticles were formed by the combination of a discontinuous flow of polymer solution (PCL) with a continuous flow of surfactant (PVA). According to **Table 3.1**, the particle size was very similar. **Figure 3.1** presents the size distribution of PCL microparticles that showed low polydispersity (26.5± 5.4 µm) with a very stable system. Lin and co-workers produced PCL microparticles with a microfluidic device and similar results were obtained.

PCL microparticles showed consistent morphology (sphericity and smooth surface) and excellent size uniformity.[6]

Figure 3.1. Production of PCL microparticles by microfluidics **A.** Microfluidics device **B.** Microscope image of PCL microparticles (10x) obtained by microfluidic device **C.** Particle size distribution of PCL microparticles obtained by microfluidics.

Due to the high number of combinations tested (three different micropillars spacing, microparticles diameters, micropillars height and patch flexibility, N= 3), considerable number of microparticles were needed. Therefore, although microfluidics achieved monodispersed microparticles, another process was to be found due the time required in production of microparticles with microfluidics. Being a faster, reproducible and precise methodology, emulsion technique was used to engineer PCL microparticles. For the purpose, a 4.5 % (w/v) PCL solution was prepared in DCM and 0.5 % (w/v) PVA solution was prepared in distilled water. PCL solution (8 mL) was added with OB1 Pressure Controllor (Elveflow, France) to PVA solution (150 mL) in continuous stirring at 800 rpm.[7] Microarticles were dried at 170 rpm in microplate agitator and then washed twice against distilled water under centrifugation at 1000 rpm for 5 min. Microparticles with different diameter ranges, namely [25-40]µm, [63-80]µm, and [100-160]µm, where selected with the aid of sieves. At the end, the sieves were washing in ultrasonic bath and dried with compressed air.

To allow a better visualization of the entrapment of microparticles within PMP, comarin-6 was dissolved in acetone (2 mg/mL) and added to the PCL solution. To each 8 mL of PCL 70 µL of comarin-6 solution was used. Comarin-PCL microparticles were produced following the same protocol described for PCL microparticles.

2.3.Production of tetracycline-loaded alginate microparticles

Alginate microparticles were produced by electrospraying technique (SprayBase, Avectas, Ireland). First, microparticles with and without tetracycline were optimized in order

to obtain a rounded shape and a diameter of 80 µm. Parameters were set as: flow rate 1.0 m/h, voltage 15 kV, and needle-to-collector distance 6 cm. To optimize the encapsulation of tetracycline, two different methodologies were performed. For unloaded microparticles a needle diameter of 22G was used with an alginate concentration of 2.0 % w/v. For tetracycline-loaded microparticles the needle diameter and the polymer concentration were decreased to 26G and 1.75 % w/v, respectively. Calcium chloride (0.1M) was used as the crosslinking bath under continuous agitation (300 rpm). In a subsequent experiment, alginate microparticles obtained by electrospray technique (10 mg) were lyophilized and then suspended in 5 mL of tetracycline solution. The suspension was allowed to stir at room temperature (RT) during 24h and then again lyophilized.[8,9] The amount of tetracycline encapsulated was determined by decrosslinking the alginate microparticles in ethylenediaminetetraacetic acid (EDTA, 0.1M) solution. Absorbance was read at 362 nm in a microplate reader (Synergy HTX, BioTek Intruments, USA) using a corning 384 quartz microplate (Hellma). Drug content and drug entrapment were calculated according to the following equations:

$$Drug\ content\ (\%\ w/w) = \frac{mass\ of\ drug\ in\ microparticles}{m_{microparticles}} \times 100$$

Equation 1

$$Drug\ entrapment\ (\%\ w/w) = \frac{mass\ of\ drug\ in\ microparticles}{mass\ of\ drug\ used\ in\ formulation} \times 100$$

Equation 2

2.4.Microparticles incorporation into PMP

The different PMP were pressed against the produced microparticles in order to promote their capture. Different combinations of particle size and distance between the pillars were obtained (**Table 3.2**). As previously mentioned, 3 different PDMS rigidity and pillars height were also used. To evaluate the entrapment efficiency, the different formulations of PMP entrapping different microparticles were weighted.

Table 3.2. Different formulations of PMP entrapped with different microparticles.

	Microparticle size (µm)		
Micropillars spacing (µm)	40	80	160
40	x	x	x
80	x	x	x
160	x	x	x

Microparticles adherence to different PMP were also investigated through different techniques: fluorescence microscopy and SEM.

Entrapment efficiency was determinate by following equation:

$$Entrapment\ efficiency\ (mg/cm^2)\ = \frac{mass\ of\ microparticles}{avaiable\ area}$$

Equation 3

Each PMP have a total area of 1.44 cm^2. The available area represents the space between the micropillars (similar to cylinders) and was defined by:

$$Avaiable\ area = \ total\ area - micropillars\ area\ \times micropillars\ number$$

Equation 4

$$micropillars\ area = 2\pi r \times micropillars\ heigth$$

Equation 5

Considering that pillars diameter of 60 µm, pillars number was achieved by:

$$micropillars\ number = \frac{total\ area}{(60 + 60 + micropillars\ spacing)^2}$$

Equation 6

2.5.Surfaces characterization

The surface of PMP either with or without PCL microparticles was visualized by scanning electron microscopy (SEM, S4100, Hitachi, Japan). Silicon wafers were also visualized by SEM. The samples were gold-sputerred and operating at 25.0 kV accelerating voltage. PMP entrapping coumarin-PCL microparticles were visualized by EGFP fluorescence microscopy (Zeiss Imager M2, Zeiss, Germany).

2.6.Mechanical Tests

The mechanical behavior of the PMP was characterized through tensile test with Shimazdu MMT-101N (Shimazdu Scientific Instruments, Japan) a load cell of 100 N and a velocity of 1 mm·min^{-1}. PMP and PMP with entrapped PCL microparticles were tested (three repeated simples). The sample thickness was measured using a micrometer with a precision of 1 μm. For each sample, the load versus cross-head displacement data from initial until rupture load were measured using a PC data acquisition system connected to the tester. The initial gauge length was set as 8 mm.[10]

Young's modulus (*E*) was calculated by dividing the tensile strength (σ) by the extensional strain (ε) in the linear (elastic) portion of the physical stress–strain curve, as described in the following equations:

$$Young's\ modulus\ (Pa) = \frac{\sigma\ (\varepsilon)}{\varepsilon}$$

Equation 7

Elongation factor (ε, adimensional) was obtained by the division between elongations at each point by the gange length (original length of the object).

$$Extensional\ strain\ (\varepsilon) = \frac{\varepsilon(t)}{Gange\ length}$$

Equation 8

Tensile strength (σ, Pa), force exerted on the object, was calculated through the division of the exerted force at each point by the cross-sectional area (width × thickness).

$$Tensile\ strength\ (\sigma) = \frac{exerted\ force\ (t)}{width\ \times thickenss}$$

Equation 9

2.7.Release Assay

The optimized system previously described as PMP with 80:80:300μm (microparticle diameter:micropillar spacing:micropillar height) with 10:1 flexibility was tested for controlled released studies under sink conditions. For this, a model antibiotic (tetracycline hydrochloride) was used, and was monitored through UV-vis spectroscopy at 362 nm. The release assays were performed in phosphate-buffered saline (PBS) solutions at physiological pH (7.4) and wounds pH (5.5). The drug release content from PMP with tetracycline-loaded alginate microparticles or tetracycline-powder microparticles was evaluated. Non-loaded alginate microparticles, and PMP without entrapped microparticles were used as controls. Briefly, the samples were immersed in 5 mL of PBS and subsequently stirred in a shaking water bath at 60 rpm and 37ºC. At predetermined time intervals, aliquots of 500 μL of PBS were withdrawn and the same volume of fresh buffer solution was added.[11] UV-spectroscopy was measured at 362 nm in a microplate reader (Synergy HTX, BioTek Intruments, USA) using a corning 384 quartz microplate (Hellma).

$$Acumulative\ tetracycline\ release\ (\%) = \frac{V_e \sum_i^{n-1} c_i + V_0 c_n}{m_{drug}} \times 100$$

Equation 10

2.8.Growth inibihition assay

The ability of PMP (6 mm diameter) entrapped with tetracycline-loaded alginate microparticles and tetracycline powder microparticles to inhibited bacterial growth was investigated using *Escherichia coli* (ATCC) and *Staphylococcus aureus* (ATCC) culture. PMP without alginate microparticles entrapped or loaded with alginate microparticles without tetracycline were used as controls. Colonies isolated from nutrient agar were inoculated to 5 mL Lysogeny broth (LB) medium (Merck) and incubated for 18–24 h in a shaking water bath at 180 rpm and 37ºC. The obtained cellular suspensions (1 mL) were centrifuged (13000g, 10 min). Pellet suspensions were then prepared in sodium chloride

(NaCl) solution (0.9% w/v). The cellular density was determinate by UV-vis spectrometry at 600 nm (UV mini-1240 UV-VIS Spectrophotometer, Shimadzu). After inoculum spreading in Muller Hinton agar medium (nzytech), samples were placed and incubated at 37°C for 24 h.[12] At the end, diameters of inhibition zones around the constructs were measured manually. Each disc diffusion test was repeated three times.

2.9.Statistics

All statistical analysis were perfomed in GraphPad using two-way ANOVA analyses of variance following the Bonferroni post-hoc test with a significant set at $p < 0.05$.

References

1. Gitlin, L., Schulze, P. & Belder, D. Rapid replication of master structures by double casting with PDMS. *Lab Chip* **9,** 3000–3002 (2009).
2. Théry, M. & Piel, M. Adhesive micropatterns for cells: a microcontact printing protocol. *Cold Spring Harb. Protoc.* **2009,** 5255 (2009).
3. Gitlin, L., Schulze, P. & Belder, D. Rapid replication of master structures by double casting with PDMS. *Lab Chip* **9,** 3000-3002 (2009).
4. Dahiya, R., Gottardi, G. & Laidani, N. PDMS residues-free micro/macrostructures on flexible substrates. *Microelectron. Eng.* **136,** 57–62 (2015).
5. Zhao, Y. *et al.* Facile preparation of fluorescence-encoded microspheres based on microfluidic system. *J. colloid*. **352,** 337-342 (2010).
6. Lin, Y., Yang, C., Wu, C., Grumezescu, A. & Wang, C. A microfluidic chip using phenol formaldehyde resin for uniform-sized polycaprolactone and chitosan microparticle generation. *Molecules*. **18,** 6521-6531 (2013).
7. Luciani, A., Coccoli, V., Orsi, S., Ambrosio, L. & Netti, P. A. PCL microspheres based functional scaffolds by bottom-up approach with predefined microstructural properties and release profiles. *Biomaterials* **29,** 4800–4807 (2008).
8. Correia, C. R., Reis, R. L. & Mano, J. F. Multilayered Hierarchical Capsules Providing Cell Adhesion Sites. *Biomacromolecules* **14,** 743–751 (2013).
9. Silva, A. S. *et al.* Aerosolizable gold nano-in-micro dry powder formulations for theragnosis and lung delivery. *Int. J. Pharm.* **519,** 240–249 (2017).
10. Sousa, M. P., Caridade, S. G. & Mano, J. F. Control of Cell Alignment and Morphology by Redesigning ECM-Mimetic Nanotopography on Multilayer Membranes. *Adv. Healthc. Mater.* **6,** 1-14 (2017).
11. Che, H. *et al.* CO_2 -switchable drug release from magneto-polymeric nanohybrids. *Polym. Chem.* **6,** 2319–2326 (2015).
12. Siafaka, P. I., Zisi, A. P., Exindari, M. K., Karantas, I. D. & Bikiaris, D. N. Porous dressings of modified chitosan with poly(2-hydroxyethyl acrylate) for topical wound delivery of levofloxacin. *Carbohydr. Polym.* **143,** 90–99 (2016).

Chapter 4- Physical supports for the immobilization of particles inspired by pollination

Lúcia F. Santos [1], A. Sofia Silva[1], Clara R. Correia[1], João F. Mano[1]

[1] Department of Chemistry, CICECO – Aveiro Institute of Materials, University of Aveiro, Campus Universitário de Santiago, 3810-193 Aveiro, Portugal

Abstract

Biomimetic systems exhibit often striking designs well adapted to specific functions that have inspired scientists and engineers in the development of new technologies and processes. In this work we explore the remarkable ability of honey bees to catch and release large amount of grains pollen during pollination. We believe that the hair spacing and height on bees‘ foreleg is relevant for leg’s ability to mechanically fix microsized grains pollen. Inspired by this observation we propose the concept of a novel micropatterned surface featuring spaced high aspect-ratio micropillars to mimic the hair of bee’s legs for microparticles entrapment. The hypothesis was validated by investigating the ability of bioinspired polydimethylsiloxane microfabricated patches to fix microparticles. Different conditions were tested, namely the geometry arrangement, spacing, height, and flexibility of micropillars combined with microparticles with variable diameters. Our results are consistent with the observations that the diameter of grain pollens is similar to the distance between the legs’ hair. Our biomimetic surfaces were explored for the fixation of solid microparticles for drug release applications, using tetracycline hydrochloride as a model antibiotic. We investigated patches entrapping (i) tetracycline hydrochloride powder or (ii) tetracycline-loaded alginate microparticles. While tetracycline powder is immediately released, the tetracycline-loaded alginate microparticles allow a controlled and sustained release of the active pharmaceutical ingredient during 5 days with a maximum cumulative release of 81.6 ± 3.8 %, also exhibiting an antimicrobial activity. Such bioinspired hairy surfaces could find applications in other fields where universal dry fixation of high-quantity of micro-objects are needed, including in agriculture (fixation of seeds or solid fertilizers),

biotechnology/chemical industry (e.g. immobilization of microorganisms and in heterogeneous catalysis) and in the new conception of cleaning utensils.

Key words: Biomimetic, drug carries, honey bee, micropatterning, patches, pollination, transdermal drug delivery.

1. Introduction

In nature, biological organisms exhibiting unique features have been a source of inspiration to the development of high performance structures and biomaterials. Commonly found in nature, different hierarchical structures range across macroscale to the nanoscale and could lead to promising applications.[1] The emerging field of biomimetics allowed the fabrication of novel soft materials and functional surfaces based on the understanding of nature designs and processes in order to solve current problems in engineering, materials science and biomedicine.[2,3]

Superhydrophobicity, self-cleaning, drag reduction in fluid flow, high and reversible adhesion, aerodynamic lift, high mechanical toughness, and self-healing are some of the numerous properties previously found in nature and employed in the development of news substrates and hydrogels.[2,4] For example, geckos, beetles, flies and other animals are some examples that have inspired the development of biomimetic adhesives due to their ability to reversibly adhere to surfaces. This capacity relies on the surface topography of their attachment pads,[5] which are covered with a pattern of microstructures, resembling the geometry of tenent hairs present in their feet.[6]

In this work we are particularly interested on the peculiar hairy structure that covers the surface of the body, in particular the legs, of honey bees, able to carry millions of particles for pollination purposes **(Figure 4.1A)**. Such insects have a typical branched hair with numerous short lateral barbs in-between pollen grains are entrapped. The hair covering the body allows the temporary retention of pollen, which is then removed by the combing action of the legs' brushes.[7–9] Thus, pollens and bees' hair legs are a naturally-optimized system that can be used to inspire the development of substrates able to mechanically fix small solid objects which could find applicability in various fields**(Figure 4.1B)**.

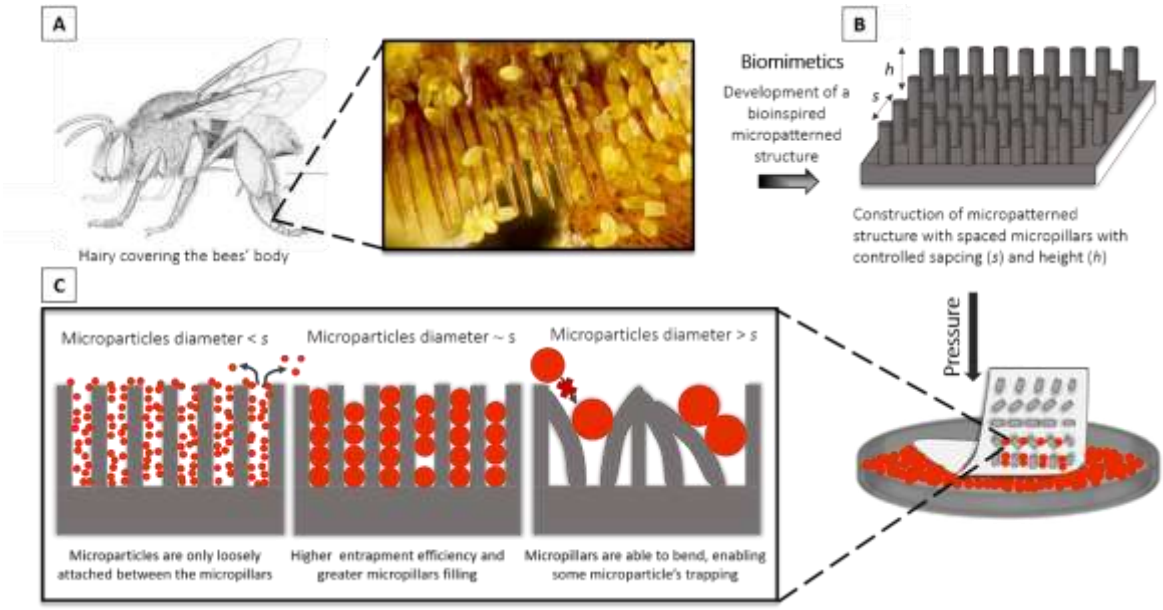

Figure 4.1. Schematic illustration of the development of the proposed biomimetic micropatterned structrure. **A.** The bees' body is covered with hairs. Grains pollen are caught between the bees' hair and their size is similar to the hair spacing; **B.** A bioinspired patch can be developed based on pollination by the construction of a micropatterning structure with micropillars with controlled spacing (*s*) and height (*h*). **C.** Capture of large amount of solid microparticles in micropillars spacing by direct contact and pressure; the entrapment efficiency will depend on the contrast between the pillars spacing (*s*) and the size of the microparticles.

We propose the development of microfabricated substrates to reproduce this natural phenomenon, by exploring the microparticles' fixation ability of micropatterned elastomeric films. We believe that such kind of substrates could be used in a wide variety of applications that require simple, non-permanent, high-content and pure-physical immobilization of solid particulate objects. We explore microparticles with variable diameters, combined with patches with different micropillars geometry arrangement, height, and spacing **(Figure 4.1C)**. We finely demonstrated the usefulness of such concept in the development of a new generation of drug delivery patches. Current problems associated with passive delivery patches have been limiting their application,[10] and one valuable solution could be the application of higher drug content to improve transcutaneous fluxes and overcome their constraints.[11] Herein, we show the development of a hierarchical biomimetic patch consisting of a polydimethylsiloxane (PDMS) micropatterned structure with micropillars entrapped with polycaprolactone (PCL) microparticles or drug-loaded alginate microparticles. We envisage the possibility of having membranes with any desired shape and size that could immobilize any

combination of drug by simple direct contact with a powder formulation. As a proof-of-concepct, tetracycline, a broad-sprectum antibiotic foreseen to act during the inflammatory phase of wounds, was used as active pharmaceutical ingredient (API). Such demonstration can extend the interest of such type of substrates able to entrap and fix solid micro-objects for other biomedical, agricultural, environmental and industrial applications.

2. Materials and Methods

2.1.Materials

All chemicals were purchased from Sigma-Aldrich and used as received, unless otherwise specified. PDMS (Sylgard® 184 silicone elastomer kit) was purchased from Dow Corning. Silicon micromolds were designed and fabricated at CENIMAT at New University of Lisbon.

2.2.Methods

2.2.1. PDMS micropatterned patches fabrication

PDMS micropatterning patches (PMP) were obtained by double casting process, as previously described.[12] Briefly, different silicon wafers were used as masters to obtain PMP (1.44 cm^2) with different distances between the micropillars (40, 80, and 160 µm) and heights (100, 300, and 550 µm). Additionally, PMP with variable flexibilities were prepared by using variable base:curing agent ratios, namely 5:1, 10:1, and 15:1. The prepared PDMS solutions were then poured onto the silicon wafers, and cured at 70°C for 2 h. To facilitate PMP-silicon detachment, silicon wafers were previously treated with a silanization protocol. Silicon wafers were cleaned with isopropanol and dried in nitrogen (N_2) and after treated with Plasma System ATTTO (Aname, Spain) for 3-4 min (30 V, 0.6 mbar), and immediately placed into a vacuum desiccator containing approximately 20µL/mold of trichloro(1H,1H,2H,2H-perfluorooctyl)silane for 2 h.[13] Same procedure was used to production of PMP using a PDMS master.

2.2.2. Production of microparticles

2.2.2.1.PCL microparticles

An emulsion technique was used to prepare the PCL microparticles.[14] PCL was dissolved in dichloromethane (DCM) (4.5% w/v) and dropwise to a stirring bath (800 rpm) of polyvinyl alcohol (PVA) (0.5% w/v). OB1 Pressure Controllor (Elveflow, France) was used as the pumping system at 5000 mbar. After mild stirring to evaporate the organic solvent, the obtained microparticles were subsequently washed with distilled water, and collected by centrifugation (200g, 5 min). Microparticles with different diameter ranges, namely [25-40]µm, [63-80]µm, and [100-160]µm, where selected with the aid of sieves. To allow a better visualization of the entrapment of microparticles within PMP, comarin-6 was dissolved in acetone (2 mg/mL) and added to the PCL solution. To each 8 mL of PCL 70 µL of comarin-6 solution was used. Coumarin-PCL microparticles were produced following the same protocol described for PCL microparticles.

2.2.2.2.Tetracycline-loaded alginate microparticles

Alginate microparticles were produced by electrospraying technique (SprayBase, Avectas, Ireland). First, microparticles with and without tetracycline were optimized in order to obtain a rounded shape and a diameter of 80 µm. Parameters were set as: flow rate 1.0 ml/h, voltage 15 kV, and needle-to-collector distance 6 cm. To optimize the encapsulation of tetracycline, two different methodologies were performed. For unloaded microparticles a needle diameter of 22G was used with an alginate concentration of 2.0 % w/v. For tetracycline-loaded microparticles the needle diameter and the polymer concentration were decreased to 26G and 2% w/v, respectively. Calcium chloride (0.1M) was used as the crosslinking bath under continuous agitation (300 rpm). In a subsequent experiment, alginate microparticles obtained by electrospray technique (10 mg) were lyophilized and then suspended in 5 mL of tetracycline solution. The suspension was allowed to stir at room temperature (RT) during 24h and then again lyophilized.[15]16] The amount of tetracycline encapsulated was determined by decrosslinking the alginate microparticles in ethylenediaminetetraacetic acid (EDTA, 0.1M) solution. Absorbance was read at 362 nm in a microplate reader (Synergy HTX, BioTek Intruments, USA) using a corning 384 quartz microplate (Hellma).

2.2.2.3.Tetracycline-powder microparticles

Tetracycline-powder microparticles were obtained by milling tetracycline hydrochloride with the aid of a mortar with agate pestle. The obtained microparticles were then separated through diameter ranges of [25-40]µm, [63-80]µm, and [100-160]µm using sieves.

2.2.3. Microparticles entrapment into PMP

The different PMP were pressed against the produced PCL or alginate microparticles in order to promote their capture. To evaluate the entrapment efficiency, the different formulations of PMP entrapping different microparticles were weighted.

2.2.4. PDMS micropatterned patches characterization

The surface of PMP either with or without PCL microparticles was visualized by scanning electron microscopy (SEM, S4100, Hitachi, Japan). Silicon wafers were also visualized by SEM. The samples were gold-sputerred and operating at 25.0 kV accelerating voltage. PMP entrapping coumarin-PCL microparticles were accessed by EGFP fluorescence microscopy (Zeiss Imager M2, Zeiss, Germany).

The mechanical behavior of different PMP was characterized through tensile test (MMT-101N, Shimazdu Scientific Instruments, Japan) with a load cell of 100 N and a velocity of 1 $mm \cdot min^{-1}$. PMP and PMP with entrapped PCL microparticles were tested (n=3). The sample thickness was measured using a micrometer with a precision of 1 µm. For each sample, the load versus cross-head displacement data from initial until rupture load was measured using a PC data acquisition system connected to the tester. The initial gauge length was set to 8 mm.

2.2.5. *In vitro* release studies

PMP with 80:80:300µm (microparticle diameter:micropillar spacing:micropillar height) with 10:1 flexibility was tested for controlled released studies of tetracycline hydrochloride through UV-vis spectroscopy at 362 nm. The release assays were performed in phosphate-buffered saline (PBS) solutions at both physiological pH (7.4) and wounds pH (5.5). The drug release content from PMP with tetracycline-loaded alginate microparticles or tetracycline-powder microparticles was evaluated. Non-loaded alginate microparticles, and PMP without entrapped microparticles were used as controls.

Briefly, the samples were immersed in 5 mL of PBS and subsequently stirred in a shaking water bath at 60 rpm and 37ºC. At predetermined time intervals, aliquots of 500 µL of PBS were withdrawn and the same volume of fresh buffer solution was added. UV-spectroscopy was measured at 362 nm in a microplate reader (Synergy HTX, BioTek Intruments, USA) using a corning 384 quartz microplate (Hellma). Drug release from swelling controlled systems (alginate microparticles) was modulated by the Kornsmeyer-Peppas equation.[16–18]

2.2.6. Growth inhibition assay

The ability of PMP (6 mm diameter) entrapped with tetracycline-loaded alginate microparticles and tetracycline powder microparticles to inhibited bacterial growth was investigated using *Escherichia coli* (ATCC) and *Staphylococcus aureus* (ATCC) culture. PMP without alginate microparticles entrapped or loaded with alginate microparticles without tetracycline were used as controls. Colonies isolated from nutrient agar were inoculated to 5 mL Lysogeny broth (LB) medium (Merck) and incubated for 18–24 h in a shaking water bath at 180 rpm and 37ºC. The obtained cellular suspensions (1 mL) were centrifuged (13000g, 10 min). Pellet suspensions were then prepared in sodium chloride (NaCl) solution (0.9% w/v). The cellular density was determinate by UV-vis spectrometry at 600 nm (UV mini-1240 UV-VIS Spectrophotometer, Shimadzu). After inoculum spreading in Muller Hinton agar medium (nzytech), samples were placed and incubated at 37°C for 24 h.[19] At the end, diameters of inhibition zones around the constructs were measured manually. Each disc diffusion test was repeated three times.

2.2.7. Statistics

All statistical analysis were perform using GraphPad using two-way ANOVA analyses of variance following the Bonferroni post-hoc test with a significant set at $p<0.05$.

3. Results

3.1.Fabrication of PDMS micropatterned patches

In order to achieve the most effective system, different constructs were fabricated to address their ability to catch and release spherical-shaped microparticles. PMP with

different flexibility were produced by varying the ratio between base and curing agent. For all the formulations investigated (5:1; 10:1; 15:1) the results, displayed in **Figure S1** (Supplementary Info), confirm that a higher base:curing agent ratio led to a higher flexibility of the mold. Different distances between the micropillars (40, 80 and 160 µm) and their height (100, 300 and 550 µm) were tested. PMP were prepared by cast molding technique, as briefly detailed in **Figure 4.2A**. The casting process consisted in pouring the pre-polymer of the elastomer over the master that was then cured and peeled off.[12] For easier manipulation purposes and to maintain silicon masters integrity negative PDMS molds were used to produce positive PDMS ones, that were later used to produce the massive number of negative replicas needed to conduct this investigation. Such negative PDMS replicas were used as substrate for the entrapment of microparticles, forming our biomimetic PMP.

To investigate the accuracy of the molding step, samples were visualized by SEM. Micrographs displaying both negative and positive PMP molds can be depicted in **Figure S2**. **Figure 4.2** also displays the silicon wafer used in this work and the obtained PMP with two different geometries herein used (square and hexagonal).

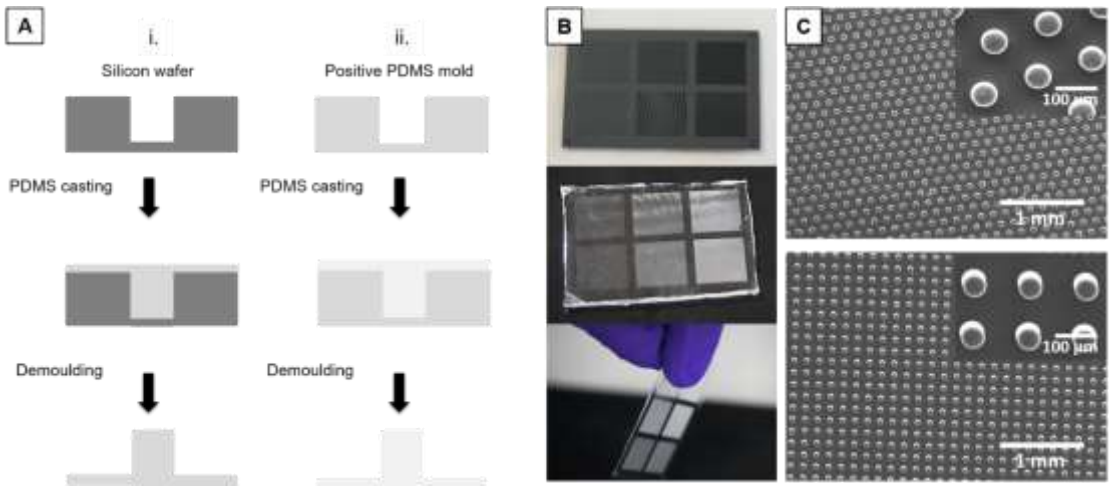

Figure 4.2. Fabrication of PDMS micropatterning patches (PMP). **A.** Schematic illustration of the fabrication of microstructured PMP by cast molding following the production of PMP using both **i.**silicon master and **ii.** inverse PDMS mold as master; **B.** Macroscopic images of the silicion wafer used in this process (top photograph) and the obtained PMP with low thickness (bottom photographs); **C.** SEM images of obtained PMP with square and hexagonal distribution of the micropillars. Scale bars are 1 mm. Magnification is 30x.

3.2.Microparticle trapping assays

In order to create an effective hierarchal patch comprising a flexible mold with maximum entrapment of microparticles, PCL microparticles were produced by emulsion technique (**Figure S3A and B**). Different sets of PCL microparticles with diameters matching the micropillars spacing, namely 40, 80, and 160 μm, were selected. Although microparticles produced through emulsion technique are highly polydisperse with a coefficient of variance (cv) of 83.2% (25 ± 20.8 μm), as demonstrated in **Figure S3C**, the sieving methodology enables to significantly decrease the cv to 15.8%, and thus obtain a monodisperse population of microparticles.

To achieve the most efficient system for microparticles trapping, different combinations of microparticles diameter, PMP flexibility, and micropillars spacing and height were investigated. A total amount of 243 combinations were tested. For the sake of simplicity, the differently spaced PMP and microparticles combinations will be numerically represented as microparticle:micropillar spacing. According to **Figure 4.1**, and more recent reports in the literature, pollen size appears to be very similar to the distance between the bees' foreleg hair, enabling a maximized accommodation of grain pollens.[7] By creating a system inspired in this organized process, it is hypothesized that the proposed biomimetic patch will be able to capture more efficiently microparticles with sizes matching the distance between the micropillars, afterwards allowing microparticles release, and consequently their content, in a sustained or controlled fashion.

3.2.1. Micropillars spacing

Based on **Figures 4.3A-C,** the entrapment efficiency is higher when the micropillars spacing and the diameter of microparticles are similar, regardless the height of the micropillars. Consequently, as the difference between the diameter of microparticles and micropillars spacing increases, the entrapment efficiency decreases. For instance, for a PMP with 300 μm of height entrapping microparticles with 40μm of diameter **(Figure 4.3A)**, the entrapment efficiency decreased from 14.0 ± 0.1 (40:40) to 12.1± 0.1 (80:40) mg/cm^2 as the spacing of the micropillars increased ($p < 0.01$**). Consequently, increasing such difference by entrapping 40 μm microparticles within PMP with 160 μm micropillars spacing (40:160), resulted in a higher significant

difference ($p < 0.0001$****) in the entrapment efficiency, which presented the lowest values of 8.3 ± 0.4 mg/cm^2. A similar trend was found for 80 μm microparticles **(Figure 4.3B)**. For instance, again for a PMP with 300 μm of height, the entrapment efficiency significantly decreased from 24.8 ± 0.4 (80:80) to 19.1 ± 0.3 mg/cm^2 (80:160) ($p < 0.0001$****) when the micropillars spacing increased from 80 μm to 160 μm. SEM micrographs (**Figure 4.3D)** corroborate these findings and also demonstrate that when microparticle size was smaller than micropillars spacing, ones were only superficially attached to the microstructures leaving the space between the micropillars empty. Micropillars roughness, displayed on **Figure S7**, may explain such microparticles' adhesion. On the other hand, when the diameter of microparticles was higher than micropillars spacing, microparticles were not able to fit in the space between. However, micropillars showed some flexibility and were able to bend, enabling a limited microparticle's trapping. For instance, when 80 μm microparticles were combined with 40 μm spaced PMP (80:40), micropillars bent to accommodate a maximum amount of microparticles and, although the PMP remained mostly filled, there was a significant reduction of the entrapment efficiency from 24.8 ± 0.4 (80:80) to 19.5 ± 0.3 mg/cm^2 ($p < 0.0001$****). The same behaviour was evidenced upon the combination of larger microparticles with the same type of PMP (160:40) where the entrapment efficiency suffers a significant decreased from 29.4 ± 1.0 (160:160) to 13.1 ± 0.5 mg/cm^2 ($p < 0.0001$****). Similar result was obtained when such larger microparticles were trapped within the 80 μm spaced PMP (160:80) showing an entrapment efficiency of 15.7 ± 0.2 mg/cm^2, similar to the 160:40 combination.

As hypothesized, the maximum entrapment efficiency was achieved when microparticles' size matched the micropillars spacing. From all the tested formulations, the 80:80 μm combination showed the highest entrapment efficiency and greatest filling of the PMP.

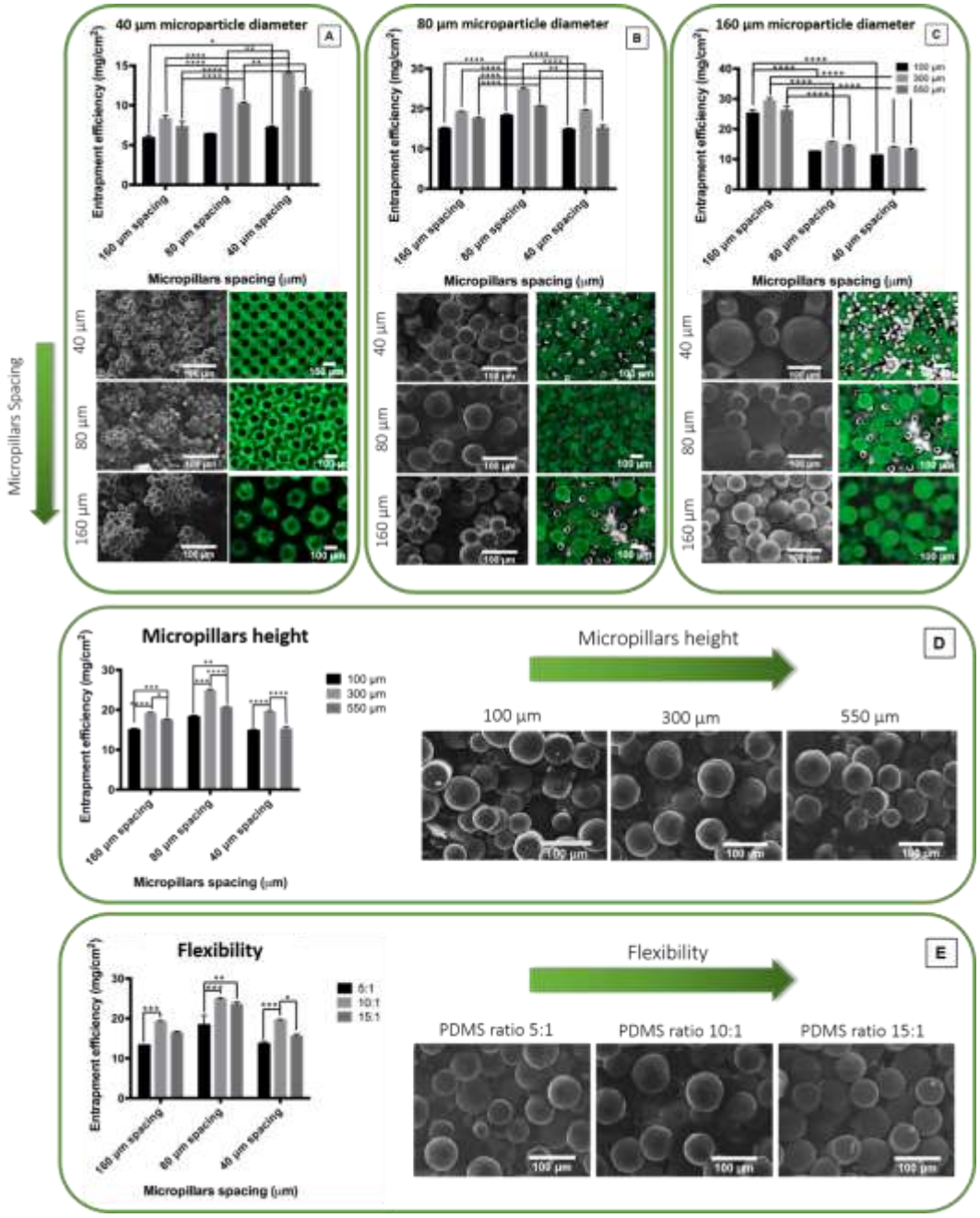

Figure 4.3. Entrapping assays of PCL microparticles within PDMS micrpatterning patches (PMP), Graphical representation of the entrapment efficiency of microparticles with different diameters, namely **A.** 40 µm, **B.** 80 µm and **C.** 160 µm, entrapped within PMP with varying micropillars spacing (40, 80 and 160 µm); **D.** Graphical representation of the entrapment efficiency of microparticles with 80 µm of diameter within PMP with 10:1 of flexibility and variable micropillars height, namely 100, 300 and 550 µm. At the right side of the graphic are shown SEM images of such PMP with variable micropillars height but only for the 80:80 system (microparticles diameter:micropillars height); **E.** Graphical representation of the entrapment efficiency of microparticles with 80 µm of diameter within PMP with 300 µm of micropillars height and variable flexibilities, namely 5:1, 10:1, and 15:1. At the right side of the graphic are shown SEM images of such PMP with variable flexibilities but only for the 80:80 system (microparticles diameter:micropillars height); P<0.1*, P<0.01**, P<0.001***, P<0.001****.

3.2.2. Micropillars height

According to **Figures 4.3A-C**, an increased entrapment efficiency of microparticles was achieved for the intermediate micropillars height with 300 µm, while the lowest micropillars of 100 µm have demonstrated to generate the lowest entrapment efficiency. Therefore, different micropillars heights, namely 100, 300, and 550 µm, with an intermediate mold flexibility of 10:1 were also tested with entrapped PCL microparticles with 80µm of diameter **(Figure 4.3 D)**. At the right side of the graphic presenting the entrapment efficiency of such PMP, are depicted the respective SEM images of the three differently height PMP for the 80:80 µm system. As visualized by SEM, the lowest micropillars of 100 µm presented the lowest entrapment efficiency since such type of PMP was only able to entrap few layers of microparticles. This is explained by the fact that the diameter of PCL microparticles of 80 µm was similar to the micropillars height of 100 µm. In fact, for the 80:80 system, an increase of the entrapment efficiency from 18.3 ± 0.4 µm to 24.8 ± 0.4 µm ($p<0.0001$****) could be observed when an increment in micropillars height from 100 µm to 300 µm occurred. Additionally, again for the 80:80 system, when comparing the lowest height of 100 µm with the highest height of 550 µm a significant increase ($p<0.01$**) in microparticles entrapment could be observed for the late. Nevertheless, such result (20.6 ± 0.4 µm) is still significantly lower than the 300 µm height PMP ($p<0.0001$****). This can be explained by the existence of empty spaces along the vertical structures of such PMP system with 550µm of height, showed in SEM images.

3.2.3. Patch flexibility

Another important parameter is the flexibility of the PMP. Different flexibilities were obtained though the variation of PDMS base and curing agent ratios. For the purpose, three different base:curing agent ratios, namely 5:1, 10:1 and 15:1, were investigated for PMP entrapping 80 µm microparticles within micropillars height of 300 µm **(Figure 4.3E)**. SEM images of such PMP with different PMP flexibilities for the 80:80 system are depicted on the right side of the graphic. For all flexibilities, the PMP were almost completely filled with entrapment efficiencies above 20 mg/cm^2. Similarly, to bee's body and foreleg hair, which are not rigid structures and bend to accommodate the maximum amount of grain pollens, some flexibility is also herein required to maximize the entrapment of microparticles. Results show that for the 80:80 system the

entrapment efficiency increased from 18.4 ± 2.3 (5:1) to 24.8 ± 0.4 mg/cm^2 (10:1) ($p<0.001$***). However, the most flexible PMP herein developed (15:1) was not able to support and retain the highest amount of microparticles, and thus a small and non-significant decrease (23.5 ± 0.6) when compared to 10:1 was verified. Overall, the results obtained demonstrate that PMP with both microparticles and micropillars spacing of 80 µm (80:80) combined with an intermediate micropillars height (300 µm) and mold flexibility (10:1 PDMS ratio) are the most profitable system with an entrapment efficiency of 24.8 ± 0.4 mg/cm^2. Therefore, such PMP was elected as an optimized hierarchal patch, and was further *in vitro* evaluated.

We hypothesise that the flexibility of the membranes could allow for the release of entrapped microparticles by a simple stretching and shaking. We expect that the average spacing between micropillars will increase due to the increase of the strain, leading to a decrease of the mechanical locking effect of the microparticles. A simple qualitative experiment was performed where we could observe that a signification fraction of entrapped microparticles could be released by a simple hand stretching combined with a mild shaking of the membrane. The shaking alone basically maintained the microparticles that were kept mechanically locked within the micropillars. Even with the outflow of compressed air over the membranes, the microparticles were found to be fixed.

3.3.Patches for drug delivery application

In order to explore the applicability of our biomimetic surface obtained in the last section, patches were established to the fixation of solid microparticles for drug delivery applications. For the proof-of-concept, tetracycline hydrochloride was used as API to *in vitro* release studies and the determination of the antibacterial activity.

3.3.1. Production of tetracycline-loaded alginate microparticles

Alginate microparticles were obtained by electrospray technique. Different parameters of the system were tested, namely by varying the flow rate, working voltage, and needle diameter. A working voltage of 15kV and 26G needle were associated with non-spherical microparticles and higher polydispersity, while lower flow rates resulted in smaller microparticles. Monodisperse microparticles with approximately 80 µm and a

spherical shape were obtained when a flow rate of 1 mL/h was combined with a 22G needle and a working voltage of 15kV. Results are displayed in **Figure 4.4.**

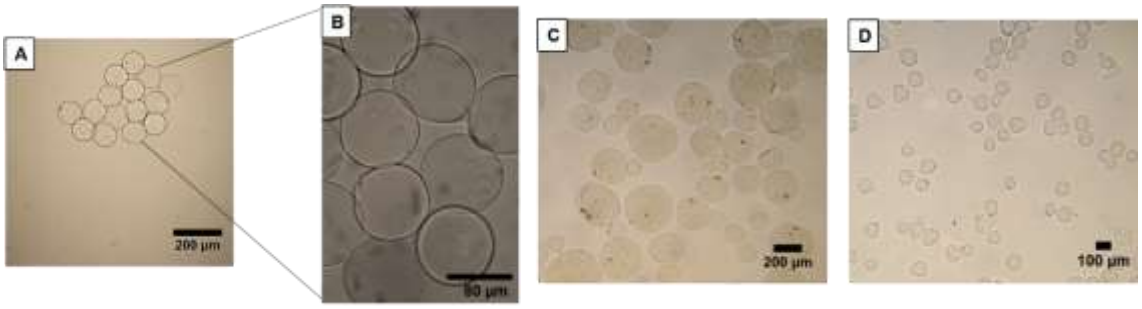

Figure 4.4. Alginate microparticles obtained by electrospray technique and visualized by light microscopy. **A.** Non-loaded alginate microparticles of with 80 µm of diameter. Scale bar is 200 µm. Parameters: 1 m.L/h flow rate, 22 G needle, and a working voltage of 15 kV. **B.** Higher magnification of A. Scale bar is 80 µm. **C.** Tetracycline-powder alginate microparticles using 2.5 mg/mL of tetracycline hydrochloride. Scale bar is 200 µm. **D.** Non-loaded alginate microparticles. Parameters: 1.75 % (w/v) alginate, 26 G needle, flow rate (1 mL/h), 15kV working voltage, and distance to the collector of 6 cm.

In the production of tetracycline-loaded alginate microparticles (TLM) two different approaches were tested. The first one consisted in previously mixing tetracycline and alginate solutions. However, drug addition to the alginate solution resulted in high polydispersity and larger microparticles with two distinct microparticles populations, namely between 60-100 µm and 250-350 µm. To overcome this limitation, different parameters for microparticles production (flow rate, voltage, needle diameter, collector distance, and tetracycline and alginate concentrations) were optimized to obtain the desired tetracycline-alginate microparticles diameter around 80 µm. The results showed that a flow rate of 1 mL/h, 15kV working voltage, 1.75 % (w/v) alginate concentration, 2.5 mg/mL tetracycline concentration, 26G needle and distance-needle to the collector of 6 cm yielded the spherical shape and small tetracycline-alginate microparticles with approximately 80 µm **(Figure 4.4 C)**. The second approach consisted in the immersion of the previously produced non-loaded alginate microparticles on a concentrated tetracycline bath (2.5 mg/mL). The most efficient approach was determined through the calculations of drug content and encapsulation efficiencies. Higher values were obtained with the second methodology resulting in a drug content of 2.10 ± 0.09 % and an encapsulation efficiency of 22.7 ± 1.0 %. Although the first approach presented a similar encapsulation efficiency (20.2 ± 1.4%), the drug content dropped substantially to 1.27 ± 0.14 %.

3.3.2. *In vitro* release studies

TLM and tetracycline powder (previously milled until the desired size of 80 µm) were entrapped in the PMP. Both constructs were incubated in PBS at pH 7.4 (physiological) and pH 5.5 (wound). TLM alone (not coupled with PMP) were also incubated. The cumulative release profile of the encapsulated drug is depicted in **Figure 4.5A.** As demonstrated, the total amount of tetracycline powder entrapped in PMP was released within 5 minutes for both pH.

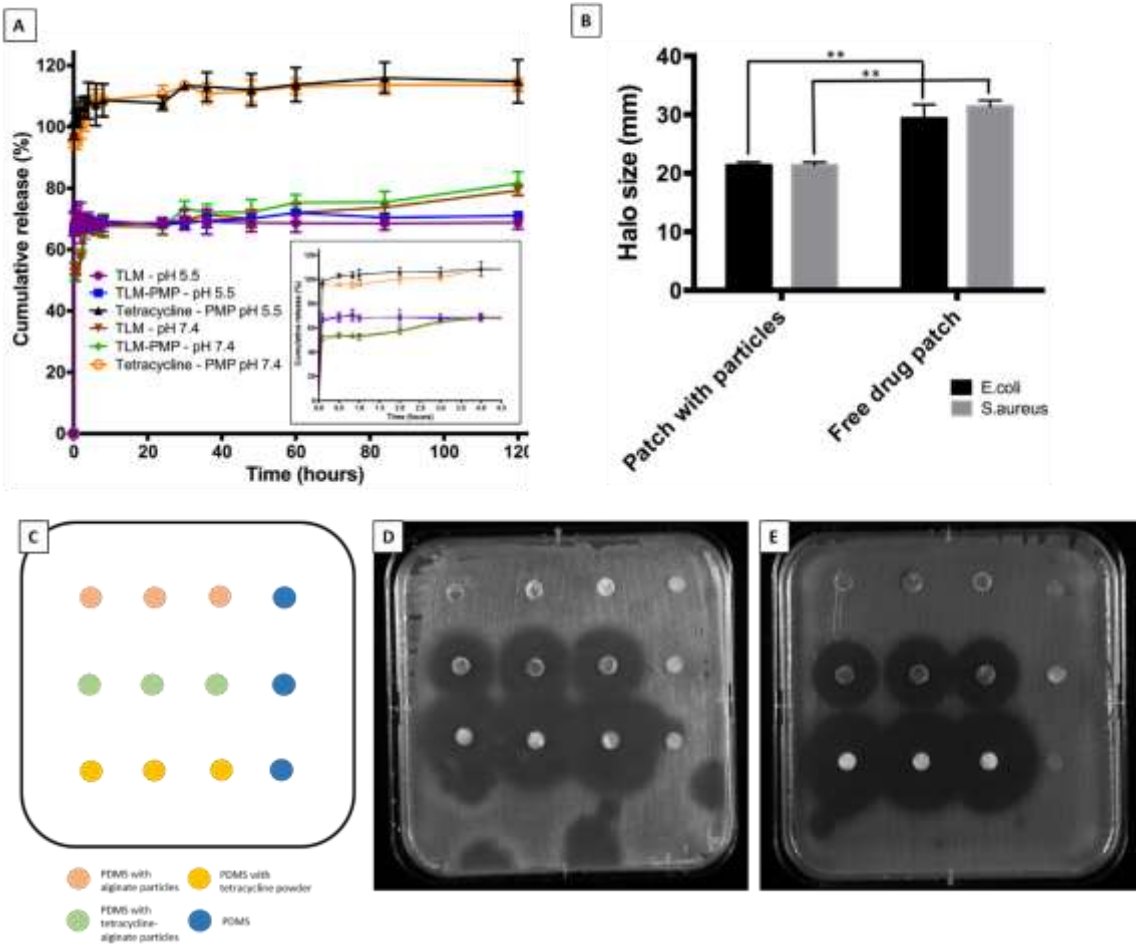

Figure 4.5. Antimicrobial activity and *in* vitro release assays from PDMS micrpatterning patches (PMP); Antimicrobial activity of the different combinations- PMP, PMP with non-loaded alginate microparticles, PMP with tetracycline-loaded alginate microparticles (TLM) and PMP with tetracycline powder against two microorganisms; **A.** *In vitro* cumulative release of tetracycline from PMP; **B.** Graphical representation of the inhibition zone (mm) of the different constructs; **C.** Disposition of the different combinations on plate; **D.** Antibiogram to Gram-negative *Escherichia coli*; **E.** Antibiogram to Gram-positive *Staphylococus*

A more controlled and sustained release of the drug was obtained through the encapsulation of tetracycline in alginate microparticles, enabling the engineering of a hierarchal patch with adequate features for drug delivery purposes. In fact, for each pH, the drug release from both systems TLM and TLM+PMP, is similar between them: 68.8 ± 2.1 and 71.1 ± 1.2, respectively for pH 5.5; and 79.3 ± 1.4 and 81.6 ± 3.8, respectively for pH 7.4 at the end of 5 days. An initial burst release is observed for these two formulations at both pH, where at least 50 % of the drug content is released within minutes.

3.3.3. Antibacterial studies of the prepared dressings

Growth inhibition assays for the different patches combinations (PMP with TMP and PMP with tetracycline powder) were performed against two common pathogens, in which tetracycline has demonstrated antibacterial activity - *E. coli* and *S. aureus*.[20] The different constructs were placed into the inoculation medium to inhibit the bacterial growth. PMP and PMP with alginate microparticles were used as controls. As expected, no inhibition zone was formed, demonstrating that such controls do not possess any inhibitory activity against the specific strains (**Figure 4.5D and 4.5E)**. In contrast, both constructs with tetracycline showed antibacterial activity against the different bacterial strains. Nevertheless, it is discernible that there is a proportional relation between drug concentration and antibacterial activity. PMP with tetracycline powder showed an enhanced antimicrobial activity due the highest drug concentration (100 % w/w). Significant smaller inhibition zones ($p<0.01$**) were achieved, in both strains, for PMP with TLM where the drug content within the patch is only 2.10 ± 0.09 % (w/w).

4. Discussion

Hair spacing on bees'foreleg is proposed to dictate leg's ability to store the microsized pollen during pollination.[7] Inspired by this extremely efficient system, where honey bees tune their body and foreleg hairs to accommodate a large amount of pollen grains, a new biomimetic structure for physically support the entrapment of microparticles was herein proposed. For this aim, a micropatterned structure able to mimic the bees' leg hair was obtained through the fabrication of PMP with spaced micropillars. Results showed that such constructs were able to entrap a large amount of different microparticles. As hypothesized, the maximum entrapment efficiency was

achieved when the diameter of microparticles matched the micropillars spacing, regardless of PMP geometry arrangement. Particularly, the PMP formulation of 80:80:300μm (microparticle diameter:micropillar spacing:micropillar height) with 10:1 flexibility, represent the most effective patch with an increased entrapment efficiency of 24.8 ± 0.4 mg/cm^2 against the 5 mg/cm^2, usually detected in the current commercially available patches approved by the US Food and Drug Administration (FDA).[21] In the biological example of honey bees, an increased hair length represents a bigger volume available to accumulate grain pollens.[7] The results herein detailed demonstrated that a compromise between height and microparticles accumulation is established. Hence, the results herein exhibited demonstrate that an intermediate height of the micropillars, increases the patch entrapment efficiency. Similar trends were obtained for all differently spaced PMP. Furthermore, the developed PMP present a simple design and it is mechanically resistant, encouraging its applications in situations where stretching and bending is likely to occur.

We also demonstrated that hydrogel microparticles could be immobilized in the developed bioinspired substrates, in order to demonstrate the adequacy of these systems to the used as patches for sustained drug release. Alginate has been widely used in hydrogels for biomedical applications, particularly in the encapsulation of a wide range of drugs, due to its low toxicity and cost.[22] TLM with an average size of 80μm, were produced through electrospray, a suitable technique to engineer monodispersed drug-loaded polymeric particles with diameters ranging from nano to micrometers,[23,24] with a drug loading of 2.10 ± 0.09 % and encapsulation efficiency of 22.7 ± 1.0 %. Martins and co-workers presented similar results with insulin-loaded alginate microparticles (1.78 ± 0.09 mm), achieving a maximum drug loading of 2.48 ± 0.01 % but higher encapsulation efficiency (80.0 ±0.8 %).[25] The authors justified the low loading capacity and encapsulation efficiency with the hydrophilic character of the drug and the large gel porosity, causing leakage of the loaded drugs and faster drug diffusion from the alginate to the crosslinking bath of calcium chloride. To overcome this limitation the alginate microparticles could be combined with other polymers. An example is the use of poli(3-hidroxibutirato-co-3-hidroxivalerato) (PHBHV) in tretacycline-loaded alginate microparticles, known to increase the drug content to 5%.[26]

Wound healing is normally divided in three steps: inflammation, proliferation and remodelling. Antibiotics, such as tetracycline, mainly act during the inflammatory phase,

which lasts for about 5 days.[27,28] The incorporation of drug carries (TLM) in the PMP allowed a more controlled and sustained release of the API for 5 days, when compared to the tetracycline powder-PMP system, where an immediate drug release was observed. The burst release can be easily explained by the probable superficial adsorption of tetracycline in the alginate microparticles. Due to the methodology herein described for drug encapsulation, it is extremely likely that the API has remained on the outermost of the particles, entrapped in their crosslinked network. Also, tetracycline's low molecular weight (444.435 $g.mol^{-1}$) may accentuate the concentration gradient, increasing osmotic pressure and causing such burst effect.[29] As result, when microparticles are placed in contact with an aqueous medium, a rapid diffusion is expected to occur. Additionally, at pH 5.5, the carboxylic acid group from alginate can be partially deprotonated ($pKa \approx 3.2$), which leads to a faster polymer dissolution, and consequently increasing such initial release. Nevertheless, after 4h, the osmotic pressure appears to be overcome for pH 5.5, probably due to alginate deterioration, and a steady state is achieved. Nevertheless, at pH 7.4, where the majority of microparticles are still intact, such osmotic pressure continues to play an active role, and a sustained release of the drug can still be observed.

Burst events followed by a controlled and sustained release of drug are of particular interest in wounds treatment, where an initial burst provides immediate relief followed by prolonged release to promote gradual healing.[29] Thereupon, these findings demonstrate that the PMP herein developed could be perfectly applied either in wound healing situations or other events that require topical transdermal delivery of a drug. Nevertheless, both constructs have manifested remarkable antimicrobial activity against gram-negative and gram-positive bacteria.

The results herein obtained suggest that such optimized and hierarchal system could be further considered for the development of bioinspired devices that provide the entrapment of huge amount of different microparticles. The fabrication of hairy substrates could be extended to other materials (including biodegradable polymers) and non-flat geometries. As reported in this work, an optimized patch could be developed for clinical applications, able to fix high quantity of drug powder or microparticles encapsulating drugs. Such entrapment could be easily done by a simple contact of the patch with any powdery product formulated from the shelf. This could be a valuable solution for the treatment of diseases that require high-drug concentration, enabling less frequent dosing, and thus significantly improving patient compliance. We hypothesize that this system

could be applied as a platform to the development of a wide variety of micropatterned structures with different applicability in, for example, biomedical, biotech and industrial fields.

5. References

1. Bhushan, B., Jung, Y. C. Natural and biomimetic artificial surfaces for superhydrophobicity, self-cleaning, low adhesion, and drag reduction. *Prog. Mater. Sci.* **56,** 1–108 (2011).
2. Bhushan, B. Biomimetics: lessons from nature-an overview. *Philos. Trans. R. Soc. A Math. Phys. Eng. Sci.* **367,** 1445–1486 (2009).
3. Nishimoto, S., Bhushan, B. Bioinspired self-cleaning surfaces with superhydrophobicity, superoleophobicity, and superhydrophilicity. *RSC Adv.* **3,** 671–690 (2013).
4. Hancock, M. J., Sekeroglu, K., Demirel, M. C. Bioinspired directional surfaces for adhesion, wetting, and transport. *Adv. Funct. Mater.* **22,** 2223–2234 (2012).
5. Reddy, S., Arzt, E., del Campo, A. Bioinspired Surfaces with Switchable Adhesion. *Adv. Mater.* **19,** 3833–3837 (2007).
6. Gorb, S., Sinha, M., Peressadko, A. Insects did it first: a micropatterned adhesive tape for robotic applications. *Bioinspir. Biomim.* **2,** 117 (2007).
7. Amador, G. J. *et al.* Honey bee hairs and pollenkitt are essential for pollen capture and removal. *Bioinspir. Biomim.* **12,** 1–11 (2017).
8. Lin, H., Qu, Z., Meredith, J. C. Soft Matter Pressure sensitive microparticle adhesion through biomimicry of the pollen – stigma interaction. *Soft Matter* **12,** 2965–2975 (2016).
9. Casteel, D. *The behavior of the honey bee in pollen collection*. (2012).
10. Brown, M. B. *et al*. Dermal and Transdermal Drug Delivery Systems: Current and Future Prospects. *Drug Deliv.* **13,** 175–187 (2006).
11. Naik, A., Kalia, Y. N., Guy, R. H. Transdermal drug delivery: overcoming the skin's barrier function. *Pharm. Sci. Technolo. Today* **3,** 318–326 (2000).
12. Gitlin, L., Schulze, P., Belder, D. Rapid replication of master structures by double casting with PDMS. *Lab Chip* **9,** 3000–3002 (2009).
13. Théry, M., Piel, M. Adhesive micropatterns for cells: a microcontact printing protocol. *Cold Spring Harb. Protoc.* **7,** 1–11 (2009).
14. Luciani, A. *et al*. PCL microspheres based functional scaffolds by bottom-up approach with predefined microstructural properties and release profiles. *Biomaterials* **29,** 4800–4807 (2008).
15. Correia, C. R., Reis, R. L., Mano, J. F. Multilayered Hierarchical Capsules Providing Cell Adhesion Sites. *Biomacromolecules* **14,** 743–751 (2013).
16. Silva, A. S. *et al.* Aerosolizable gold nano-in-micro dry powder formulations for theragnosis and lung delivery. *Int. J. Pharm.* **519,** 240–249 (2017).
17. Ritger, P. L., Peppas, N. A. A simple equation for description of solute release I. Fickian and non-fickian release from non-swellable devices in the form of slabs, spheres, cylinders or discs. *J. Control. Release* **5,** 23–36 (1987).
18. Siepmann, J., Siepmann, F. Mathematical modeling of drug delivery. *Int. J. Pharm.* **364,** 328–343 (2008).

19. Siafaka, P. I. *et al*. Porous dressings of modified chitosan with poly(2-hydroxyethyl acrylate) for topical wound delivery of levofloxacin. *Carbohydr. Polym.* **143,** 90–99 (2016).
20. Shahverdi, A. R. *et al*. Synthesis and effect of silver nanoparticles on the antibacterial activity of different antibiotics against *Staphylococcus aureus* and *Escherichia coli*. *Nanomedicine Nanotechnology, Biol. Med.* **3,** 168–171 (2007).
21. Pastore, M., Kalia, Y., Horstmann, M. Transdermal patches: history, development and pharmacology. *Br. J. Pharmacol.* **172,** 2179–2209 (2015).
22. Martín, M. J. *et al.* Development of alginate microspheres as nystatin carriers for oral mucosa drug delivery. *Carbohydr. Polym.* **117,** 140–149 (2015).
23. Wang, Y. *et al.* Controlled release behaviour of protein-loaded microparticles prepared via coaxial or emulsion electrospray prepared via coaxial or emulsion electrospray. *J. Microencapsul.* **30,** 490–497 (2013).
24. Park, H. *et al.* Fabrication of cross-linked alginate beads using electrospraying for adenovirus delivery. *Int. J. Pharm.* **427,** 417–425 (2012).
25. Martins, S. *et al.* Insulin-loaded alginate microspheres for oral delivery – Effect of polysaccharide reinforcement on physicochemical properties and release profile. *Carbohydr. Polym.* **69,** 725–731 (2007).
26. Sendil, D. *et al*. V. Antibiotic release from biodegradable PHBV microparticles. *J. Control. Release* **59,** 207–217 (1999).
27. Martin, P. Wound healing--aiming for perfect skin regeneration. *Science* **276,** 75–81 (1997).
28. Broughton 2nd, G., Janis, J. E., Attinger, C. E. The basic science of wound healing. *Plast. Reconstr. Surg.* **117,** 12–34 (2006).
29. Huang, X., Brazel, C. S. On the importance and mechanisms of burst release in matrix-controlled drug delivery systems. *J. Control. Release* **73,** 121–136 (2001).

Supporting Information

Physical Supports for the immobilization particles inspired by pollination.

Lúcia F. Santos [1], A.Sofia Silva[1], Clara R. Correia[1], J.F. Mano[1]

[1] Department of Chemistry, CICECO – Aveiro Institute of Materials, University of Aveiro, Campus Universitário de Santiago, 3810-193 Aveiro, Portugal

Contents

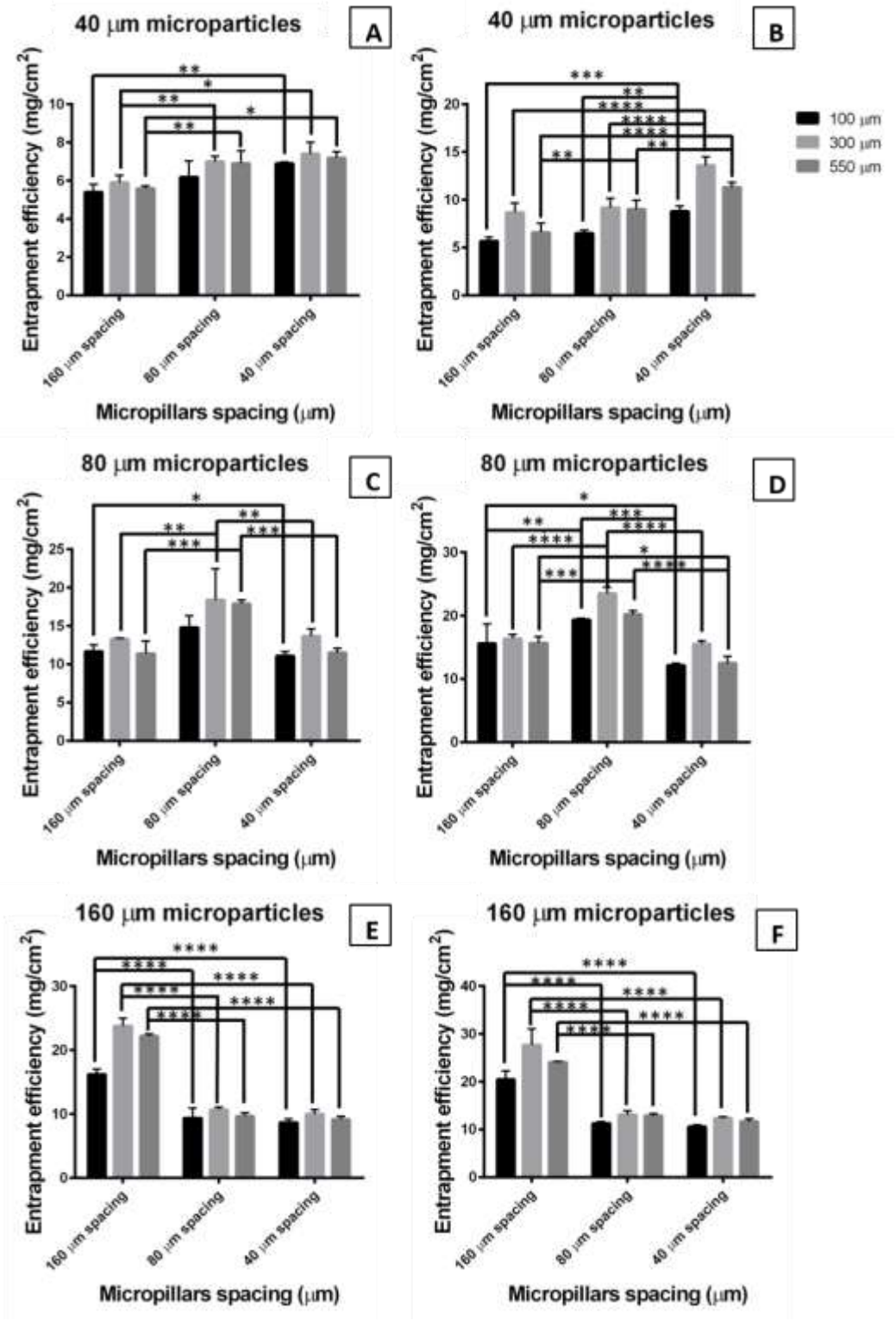

Figure S1. Graphical representation of the entrapment efficiency of. microparticles' trapping assays. **A.** microparticles with 40 µm of diameter within PMP with 5:1 of flexibility; **B.** microparticles with 40 µm of diameter within PMP with 15:1 of flexibility; **C.** microparticles with 80 µm of diameter within PMP with 5:1 of flexibility; **D.** microparticles with 80 µm of diameter within PMP with 15:1 of flexibility; **E.** microparticles with 160 µm of diameter within PMP with 5:1 of flexibility; **F.** microparticles with 160 µm of diameter within PMP with 15:1 of flexibility.

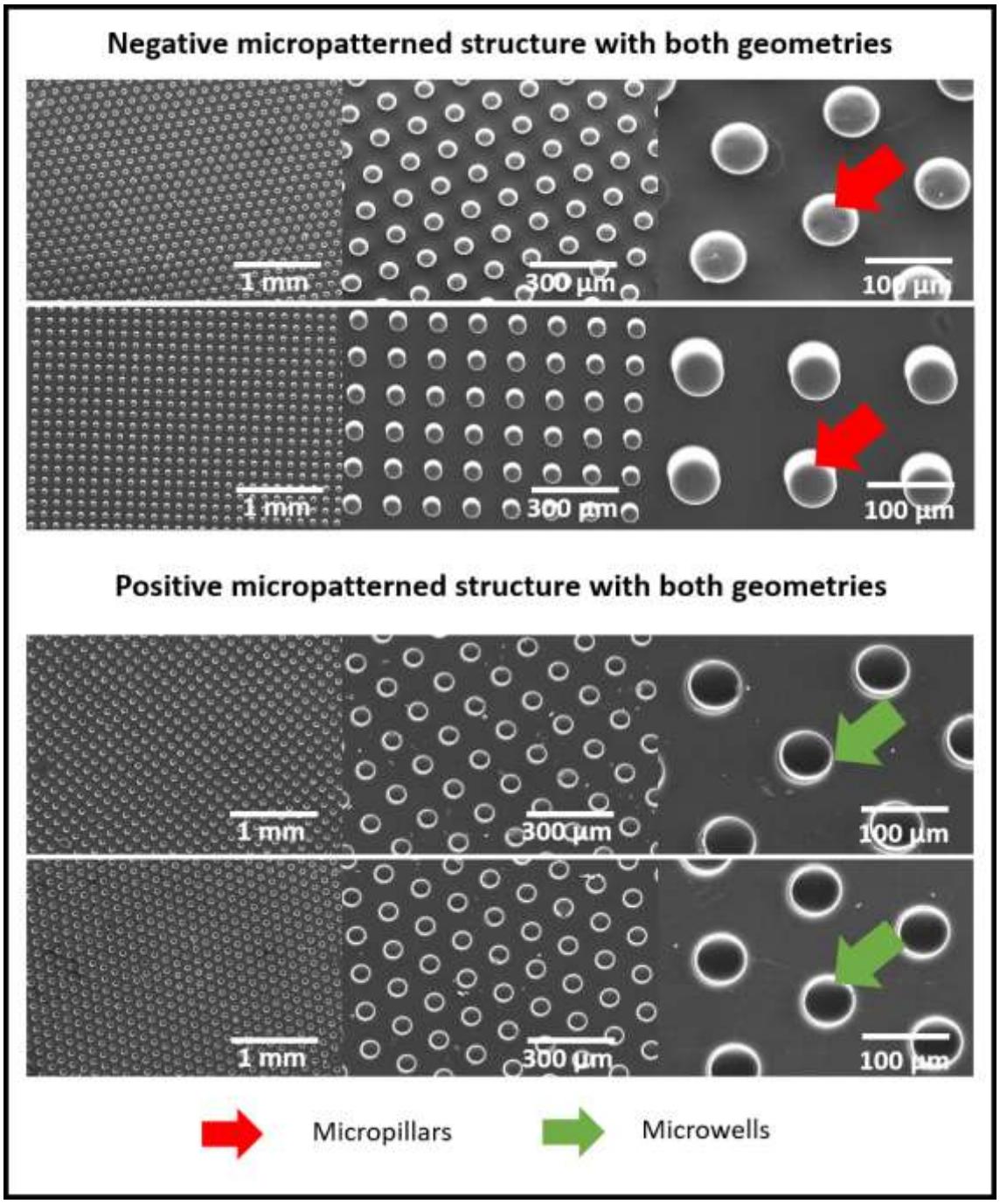

Figure S2. SEM images of negative and positive PMP with both geometries (square and hexagonal).

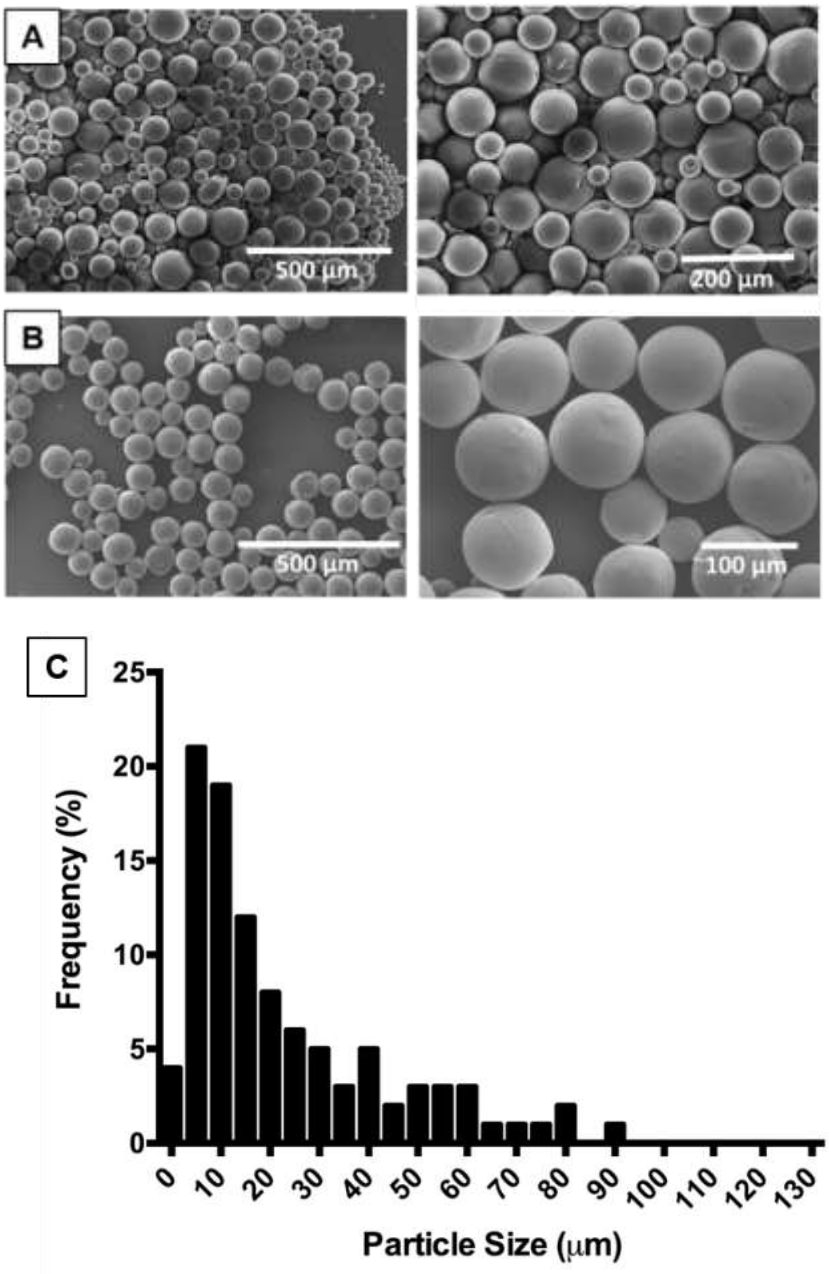

Figure S3. PCL microparticles obtained by emulsion technique; **A.** SEM images of PCL microparticles before sieving; **B.** SEM images of PCL microparticles after sieving; **C.** Microparticle size distribution of PCL microparticles produced by emulsion technique.

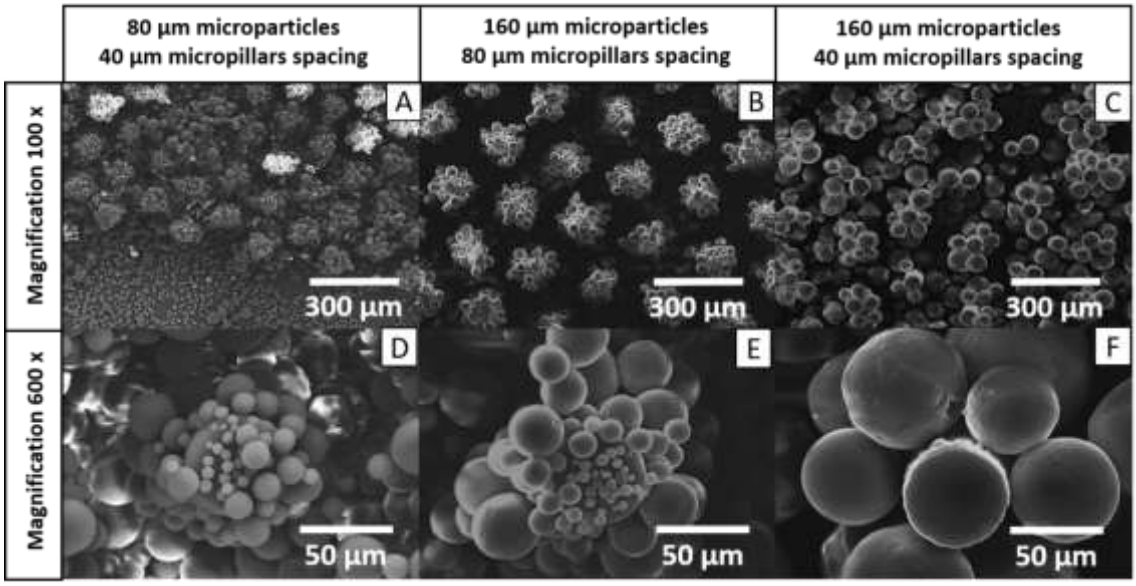

Figure S4. SEM images of PMP with microparticles diameters inferior to micropillars spacing; **A.** 40 µm microparticles with 80 µm micropillars spacing. Magnification 100x; **B.** 40 µm microparticles with 160 µm micropillars spacing. Magnification 100x; **C.** 80 µm microparticles with 160 µm micropillars spacing. Magnification 100x; **D.** 40 µm microparticles with 80 µm micropillars spacing. Magnification 600x; **E.** 40 µm microparticles with 160 µm micropillars spacing. Magnification 600x; **F.** 40 µm microparticles with 160 µm micropillars spacing. Magnification 600x.

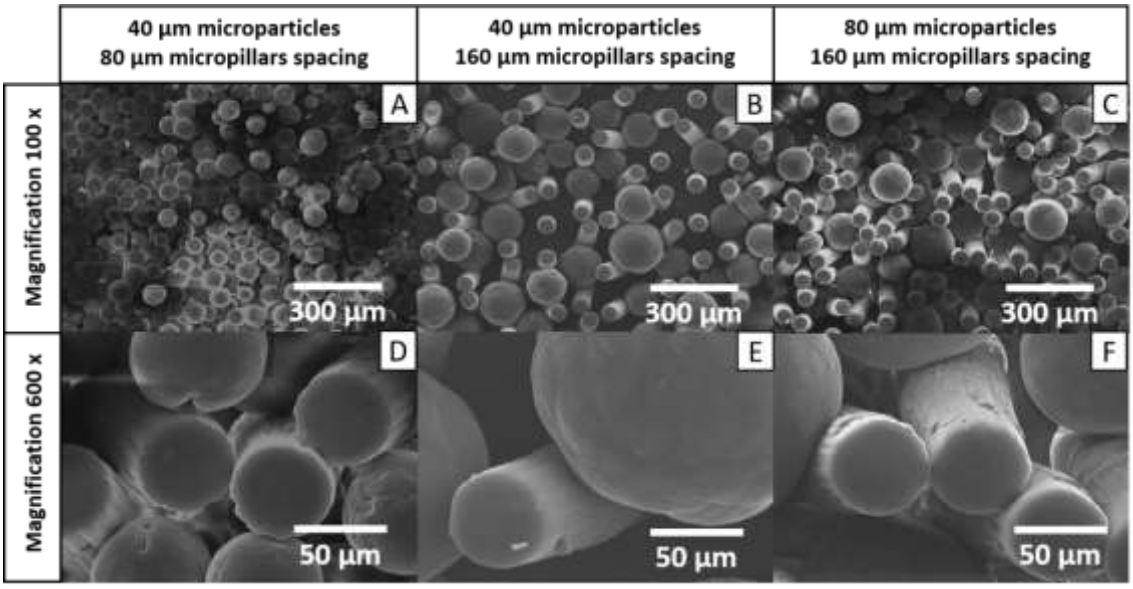

Figure S5. SEM images of PMP with microparticles diameters superior to micropillars spacing; **A.** 80 µm microparticles with 40 µm micropillars spacing. Magnification 100x; **B.** 160 µm microparticles with 80 µm micropillars spacing. Magnification 100x; **C.** 160 µm microparticles with 40 µm micropillars spacing. Magnification 100x; **D.** 80 µm microparticles with 40 µm micropillars spacing. Magnification 600x; **E.** 160 µm microparticles with 80 µm micropillars spacing. Magnification 600x; **F.** 160 µm microparticles with 40 µm micropillars spacing. Magnification 600x

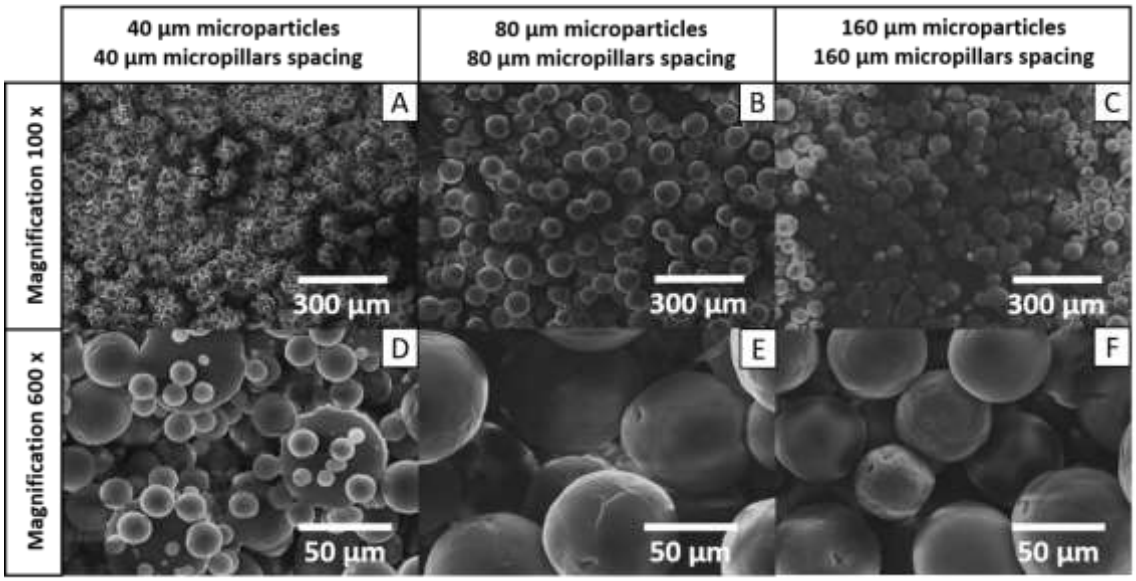

Figure S6. SEM images of PMP with microparticles diameters similar to micropillars spacing; **A.** 40 µm microparticles with 40 µm micropillars spacing. Magnification 100x; **B.** 80 µm microparticles with 80 µm micropillars spacing. Magnification 100x; **C.** 160 µm microparticles with 160 µm micropillars. Magnification 100x spacing; **D.** 40 µm microparticles with 40 µm micropillars spacing. Magnification 600x; **E.** 80 µm microparticles with 80 µm micropillars spacing. Magnification 600x; **F.** 160 µm microparticles with 160 µm micropillars. Magnification 100x spacing.

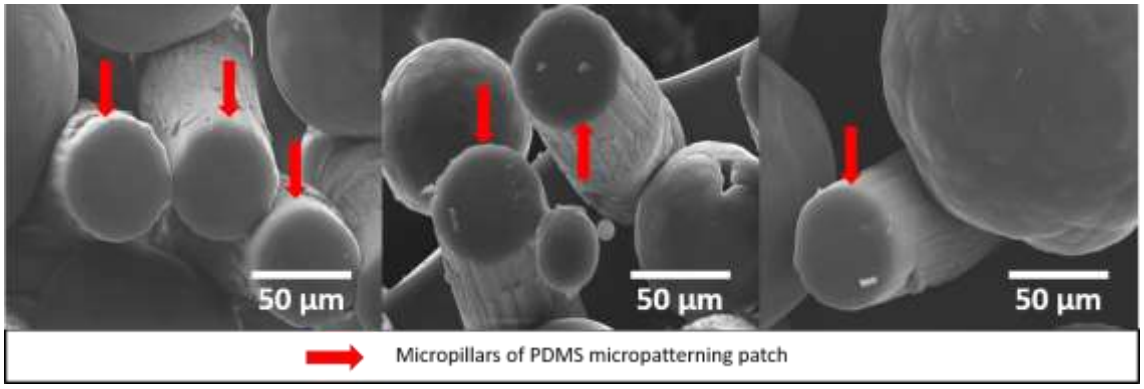

Figure S7. SEM images of PMP with PCL microparticles entrapped between the micropillars.

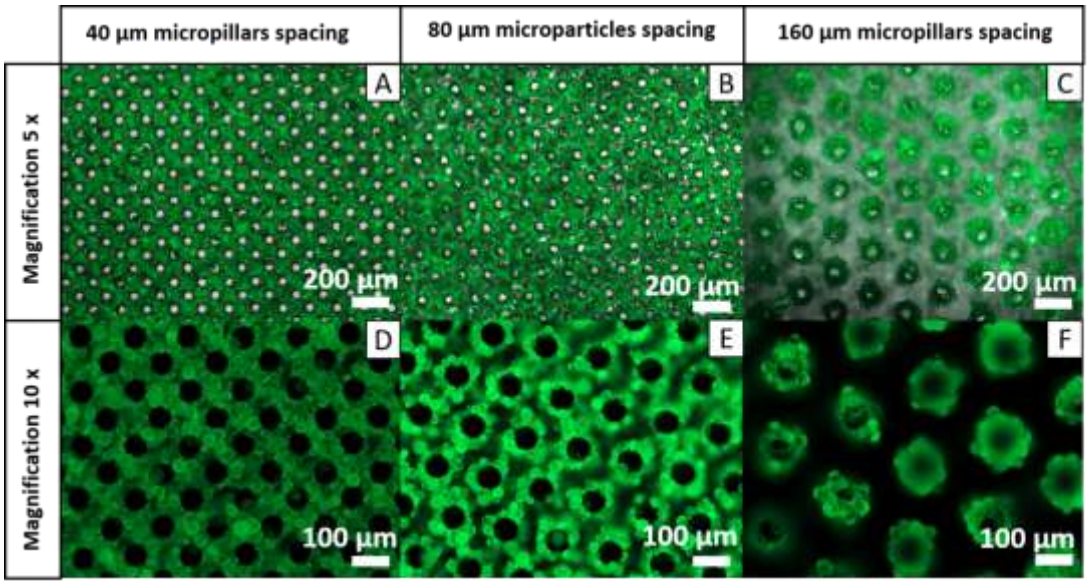

Figure S8. Fluorescence microscopy of PMP with 40 µm fluorescent PCL microparticles and with different micropillars spacing: **A.** 40 µm. Magnification 5x; **B.** 80 µm. Magnification 5x; **C.** 160 µm.. Magnification 5x; **D.** 40 µm. Magnification 10x; **E.** 80 µm. Magnification 10x; and **F.** 160 µm.. Magnification 10x.

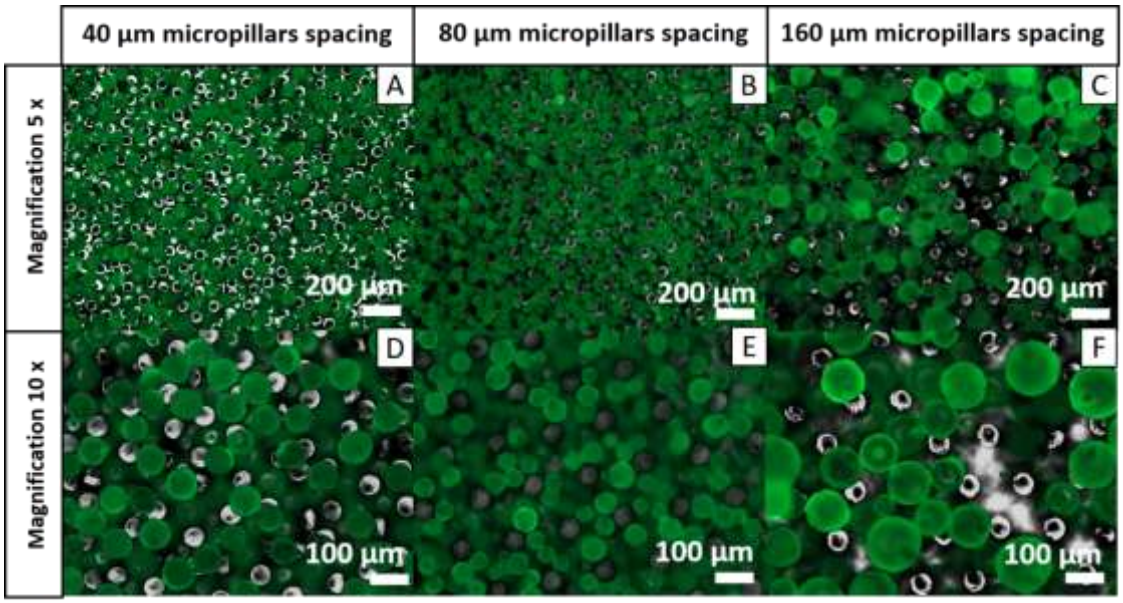

Figure S9. Fluorescence microscopy of PMP with 80 µm fluorescent PCL microparticles and with different micropillars spacing: **A.** 40 µm. Magnification 5x; **B.** 80 µm. Magnification 5x; **C.** 160 µm.. Magnification 5x; **D.** 40 µm. Magnification 10x; **E.** 80 µm. Magnification 10x; and **F.** 160 µm.. Magnification 10x.

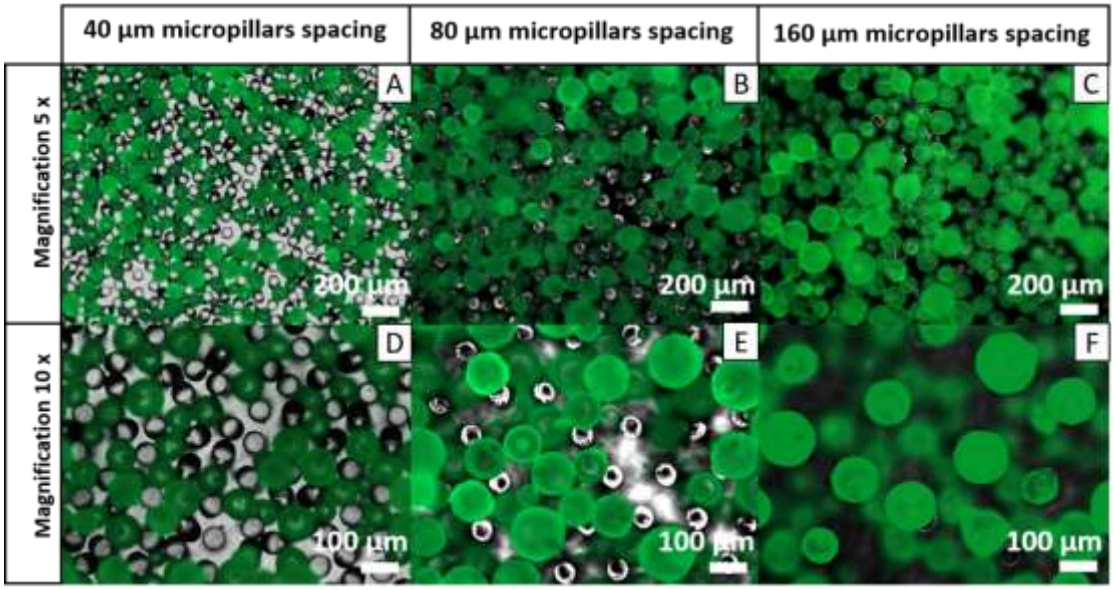

Figure S10. Fluorescence microscopy of PMP with 160 µm fluorescent PCL microparticles and with different micropillars spacing: **A.** 40 µm. Magnification 5x; **B.** 80 µm. Magnification 5x; **C.** 160 µm.. Magnification 5x; **D.** 40 µm. Magnification 10x; **E.** 80 µm. Magnification 10x; and **F.** 160 µm.. Magnification 10x.

Table S2. Production of alginate microparticles by electrospray. Different parameters were tested using alginate solution 2% (w/v), diameter tube of 0.5 mm and distance to the collector. of 6 cm.

Flow rate (mL/h)	Voltage (kV)	Needle	Shape	Size
10	10	26G	2 populations (spherical)	± 200 µm ± 110 µm
5	10	26G	Spherical	> 120 µm with polydispersity
	15	26G	Shapeless	-
1	15	26G	Shapeless	Very large and high polydispersity
	15	22G	Spherical	80-90 µm

Chapter 5- Final Overview, concluding remarks and future prospects

The development of novel and pioneering therapeutic devices is emerging nowadays and one of the major goal includes the development of new and optimized drug delivery systems (DDS) capable of enhancing conventional treatments efficacy and/or to avoid the commonly associated side effects.

CHAPTER 1 encompasses the thesis motivation combined with the wound healing concerns and with the advantages that can arise from the development of a bioinspired optimized transdermal DDS. Inspired by animals such as insects, many biomimetic synthetic adhesives have been studied in order to support macroscopic masses. Honey bees, for instance, have a typical branched hair and pollen grains are caught and held between the barbs of adjacent hair. In pollination, the hairy covering the body allows the temporary retention of pollen, followed by removal through the combined action of legs' brushes. An optimized bioinspired system can, therefore, be developed based on the pollination process though the adhesion between particles and micro-patterned soft matter surfaces.

Transdermal drug delivery has been investigated as a successful drug delivery platform. Due to their simple design, application and low production cost, patches still the most commonly transdermal DDS present in the market. In order to recognize their benefits and limitations, CHAPTER 2 makes a review that highlights the efforts developed in last years regarding the production of patches with different designs and their potential application in drug delivery. Current commercially available transdermal patches and clinical trials are also included. Although major achievements have been attained in the development of more sophisticated patches, some limitations still need to be overcome. In fact, drug' physicochemical properties continue to play an important role in its transport through the skin layers. Consequently, low transcutaneous flux, drug incorporation and retention in the patch still restraint their application.

The work detailed in this thesis reveals the extraordinary advantages of combining the biomimetic concept with microfabrication techniques to develop a robust bioinspired hierarchal patch based on the extraordinary and organized bee’s ability to catch and release the pollen during pollination in order to overcome the current patches limitations. The major goals of the present thesis were: i) the development of a new design of a micropatterned

patch with micropillars (that mimics bees' legs) to catch a certain amount of drug; ii) the engineering of a novel and optimized system for transdermal drug delivery purposes iii) to support the hypothesis that grains pollen are catch between hair legs because this distance is equal to grains pollen sizes and define the most effective system. For this purpose, different conjugations of a system composed of a PDMS micropatterning patch together with differently sized drug microparticles were investigated to act in a controlled and sustained manner during the inflammatory phase of a wound.

CHAPTER 3 thoroughly described the materials and methods and also presents the results and discussion of preliminary steps performed during the development of the work.

With the goal of designing an optimized patch, in CHAPTER 4 a robust bioinspired patch with simple design was successful engineering based on pollination process. A PDMS micropatterning patch with micropillars was obtained by casting process. Differently sized PCL microparticles (obtained by emulsion technique) were combined with different PDMS micropatterning patch to achieve the most effective system. The patch filling with microparticles was accessed by SEM and fluorescence microscopy. The hypothesis previous described was supported. An optimized system was achieved through the perfect combination of microparticles' diameters and micropillars distance from the patch to controlled and sustained release of the drug. In fact, an entrapment efficiency of 24.8 ± 0.4 $mg \cdot cm^{-2}$ was achieved with a size patch of 1.44 cm^2, improving to a great extend the commercially available patches. According to Table 2.3 (CHAPTER 2), the current patch drugs approved by FDA in the market present a dose much lower than system proposed, less than 5.1 $mg \cdot cm^{-2}$ (36 mg in 7 cm^2). It is foreseen that the proposed hierarchal patches will be a valuable solution for the treatment of diseases that require high-drug concentration enabling less frequent dosing, therefore improving patient compliance.

The release profile was determinate for two different systems: patches with both tetracycline powder microparticles and tetracycline-loaded alginate microparticles, a model antibiotic, expected to act during the inflammatory phase of the wound healing process. While tetracycline powder was immediately release, the other ones allowed a controlled release for 5 days. Drug carriers (tetracycline-loaded alginate microparticles) allowed a more sustained drug release when compared to tetracycline powder. The hierarchical patch activity was verified through antimicrobial assays, proving their antimicrobial action against both gram-negative and gram-positive bacteria. Still, this patch is not limitative, being a

platform that can be applied to a large pool of drugs and that can be coupled with other techniques to develop a wide variety of patches.

Ultimately, the investigation conducted in this thesis and the findings that resulted from it enabled the successful development of potential bioinspired patch for clinical applications. The goals of this thesis were successfully achieved and bring new insights that could solve the current problems associated with passive drug delivery patches.

Although the work herein detailed may present huge advances in biomimetic systems for transdermal drug delivery and patches designs, more efforts need to be performed to translate these approaches into clinical applications. *In vivo* contributions regarding the use of PDMS micropattermig patch must be addressed in order to convince the pharmaceutical industries to adopt such strategy. Accurate pharmacokinetics and pharmacodynamics studies, (meaning what happens to the drug microparticles after their deposition in the skin and what are the effects of such particles/biomolecules in the body, respectively) need to be fully investigated to assure clinical relevance. Moreover, biocompatible and biodegradable polymers, mostly natural ones have been received careful attention due to their biocompatibility, low toxicity and susceptibility to degradation by human enzymes. Alternatives to PDMS must be debated.

Forthcoming works that can arise from this thesis and be implemented in a near future include:

. i) Replacement of PDMS patches engineered in CHAPTER 4 by natural and/or biodegradable polymers.

. ii) *In vivo* assays - determination of transcutaneous flux, plasma level and biocompatibility assays.